**UNIVERSIDAD DE ANTIOQUIA**

**Technical, economic, and environmental evaluation of different Fenton-based processes for treating hospital wastewater**

Claudia Mildred Grisales Cifuentes

Trabajo de investigación para optar al título de Magíster en Ingeniería Ambiental

Director
Ricardo Antonio Torres Palma, Doctor (PhD)

Asesor
Efraím Adolfo Serna Galvis, Doctor (PhD)

Universidad de Antioquia
Facultad de Ingeniería

Maestría en Ingeniería Ambiental

Medellín, Antioquia, Colombia

2022

| Cita | (Grisales Cifuentes; Serna Galvis & Torres Palma, 2018) |
|---|---|
| **Referencia**<br><br>**Estilo APA 7 (2020)** | Grisales Cifuentes, C.M., Serna Galvis, E.A., & Torres Palma, R. A. (2022. *Technical, economic, and environmental evaluation of different Fenton-based processes for treating hospital wastewater* [Tesis de maestría]. Universidad de Antioquia, Medellín, Colombia. |

Maestría en Ingeniería Ambiental, Cohorte XXII.

Grupo de Investigación Remediación Ambiental y Biocatálisis.

Centro de Investigación en Ciencias Exactas y Naturales (CIEN).

**UNIVERSIDAD
DE ANTIOQUIA**
Vicerrectoría de Docencia

Sistema
de Bibliotecas

**Repositorio Institucional:** http://bibliotecadigital.udea.edu.co

Universidad de Antioquia - www.udea.edu.co

**Rector:** John Jairo Arboleda Cespedes

**Decano/Director:** Jesús Francisco Vargas.

**Jefe departamento:** Pedro León Simanca.

## TABLE OF CONTENT

## LIST OF TABLES

## LIST OF FIGURES

# ABSTRACT

Advanced Oxidation Processes (AOPs) are gaining attention to remove pharmaceuticals from hospital wastewaters (HWW). In this study, the feasibility of applying Fenton-based technologies (carbocatalysis and photo-Fenton), and assessing their technical, economic, and environmental performance was evaluated. For the technical criterion, Box-Behnken experimental designs were applied; to establish the economic aspect, reagents and electric energy consumptions during the operation of processes were considered, while the environmental impact was determined using life cycle assessment. Initially, it was tested a carbocatalytic process using a biochar from palm fiber wastes to activate different oxidants (hydrogen peroxide, peroxymonosulfate, and persulfate) during the elimination of three pharmaceuticals (valsartan, cephalexin, acetaminophen) belonging to diverse therapeutic groups. Secondly, the photo-Fenton process, at natural pH, using peroxymosulfate in place of hydrogen peroxide for the elimination of a representative pharmaceutical (valsartan) in simulated and actual HWW, was tested. The modification of the process by the addition of citric acid was also evaluated. Finally, a comparison between carbocatalysis and photo-Fenton (using Fe(II)+PMS+UVA with citric acid) was done.

Carbocatalytic treatment was more efficient against compounds, such as valsartan, recalcitrant to conventional oxidants and hardly adsorbed on the carbonaceous material. This process involved hydroxyl radical and singlet oxygen in the target pollutant degradation. Under optimal conditions, the carbocatalytic process reached up to 90% of the removal of pharmaceuticals in HWW. In turn, the Fe (II)+PMS+UVA process was able to degrade the target pharmaceutical by the action of both hydroxyl radical and sulfate radical, the process performance was improved by the addition of citric acid (resulting in a significant decrease of the treatment time). Furthermore, this photo-Fenton system led to removals between 30 and 90% of the pollutant in HWW.

The economic calculations for the operation of the processes showed that carbocatalysis presented higher costs (11.057 USD $m^{-3}$) than Fe (II)+PMS+UVA in presence of citric acid (4.92 USD $m^{-3}$). The costs associated with the biochar preparation represented 82% of the value reported for the total operational cost in the carbocatalysis process. Meanwhile, the operational costs associated

with the consumption of reagents represented ~ 99% of the value reported for the photo-Fenton process.

The environmental impact analysis indicated that Fe (II)+PMS+UVA (with citric acid) process had a global warming potential of ~0.517 Kg $CO_2$-Eq, which was six-fold lower than that for carbocatalysis (2.87 Kg $CO_2$-Eq). The factor with the greatest environmental footprint for the carbocatalytic process was the biochar preparation, whereas in the Fe (II) +PMS + UVA processes, the reagents synthesis, and energy consumption were the factors with the main influence on the environmental impact. At the end, the processes comparison, considering the three criteria (technical, economic, and environmental) revealed that the Fe (II)+PMS+UVA in the presence of citric acid system was more suitable than carbocatalysis to remove the target pharmaceutical compounds in HWW.

**CHAPTER I**

**BACKGROUND AND THEORETICAL FRAMEWORK OF THE RESEARCH WORK**

This chapter begins by depicting the problem statement, i.e., contaminants of emerging concern in water, and hospital wastewater as a main source of them (section 1.1), followed by the theoretical framework of the work (section 1.2). Then, the hypothesis (section 1.3) and objectives of the research are presented (section 1.4). At the end of the chapter, it is detailed the cases studied in the work (section 1.5).

## 1.1.    Problem statement

The presence of contaminants of emerging concern (CECs), such as pharmaceuticals and personal care products in water bodies, is gaining attention due to their potential negative effects on the environment and human health (Anjali & Shanthakumar, 2019; Castillo Meza et al., 2020; A. H. Khan et al., 2020; Ouarda et al., 2019). Hospitals have been identified as one of the main contributors of CECs (especially pharmaceuticals) (Boillot et al., 2008; Mackuľak et al., 2019; Rodriguez-Mozaz et al., 2018; Paola Verlicchi et al., 2012). Despite the low concentration of pharmaceuticals (ranging from ng $L^{-1}$ to µg $L^{-1}$), the hospital wastewater (HWW) typically has 4-50 times more concentrated pollutants than urban wastewater (UWW) (Paola Verlicchi et al., 2012). Thus, HWW cause several environmental and health concerns such as antibiotic resistance, endocrine disruption, carcinogenicity, and toxicity (Chonova et al., 2018; Ouarda et al., 2019).

Several studies had reported the potential toxicity of HWW to the aquatic environment. Hamjinda et al. (Hamjinda et al., 2018) informed the negative effects of HWW on algae and microcrustacean growth caused by antibiotics, especially norfloxacin and ciprofloxacin, at concentrations of 12.11 and 9.60 µg $L^{-1}$, respectively. Perrodin and Orias (Perrodin & Orias, 2018) concluded that the multiple pollutants present in HWW may lead to additive or synergistic effects that result in strong negative impacts on aquatic ecosystems. Also, Weissbrodt et al. (Chonova et al., 2018) have reported that the toxicity of HWW is 5-15 times higher than domestic wastewater. It is important to mention that substances such as analgesics and antibiotics are the most frequent pharmaceuticals

in HWW (Efraim A. Serna-Galvis et al., 2019; Efraím A. Serna-Galvis et al., 2017, 2019b; Paola Verlicchi et al., 2012).

In developing countries, HWW are usually discharged in urban sewer systems or directly discharged on water bodies without any treatment (Kumari et al., 2020; Efraim A. Serna-Galvis et al., 2019). Another major issue related to HWW is the inability of conventional wastewater treatment plants (WWTPs) to eliminate many pharmaceuticals, e.g., antibiotics, which are finally released to the aquatic ecosystems (Suarez et al., 2009). To face this issue, different alternatives of treatment have been assessed including the use of coagulation-flocculation and flotation (Saitoh et al., 2017; Suarez et al., 2009), biological treatments (especially biological membrane reactor, MBR) (Chiarello et al., 2016; Nguyen et al., 2017; Vo et al., 2019), and adsorption using activated carbon (Alvarino et al., 2020; Lima et al., 2019). However, the factor that limits the use of MBR techniques is the lack of robustness to the variability of pharmaceutical compounds in real wastewater. Moreover, in the case of coagulation-flocculation, flotation, and adsorption processes, their main disadvantage is associated with the that they promote a phase change more than degradation/transformation of the pollutants (Belalcázar-Saldarriaga et al., 2018b; Chiarello et al., 2016; Suarez et al., 2009).

Advanced oxidation processes (AOPs) are gaining attention to remove pharmaceuticals from HWW (Efraim A. Serna-Galvis et al., 2019; Efraím A. Serna-Galvis et al., 2017, 2019b). They produce highly reactive oxygen species (ROS) that can efficiently degrade CECs (Anjali & Shanthakumar, 2019; Kim et al., 2020). AOPs involve formation and utilization of hydroxyl radicals (HO•, $E° = 2.8$ V), and more recently sulfate radicals (SO$_4$•$^-$, $E° = 2.5$-$3.1$ V), singlet oxygen ($^1O_2$), and superoxide radical anion (O$_2$•$^-$), for degrading pollutants (Devi et al., 2016; Jianlong Wang & Wang, 2018). A well-known AOP is the Fenton process, in which, HO• is formed from the reaction of the ferrous ion with hydrogen peroxide (as shown in Eq. (1)). Analogously, the reaction of the ferrous ion with persulfate (PS) or peroxymonosulfate (PMS) produces SO$_4$•$^-$ (Eqs. 2-3) (Devi et al., 2016; Jianlong Wang & Wang, 2018).

$$Fe^{2+} + H_2O_2 \rightarrow Fe^{3+} + HO \cdot + OH^- \hspace{3cm} \text{Eq. (1)}$$

$$Fe^{2+} + S_2O_8^{2-} \rightarrow SO_4^{\cdot-} + Fe^{3+} + SO_4^{2-} \hspace{2.5cm} \text{Eq. (2)}$$

$$Fe^{2+} + HSO_5^- \rightarrow SO_4^{\cdot-} + Fe^{3+} + OH^- \hspace{2.7cm} \text{Eq. (3)}$$

Fenton process requires the operation in a narrow pH range (2.8-3.0), to avoid the iron precipitation, and reduce undesirable reactions (Belalcázar-Saldarriaga et al., 2018b; Luis Miguel Salazar et al., 2019). This represents a technical limitation, considering that the common pH for HWW varies from 6.3 to 9.2, and the pH adjustment generates a high consumption of acid and hydroxide in acidification and neutralization steps, in addition to increasing the presence of ions in the water matrix (Grisales et al., 2019; N. A. Khan et al., 2020; Paola Verlicchi et al., 2012). Additionally, economic and environmental assessments (which are factors to consider at large-scale applications) (Belalcázar-Saldarriaga et al., 2018b; Grisales et al., 2019; Luis Miguel Salazar et al., 2019) for treating HWW by the Fenton based process are a lack. Therefore, with the purpose to face the above-mentioned limitations, in this research, Fenton and alternative catalytic processes (carbocatalysis and Fe (II)+PMS+UVA) were evaluated to degrade three pharmaceuticals with chemical structure different and relevant consumption (Cephalexin, Valsartan, Acetaminophen) and typically present in HWW matrices, establishing the most efficient technology from a technical, economic, and environmental point of view.

## 1.2.    Background of the study

Recent studies have focused their attention on the use of Peroxydisulfate (PDS) and Peroxymonosulfate (PMS) instead of the traditional Fenton process, as oxidizing agents to produce sulfate radical or other species capable of effectively degrading CECs. It can be mentioned that $SO_4^{\bullet-}$ has some remarkable advantages on $HO^\bullet$, including higher selectivity and longer half-life time ($SO_4^{\bullet-}$ = 3-4 x $10^{-5}$ s vs. $HO^\bullet$ = 2 x $10^{-8}$ s) (Oh et al., 2016; Luis Miguel Salazar et al., 2019; Jianlong Wang & Wang, 2018). To generate $SO_4^{\bullet-}$, both PDS and PMS can be activated through heat, radiation, ultrasound, or metal ions (e.g., $Fe^{2+}$, $Co^{2+}$, $Mn^{2+}$, Eqs. 2-3).

According to the advantages mentioned above, $SO_4^{\bullet-}$ has been successfully applied to degrade organic pollutants commonly found in HWW (e.g., antibiotics) (Kim et al., 2020; Pirsaheb et al., 2020; Rodríguez-Chueca, Garcia-Cañibano, et al., 2019). Figure 1 depicts the growing increase in the number of studies on sulfate radical advanced oxidation processes (SR-AOP) applications in facing the removal of pharmaceuticals, during the last two decades.
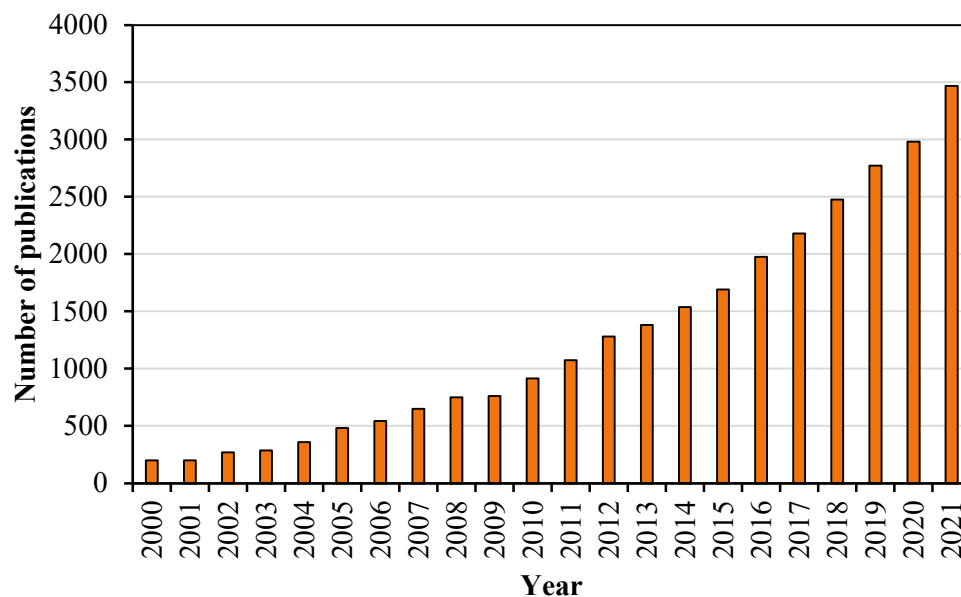
**Figure 1.** Number of publications (2000-2021) on applications of sulfate radicals for
pharmaceutical degradation (Scopus database, January 2022)

As presented in Section 1.1, Fenton-based processes have the problem of iron precipitation.
However, in persulfate/Iron (PDS/Fe) and peroxymonosulfate/Iron (PMS/Fe) systems, a decrease
in the catalyst precipitation can be achieved using complexing agents. For instance, Dong et al.
(Dong et al., 2017) assessed the role of four complexing agents in the degradation of iopamidol (a
pharmaceutical) by PDS/Fe(III), finding that the degradation of iopamidol was accelerated,
especially with gallic acid, increasing the degradation rate constant more than 10 times due to an
enhancement of the Fe (III) reduction and the PDS decomposition to generate more radicals.
Similarly, Shi et al. (Shi et al., 2019) introduced protocatechuic acid (PCA) as a complexing agent
in the PMS/Fe (II) system to degrade ciprofloxacin, showing that the PMS/Fe(II)/PCA system has
a superior degradation ability than PMS/Fe (II) system, owing to the high generation of ROS, and
fast transformation of Fe (III) to Fe (II) because of the formation of a PCA-Fe chelate, which
decreased the iron precipitation.

On the other hand, carbonaceous materials (e.g., activated carbon, graphene, carbon nanotubes,
and biochar) have been used as new/alternative catalysts (i.e., carbocatalysis) to activate PDS and
PMS recently (Devi et al., 2016; Luo et al., 2019; Jianlong Wang & Wang, 2018). One of the

greatest advantages of carbonaceous materials (CBM) is the extensive feedstock available to produce them, which includes industrial wastes and bio-wastes, commonly woods, activated sludge, agriculture wastes, urban and domestic wastes, manures, and algae (Shan et al., 2020; Jianlong Wang & Wang, 2018; Xiang et al., 2020).

The use of carbonaceous materials (CBM) is attractive due to noticeable properties such as huge specific area, high pore volume and conductivity, low costs, and recyclability. Indeed, CBM can remove CECs in wastewater by adsorption, and with the addition of an oxidizing agent (e.g., PDS, PMS, or $H_2O_2$), pollutants are degraded by the ROS action (Shan et al., 2020; Jianlong Wang & Wang, 2018). Table 1 depicts an overview of recent publications related to the evaluation of carbocatalysis to degrade pharmaceuticals. Such studies report a high efficiency in most cases and the possibility to operate at near-neutral conditions. Additionally, biochar (BC, produced by the thermal decomposition of biomass) represents a novel CBM, which is gaining attention for the degradation of organic contaminants (Shan et al., 2020; Jianlong Wang & Wang, 2018), because of the high efficiency of the process plus the possibility of catalytic activity recovery by thermal treatment of the used biochar (Li et al., 2020; Mian & Liu, 2020; Jia Wang et al., 2020). Furthermore, the wide availability of bio-wastes and low-cost synthesis of BC make this CBM a good alternative for wastewater treatments, contributing management, re-utilization of wastes, and water decontamination (Nidheesh et al., 2021; Shan et al., 2020).

Apart from the technical and operational aspects of the AOPs, it is very important to consider the use of theoretical tools like the life cycle assessment (LCA) to establish the environmental and costs calculation. LCA allows identifying the main critical stages in the processes to propose alternatives with a low overall environmental impact (Belalcázar-Saldarriaga et al., 2018b; Grisales et al., 2019). It can mention that some studies about pharmaceutical degradation have shown that reagents and electricity consumption are the main contributors to the overall carbon footprint (CFP) (Foteinis, Maria, et al., 2018; Foteinis, Monteagudo, et al., 2018; Rodríguez et al., 2016; Sbardella et al., 2020). For instance, Foteinis et al. (Foteinis, Monteagudo, et al., 2018) evaluated the 7a-ethynylestradiol removal by different AOPs, where the use of simulated irradiation increases the environmental footprint up to a factor of 5 higher than natural solar irradiation, attributed to electricity consumption by the lamp (81.3% of the total CFP). Other authors such as Rodríguez et al. (Rodríguez et al., 2016), Foteinis et al. (Foteinis, Maria, et al., 2018), and Sbardella et al.

(Sbardella et al., 2020)  have demonstrated that the chemical reagents, mainly the oxidizing agents ($H_2O_2$, PDS, and PMS), are the major contributors to the environmental footprint of the processes. The identification of these critical stages along with economic considerations allows the evaluation of new alternatives or implementation of variations on the processes to enhance the sustainability of AOPs and favor their use at a large scale (Belalcázar-Saldarriaga et al., 2018b; Luis Miguel Salazar et al., 2019).

**Table 1.** Recent studies on pharmaceutical removal through AOPs catalyzed by carbonaceous-based material.

| Carbon-based material | Oxidant agent | Pharmaceuticals | Significant findings | Reference |
|---|---|---|---|---|
| Red mud | PMS | Flumequine and ciprofloxacin | A complete removal of pharmaceuticals was achieved after six hours of treatment, with [PMS]=1.0 mM, [RM]=0.05 g $L^{-1}$, [HA]=0.05 mM and pH=7.0±0.1 | (Kim et al., 2020) |
| Oily sludge (OSC) | PMS | Norfloxacin | Removal efficiency of 95.1% was achieved with the following experimental conditions: T=25°C, pH=7, [PMS]=0.8 mM, catalyst dose of 1 g $L^{-1}$ ($COFe_2O_4$/OSC), t=60 min | (Wei et al., 2020) |
| Swine bone biochar (BBC) | PDS | Acetaminophen (ACT) | Complete removal of acetaminophen after 60 minutes of treatment with the following experimental conditions: [ACT]=20 mg $L^{-1}$, [PDS]=1 g $L^{-1}$, [BBC]=0.1 g $L^{-1}$, T=25°C | (Zhou et al., 2020) |
| Sewage sludge biochar | $H_2O_2$ | Ciprofloxacin (CIP) | Removal efficiency of 93% was achieved. Experimental conditions: pH=7, [$H_2O_2$]=1.0 mM, T=25°C, t=24 h, [CIP]=1 mg $L^{-1}$, [BC]=0.4 g $L^{-1}$ | (Luo et al., 2019) |

| | | | | |
|---|---|---|---|---|
| Coffee grounds biochar | PDS | Sulfamethoxazole (SMX) | Almost complete degradation of SMX, using [BC]=200 mg L$^{-1}$, [PDS]=1 g L$^{-1}$, t=75 min, [SMX]=500 µg L$^{-1}$ | (Lykoudi et al., 2020) |
| Modified sludge bio-hydrochar (IBHC) | PDS | Tetracycline (TC) | Activation of PS by IBHC allows to achieve a removal of 99.72% of TC. Experimental conditions: [TC]=60 mg L$^{-1}$, [IBHC]=0.2 g L$^{-1}$, [PDS]=5 mM, pH=4, T= 25°C | (Wei et al., 2020) |
| Biochar | PDS | Sulfamethoxazole (SMX) | Almost complete degradation of SMX after 24 h. Experimental conditions: [SMX]=10 µM, [BC]=2 g L$^{-1}$, [PDS]=1 mM, T=25°C, pH=9 | (Zhang et al., 2020) |
| Biochar (rice husk) | PMS | Tetracycline (TC) | Removal efficiency > 90% after an hour of treatment. Experimental conditions: pH=6, T=22°C, [PMS]=5 mM, and 0.2 g of BC. | (Huong et al., 2020) |
| Biochar and activated carbon (AC) | PDS | Sulfamethoxazole (SMX) | After 150 min of treatment, 88.7% and 91.2% of SMX was degraded in the BC (Produced at 700°C)/PDS and AC/PDS, respectively. Operational conditions: [BC]=[AC]=0.1 g L$^{-1}$, [SMX]=0.5 mg L$^{-1}$, [PDS]=0.5 mM, T=25°C, pH=7.2 | (Liang et al., 2019) |

| | | | | |
|---|---|---|---|---|
| Fe impregnated biochar (FBC), produced from maize straw and peanut shell | $H_2O_2$ | Sulfamethoxazole (SMX) | After 2 hours of treatment, 100% removal of SMX was achieved. Experimental conditions: [FBC]=1 g L$^{-1}$, [SMX]=10 µM, [$H_2O_2$]=3 mM, pH=5, T=25°C | (Xiang et al., 2020) |
| Granular activated carbon (GAC) and carbon nanotube | PDS | Acetaminophen (ACT) | Complete removal of ACT was achieved after 90 min in GAC/PDS system, and after 60 min in CNT/PDS system. Operational conditions: [GAC]=1 g L$^{-1}$, [CNT]=0.1 g L$^{-1}$, [ACT]=10 mg L$^{-1}$, [PDS]=0.21 mM, T=25°C. Removal efficiency was not affected under a pH of 3-7 in both systems. | (Pham et al., 2020) |
| Graphitized biochar (GBC) | PDS | Sulfamethoxazole (SMX) | 98% of removal after 2 hours of treatment, with the following experimental conditions: [SMX]=10 mg L$^{-1}$, [PDS]=0.10 mM, [GBC]=0.1 g L$^{-1}$, T=25°C, pH=5.4 | (Du et al., 2020) |

Considering the presented background, this work is focused on the evaluation of Fenton-based processes (replacing $H_2O_2$ by PMS, and the use of complexing agents) and carbocatalysis (change of ferrous ions by a CBM) to degrade relevant pharmaceuticals in HWW matrices, establishing the most efficient technology from technical, economic, and environmental points of view.

## 1.3.    Hypothesis

The evaluation of Fenton-based processes (considering the substitution of $H_2O_2$ by PMS, and the addition of iron complexing agents) or analogous systems (which use a CBM as an alternative catalyst) under technical, environmental, and economic criteria leads to a feasible system to degrade pharmaceuticals in HWW at near neutral-pH.

## 1.4 Objectives

### 1.4.1    General objective

To evaluate technical, economic, and environmental aspects of different catalytic processes for treating hospital wastewater

### 1.4.2.    Specific objectives

- To identify and select representative pharmaceuticals present in Hospital wastewater, to be used for the development of the research work.
- To evaluate the utilization of a CBM as an alternative catalyst to activate $H_2O_2$, PDS, and PMS in the removal of contaminants from hospital wastewater.
- To identify the effect of the main variables that maximize the efficiency of the carbocatalytic process to degrade pharmaceuticals.
- To determine the operating conditions of the Fenton-based process that allow maximum efficiency to eliminate pharmaceuticals.
- To evaluate/compare the considered processes (carbocatalysis and Fenton-based system) in terms of environmental and economic performance.

## 1.5.    Stages of the research

To achieve the objectives above-presented, this research work consisted of the following four general stages:

a.      *Physical-chemical characterization of hospital wastewater and selection of the target pharmaceuticals.* To develop this step measurements of macro-parameters (such as pH, chemical oxygen demand, total solids, and conductivity) and micropollutants (i.e., pharmaceuticals) were performed.

b.    *Evaluation of the carbocatalytic process.* To achieve the objectives associated with this item, a CBM as an activator of three oxidizing agents ($H_2O_2$, PDS, and PMS) was tested, and the synergistic effect of three oxidizing agents in the removal of the target pharmaceuticals was evaluated. Also, for the selection of the proper operating conditions for the carbocatalytic process, an experimental design was developed; and the effect of pH, catalyst dose, and oxidizing agent concentration was studied. The degradation routes involved in this process were established by the addition of suitable scavengers of radicals. The application of the process to simulated and real hospital wastewater containing the target pharmaceutical was assessed. Moreover, the treatment extent (to evidence positive impacts of the process) was established through phytotoxicity essays.

c.    *Evaluation of the Fenton-based process.* The selection of operational conditions for the Fenton-based process involved an experimental design, considering as variables light power, iron amount, and oxidizing agent (PMS) concentration. The degradation routes in this process were established by the addition of radical scavengers. Furthermore, the intensification of the Fenton-based process by the addition of an organic acid was tested (different concentrations of the acid organic were evaluated). Also, the process was applied to simulated and real hospital wastewater containing target pharmaceuticals, and to determine the treatment extent phytotoxicity essays were developed.

d.    *Identification of the most promising oxidation processes for treatment of real wastewaters at pilot plant scale.* For this stage, an environmental and economic analysis was performed employing an LCA and costs calculation, respectively.

**CHAPTER II**

**CHARACTERIZATION OF THE HOSPITAL WASTEWATER, AND SELECTION OF THE TARGET PHARMACEUTICALS**

## 2.1. Introduction

In this chapter, the macro-composition of the real hospital wastewater (RHWW) from Tumaco-Colombia was determined initially by measuring chemical oxygen demand (COD), pH, conductivity, and total solids (TS). Then, the selection of target pharmaceuticals for the development of this research is presented. Finally, the quantification of the target pharmaceutical in the considered HWW was discussed.

## 2.2. Materials and methods

### 2.2.1. Reagents

Potassium dichromate from Merck ($K_2Cr_2O_7$, ACS reagent, $\geq$99.0%), sulfuric acid ($H_2SO_4$, Sigma Aldrich, 96%), silver sulfate provided by Merck ($Ag_2SO_4$, ACS reagent, $\geq$99.5%), and mercuric sulfate purchased from Merck ($HgSO_4$, ACS reagent, $\geq$99%) were used for the COD analysis.

The RHWW sample was directly taken from the effluent of the local hospital in Tumaco-Colombia. The RHWW corresponded to the recollection of the effluent during one typical day of the hospital operation. The sample was preserved at 4°C until the treatment application. The hospital in Tumaco-Colombia has both medical (i.e., ambulatory services e.g., diagnosis), emergency and first aids section, operations section, intensive care unit, hospitalization area, and clinic laboratory) and non-medical sections (i.e., toilets, kitchens, and laundries) (Municipio de Tumaco, 2018). It serves an average population of ~200000 habitants. The hospital is a small size institution (i.e., it has 122 beds); thus, this has an effluent flow < 200 $m^3$ $day^{-1}$ (Paola Verlicchi et al., 2010).

Pharmaceutical reference standards for LC-MS/MS analysis of the RHWW were acquired from Sigma-Aldrich. More details on reagents and chemicals used in the analysis can be found in

(Botero-Coy, Martínez-Pachón, Boix, Rincón, Castillo, Arias-Marín, Manrique-Losada, Torres-Palma, Moncayo-Lasso, & Hernández, 2018).

### 2.2.2. Analytical methods

COD was determined according to Standard Methods for Examination of Water and Wastewater 5220 (closed reflux procedure using a Velp Thermo-reactor and measuring the absorbance in a Mettler-Toledo UV5 spectrophotometer), (Efraim A. Serna-Galvis et al., 2015). Total solids were determined by applying the Standard Methods 2540 B, a well-mixed sample (40 mL) was evaporated in a weighed dish and dried to constant weight in a stove (1Dies, MOD.D-53) at 104°C. The pH was directly measured using a pH93 pH-meter. Conductivity was determined by direct measurement using a Lab945 SI Analytics conductimeter (Efraím A. Serna-Galvis et al., 2019a).

The quantification of the target pharmaceuticals in the considered RHWW was performed by liquid chromatography coupled to tandem mass spectrometry with triple quadrupole analyzer, injecting 100 μL in the UHPLC-MS/MS (Waters Acquity UPLC system interfaced to a triple quadrupole mass spectrometer Xevo TQS (Waters) equipped with an orthogonal Z-spray electrospray ionization interface (ESI) operated in positive mode). Chromatographic separation was performed using an Acquity UPLC BEH C18 column (1.7 μm, 100 mm x 2.1 mm), with a gradient mobile phase $H_2O$/MeOH, both 0.01% HCOOH and 1mM $NH_4Ac$, at a flow rate 0.4 mL min$^{-1}$ (Botero-Coy, Martínez-Pachón, Boix, Rincón, Castillo, Arias-Marín, Manrique-Losada, Torres-Palma, Moncayo-Lasso, & Hernández, 2018).

### 2.3. Results and discussion

### 2.3.1. Macro-components of the hospital wastewater

Table 2 presents the macro-parameters of the utilized RHWW. The considered sample contained moderate COD ~254 mg L$^{-1}$. The main contributions to this COD value can be associated with the organic macro-components (e.g., substances from toilets, kitchens, and laundry activities) (Carraro et al., 2016; P. Verlicchi et al., 2010). Besides, the HWW from Tumaco-Colombia had similar values of COD and pH as reported for hospital wastewaters from Brazil, France, and Indonesia

(Carraro et al., 2016; Emmanuel et al., 2005). Also, it can be noted that the conductivity and solids

content agree with the values for typical hospital wastewater (see Table 3).

**Table 2.** Macro-components in the RHWW from Tumaco-Colombia (14th April 2019).

| Parameters | RHWW |
|---|---|
| pH | 6.79 |
| Conductivity (uS cm$^{-1}$) | 379.30 |
| Total solids (mg L$^{-1}$) | 272.50 |
| COD (mg L$^{-1}$) | 253.57 |

**Table 3.** Average range of macro-parameters of typical hospital wastewater (THWW)*.

| Parameters | THWW |
|---|---|
| pH | 6.3-9.2 |
| Conductivity (μS cm$^{-1}$) | 297-1000 |
| Total solids (mg L$^{-1}$) | 150-160 |
| COD (mg L$^{-1}$) | 120-500 |

*Data from Verlicchi et al. (Paola Verlicchi et al., 2012);  Kumari et al. (15)

### 2.3.2.  Selection of the target pharmaceuticals, and their presence in the RHWW
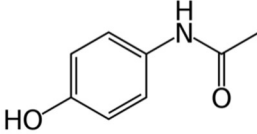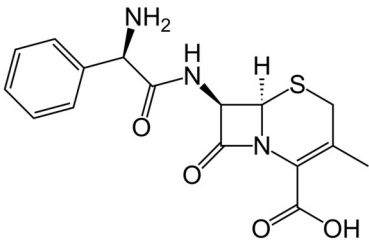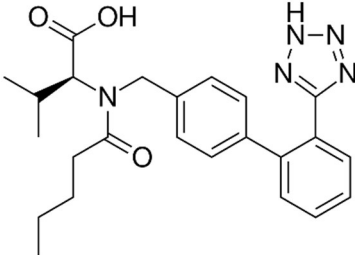
In Colombia, acetaminophen is highly consumed; consequently, high concentrations of this analgesic and antipyretic compound have been reported in hospital wastewater, raw municipal wastewater, and effluents of municipal wastewater treatment plants (Botero-Coy, Martínez-Pachón, Boix, Rincón, Castillo, Arias-Marín, Manrique-Losada, Torres-Palma, Moncayo-Lasso, & Hernandez, 2018; Efraim A. Serna-Galvis et al., 2019; Efraím A. Serna-Galvis et al., 2019a). For these reasons, acetaminophen (also known as paracetamol) was selected as one of our target pharmaceuticals.

Cephalosporins belong to the most consumed antibiotics in Latin-American countries (Wirtz et al., 2013). Indeed, cephalexin (a representative cephalosporin) is widely prescribed in hospitals (López & Garay, 2016) and free-sold in the drug stores in Colombia (Álvarez et al., 2012; Machado-Alba & González-Santos, 2009; Peña, 2015). Additionally, cephalexin is also used in veterinary contexts (García, 2010). Thereby, this antibiotic was also chosen to perform the present research.

On the other hand, sartan-type pharmaceuticals such as valsartan are among the most worldwide consumed antihypertensives. For example, ~9 million valsartan prescriptions were done in the USA during 2017 (ClinClac, 2018; Martínez-Pachón et al., 2021). Indeed, valsartan has been found in hospital wastewater and effluents of municipal wastewater treatment plants in Colombia (Botero-Coy, Martínez-Pachón, Boix, Rincón, Castillo, Arias-Marín, Manrique-Losada, Torres-Palma, Moncayo-Lasso, & Hernandez, 2018; Efraim A. Serna-Galvis et al., 2019; Efraím A. Serna-Galvis et al., 2019a). Furthermore, this antihypertensive is easily bio-transformed into valsartan acid. Valsartan-acid is a very mobile compound and represents a risk in the environment because of its persistent nature (Berkner & Thierbach, 2014; Nödler et al., 2013). Hence, valsartan was the third target pharmaceutical to be considered in this work.

**Table 4.** Chemical structure and pKa of the selected pharmaceuticals.

| Pharmaceuticals | Chemical structure | pKa |
|---|---|---|
| Acetaminophen | | 9.4 (pKa) |

| | | |
|---|---|---|
| Cephalexin | | 3.45 (pKa1)<br>7.44 (pKa2) |
| Valsartan | | 4.7 (pKa) |

It is important to mention that acetaminophen, cephalexin, and valsartan have different chemical structures (Table 4), and they provide a wide variety of functional groups, which make them representative pharmaceuticals. Besides, the target pharmaceuticals were quantified in the RHWW from Tumaco (Table 5). We can note that acetaminophen was found at the typical levels of this analgesic in hospital wastewater around the world, which is ranged from 10 to 1000 $\mu g\ L^{-1}$ (P. Verlicchi et al., 2010). Likewise, valsartan was at levels close to the reported for hospital wastewaters in Spain (0.05-0.11 $\mu g\ L^{-1}$), (Mir-Tutusaus et al., 2017). Despite, cephalexin was not measured in the considered HWW (probably due to this antibiotic could experience hydrolysis, which limits its detection), it must be mentioned that this antibiotic is reported in effluents of wastewater treatment plants in Hong Kong at the range of 0.18-4.00 $\mu g\ L^{-1}$ (Al-Riyami et al., 2018), therefore it was selected as the target contaminant.

**Table 5.** Target pharmaceuticals in the RHWW from Tumaco-Colombia (April 14th, 2019).

| Compound | Concentration in RHWW ($\mu g\ L^{-1}$) |
|---|---|
| Acetaminophen | 118.02 |

| | |
|---|---|
| Cephalexin | Not measured |
| Valsartan | 0.02 |

## 2.4. Conclusions

The macroparameters of the considered RHWW were according to the typical values for these matrices around the world. Due to the structural variety, high consumption, and presence in wastewater, acetaminophen, cephalexin, and valsartan were chosen as the target pharmaceuticals. Indeed, acetaminophen and valsartan were already measured at µg $L^{-1}$ levels in the RHWW.

## CHAPTER III

## BIOCHAR FROM PALM FIBER WASTES AS AN ACTIVATING AGENT OF DIFFERENT OXIDANTS FOR THE ELIMINATION OF PHARMACEUTICALS IN HWW

### 3.1. Introduction

This chapter begins by depicting the main characteristic of the biochar (BP, obtained from oil palm fiber wastes) as adsorbent, followed by an evaluation of the activation properties of the biochar (i.e., carbocatalysis). Then, the evaluation of the effect of pH, PMS, and biochar concentration, and its optimization/validation, followed by the study of the oxidative pathways are presented. At the end of the chapter, it is detailed the reusability of the biochar, matrix effect during the process, and the extension of treatment. It should be mentioned that to understand fundamental aspects of the carbocatalytic process, the initial experiments were carried out in distilled water. Subsequently, both simulated and actual hospital wastewater were used.

### 3.2 Materials and methods

### 3.2.1.  Preparation of the Biochar

Oil palm fiber (an agro-industrial waste from Meta, Colombia) was used to prepare the adsorbent material (biochar). The palm fiber was impregnated with $ZnCl_2$ (3 mol $L^{-1}$, extra pure grade, Duksan) and stirred at 200 rpm for 24 h.  Subsequently, it was heated at 5°C $min^{-1}$ up to the desired activation temperature (550 °C), which was kept for 30 min. After activation, the material was rinsed with HCl (2 mol $L^{-1}$, Merck, 57%) and stirred at 150 rpm for 3 h to remove the excess of $ZnCl_2$ and other impurities. Then, the carbonaceous material was washed with distilled water until neutral pH (pH 6.8–7.0), followed by drying at 105 °C for 24 h. Finally, the material was milled and sieved to obtain a uniform size between 0.1 and 37 μm.

### 3.2.2. Reagents

Acetaminophen (ACE, $C_8H_9NO_2$, Bellchem, purity >99%), cephalexin (CPX, $C_{16}H_{17}N_3O_4S$, Syntofarma, purity >99%) and valsartan (VAL, $C_{24}H_{29}N_5O_3$, MK®, 160 mg/capsule) were the used pharmaceuticals. Oxone® ($2KHSO_5 \cdot KHSO_4 \cdot K_2SO_4$) from Sigma-Aldrich® was used as the source of PMS; in addition, hydrogen peroxide ($H_2O_2$, 30% w/w, Merck), and sodium persulfate ($Na_2S_2O_8$, Panreac) were also tested as oxidants. Formic acid from Carlo Erba was also used. Methanol ($CH_3OH$, Sigma-Aldrich, ACS, 99.9%), Tert-butyl alcohol (($CH_3$)$_3COH$, Merck, ACS reagent, ≥99.0%), p-Benzoquinone ($C_6H_4(=O)_2$, Merck, reagent grade, ≥98%), and Furfuryl alcohol ($C_5H_6O_2$, Merck, 98%) were used as scavengers. For chromatographic analyses, ultrapure water obtained from a Millipore Milli-Q® system was used. All solutions of the pharmaceuticals were prepared using distilled water. The concentrations of the target pharmaceuticals were chosen according to the experience acquired in previous works by the GIRAB research team, and considering the LOQ for the HPLC methods utilized to follow the evolution of pharmaceuticals during the treatments.

### 3.2.3. Reaction system

The experiments were performed in a batch system, which consisted of an aqueous sample (100 mL) of each pharmaceutical (CPX, VAL, or ACE), the addition of the BP in the absence or presence of the oxidants (i.e., $H_2O_2$, PMS or PDS), using a beaker under constant stirring at 200 rpm. The target pharmaceuticals were treated individually. Figure 2 shows a scheme of the reaction system.
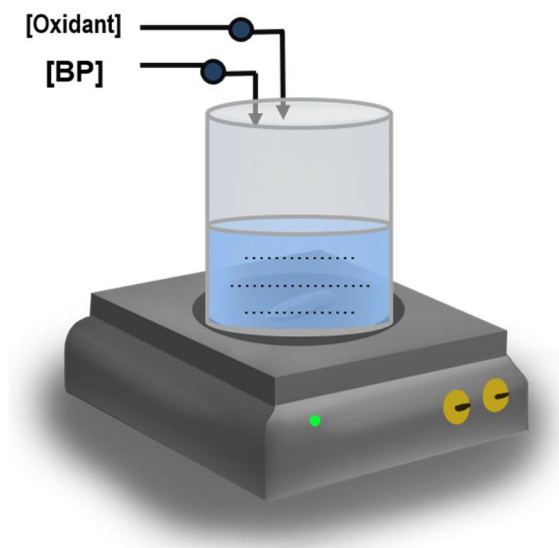
**Figure 2.** Scheme of the reaction system for carbocatalysis.

### 3.2.4. Analytical determinations

The concentration of the pharmaceuticals was determined using a UHPLC Thermo Scientific Dionex UltiMate 3000 instrument equipped with an Acclaim™ 120 RP C18 column (5 μm, 4.6 x 150 mm) and a diode array detector. The injection volume was 20 μL, and mixtures of formic acid (10 mmol L-1, pH 3.0)/acetonitrile were used as mobile phase. Table 6 summarizes the chromatographic conditions used for the tested pharmaceuticals. At different times, samples were extracted and filtered with 0.2 μm mixed cellulose ester filters. Samples for HPLC analyses were quenched with methanol. Removal percentage (RP) was calculated with Eq. (4). Here, $C_0$ and $C_t$ represent the concentration of the initial sample (t = 0 min) and at any t instant (t > 0), respectively.

$$RP = \left(\frac{C_0 - C_t}{C_0}\right) * 100 \qquad\qquad \text{Eq. (4)}$$

**Table 6.** Chromatographic conditions the pharmaceutical compounds quantification.

| Pharmaceutical compounds | Wavelengths of detection (nm) | Mobile phase methanol/formic acid/acetonitrile (% v/v/v) | Flow in isocratic mode (mL min-1) |
|---|---|---|---|
| Acetaminophen | 243 | 0/85/15 | 0.45 |

| Cephalexin | 254 | 0/80/20 | 0.5 |
| Valsartan | 254 | 10/44/46 | 1 |

To characterize the adsorption of the pharmaceuticals on the BP, infrared analyses and computational calculations were carried out. Infrared analyses were performed using a Spectrum Two (PerkinElmer, Waltham, Massachusetts, USA) with Fourier transform and attenuated total reflectance (ATR-FTIR). Also, theoretical calculations were used to analyze the most favorable interactions between the prepared biochar (BP) and the pharmaceuticals. A 20-membered carbon ring was employed to represent typical carbonaceous materials, according to comprehensive consideration of computational cost and accuracy. All the calculations were performed with the Gaussian09 software package (*Gaussian 09, R. A. 0. et al. Gaussian 09, Revision A.01*) using the DFT-B3LYP method and a set of 6–31+g (d, p) bases, which have been widely used for the study of these systems (H. Wang et al., 2019; Yao et al., 2020). Geometry optimization calculations were conducted by taking into account the solvent effect, which considers long-range implicit hydration by applying the integral equation formalism variant of the polarized continuum model (IEFPCM) (Keith & Frisch, 1994).

### 3.2.5. Synergy evaluation

The synergy (S) for the combination of BP with, $H_2O_2$, PMS, or PDS was quantified as the normalized difference between the removal percentage obtained under the combined process ($P_{combined}$) and the sum of those obtained under the application of the individual processes ($P_i$) as shown in Eq. (5). A positive value stands for synergistic effect, a negative value for an antagonistic effect, and zero stands for a simpler cumulative effect (Dewil et al., 2017).

$$S = \frac{P_{combined} - \sum_1^n P_i}{P_{combined}} \qquad \text{Eq. (5)}$$

### 3.2.6. Experimental design

A Box-Behnken experimental design was used to determine the effect of concentrations of oxidizing agent ($X_1$), BP dose ($X_2$), and pH ($X_3$) on the removal percentage. This design and selection of the best operational conditions were made with a free trial version of Design-Expert® (Stat-Ease, Inc.). The model quality was assessed by means of variance analysis (ANOVA), $r^2$, and

adjusted $r^2$ ($r^2$Adj) (Myers, RH.; Mongotmery, DC.; Anderson, 1997). The objective of the process was to attain 90% of the removal of pharmaceuticals. The Design-Expert optimization module was used to select the combination of variables that will allow a reduction in reagent consumption and warrant the objective of the treatment. A detailed description of the methodology used in the experimental design, statistical analysis, and selection of the best operational condition can be found in the software user's manual of Design- Expert® V10.

### 3.2.7.   Determination of degradation routes

Quenching experiments were used to identify the contribution of reactive oxygen species (ROS) produced during oxidative degradation of the pollutants by carbocatalysis. These studies are developed to establish the oxidation pathway and the mechanism of the BP-PMS system. Methanol (MeOH) was used as a quencher of sulfate and hydroxyl radicals, tert-butyl alcohol (TBA) as a quencher of hydroxyl radical, while furfuryl alcohol (FFA) and benzoquinone (BQ) were used as quenchers of singlet oxygen and superoxide radical, respectively (Bielski et al., 1985; Chen et al., 2018).

### 3.2.8.   Matrix effects

In this study, we evaluated the carbocatalytic process selected using simulated hospital wastewater (SHWW) and real hospital wastewater (i.e., RHWW) to identify the role of the matrix effect on the system. The global chemical composition and characteristics of simulated hospital wastewater can be seen in Table 7, while the chemical characteristics of real hospital wastewater can be seen in Table 3.

**Table 7.** Composition of the simulated hospital wastewater (SHWW).

| Component | Concentration ($\mu mol\ L^{-1}$) |
|---|---|
| NaCl | 51300 |
| $NH_4Cl$ | 940 |
| $Na_2SO_4$ | 710 |
| KCl | 1340 |
| $KH_2PO_4$ | 370 |

| | |
|---|---|
| $CaCl_2*2H_2O$ | 340 |
| Urea | 21000 |
| pH | 6,5 |

### 3.2.9. Treatment extent-Phytotoxicity

Phytotoxicity assays were performed using commercial seeds of lettuce (*Lactuca sativa*), taking as reference the germination index (G.I.). The number of germinated seeds in the analyzed sample (NGS) and their control (NGC), and the average length of roots for the sample (LRS) and the control (LRC) were used to determine the G.I. as indicated in Eq. (6). A seed was considered as germinated when the length of the root exceeded 5 mm (Belalcázar-Saldarriaga et al., 2018b; Libralato et al., 2016).

$$G.\, I.\, (\%) = \left(\frac{N_{GS}}{N_{GC}}\right) x \left(\frac{L_{RS}}{L_{RC}}\right) x 100 \qquad\qquad Eq.\ (6)$$

To determine the phytotoxic effect, the sample (5mL) previously filtered (pH $7.0 \pm 0.2$) was added to a Petri dish containing 20 seeds supported on a Whatman No. 1 filter paper. For control texts, 5 mL of distilled water at pH $7.0 \pm 0.2$ were utilized. Phytotoxicity assays were performed in absence of solar radiation at a constant temperature, following the methodology reported by Libralato et al (Libralato et al., 2016).

### 3.3. Results and discussion

### 3.3.1. Adsorption of pharmaceuticals in distilled water on the biochar

The adsorption capability of the biochar (BP, whose main physical-chemical characteristics has been already reported (Grisales-Cifuentes et al., 2021) (see Table 8) to remove the target pharmaceuticals from distilled water, was tested initially. The initial biochar concentration was chosen according to the experience acquired in previous works by the GIRAB research group, and after the verification of the carbocatalytic activity of BP, an experimental design was employed to determine the optimal concentration of the reagents involved in the process (see section 3.3.3).

**Table 8**. Main characteristics of the carbonaceous material prepared from palm fiber.

| N₂ Physisorption | | | | | | |
|---|---|---|---|---|---|---|
| *$S_{BET}$ $(m^2 g^{-1})$ | $S_{\mu p}$ $(m^2 g^{-1})$ | $S_{EXT}$ $(m^2 g^{-1})$ | $V_{\mu p}$ $(cm^3 g^{-1})$ | $V_{EXT}$ $(cm^3 g^{-1})$ | $V_{TP}$ $(cm^3 g^{-1})$ | $D_{AP}$ (nm) |
| 76.050 | 62.564 | 113.486 | 0.0359 | 0.0797 | 0.1156 | 6.1 |

| Elemental analysis (%) | | | | |
|---|---|---|---|---|
| N | C | H | O | S |
| 0.60 | 78.00 | 2.20 | 18.10 | 0.60 |

| Functional groups (mmol/g) | | |
|---|---|---|
| Phenolic | Lactonic | Carboxylic |
| 0.233 ±0.031 | 0.092 ± 0.018 | 1.343 ± 0.012 |

| FTIR | |
|---|---|
| **Main signals** $(cm^{-1})$ | 3300, 2950, 1700, 1510 and 1400-1000 |

*Specific surface area ($S_{BET}$), micropores surface area ($S_{\mu p}$), external surface area ($S_{EXT}$), volume of the micropores ($V_{\mu p}$), external volume ($V_{EXT}$), the total pore volume ($V_{TP}$), average pore diameter ($D_{AP}$).

Fig. 3 shows the adsorption curves and the control experiments without the biochar (black lines in this figure) and indicated that the pollutants were not removed by hydrolysis, and adsorption phenomena are involved in the interaction with the biochar in absence of the oxidants.

From Fig. 3, it can be noted that valsartan (VAL) and cephalexin (CPX) followed a similar trend, leading to removals of ~30% during the first 15 min of treatment and after this time the adsorption equilibrium is achieved. Meanwhile, acetaminophen (ACE) exhibited higher adsorption in 15 min (~50%) and reached its equilibrium at 30 min of treatment. To explain these adsorption results, the pKa values of the selected pollutants were considered (Table 4). The predominant forms of the substances depend on the pH of the aqueous solution. Thus, as the experimental pH was 5.5, under these work conditions, acetaminophen (ACE, pKa=9.4) is in its neutral form. In turn, valsartan (VAL, pKa=4.7) and cephalexin (CPX, pKa=3.45 and 7.44) are in their anion and zwitterionic forms, respectively. At the same time, as the biochar has a PZC of 4.1, this has a predominance of

negative superficial charges at the working pH. Therefore, due to the presence of negative charges on the structures of VAL and CPX, they may experiment some electrostatic repulsion by the carbonaceous material (Bangari & Sinha, 2019; Paredes-Laverde et al., 2018). Consequently, VAL and CPX have lower adsorption than ACE on the biochar.

The three pharmaceuticals have diverse functional groups (Table 4). The antihypertensive valsartan possesses a biphenyl, a tetrazole ring, an amide, and a carboxylic acid. The analgesic acetaminophen is made of an acetamide plus phenol. Meanwhile, the antibiotic cephalexin has a central β-lactam bonded to a cyclic thioether and an amide; cephalexin also contains an amine, a benzene ring, and a carboxylic acid.
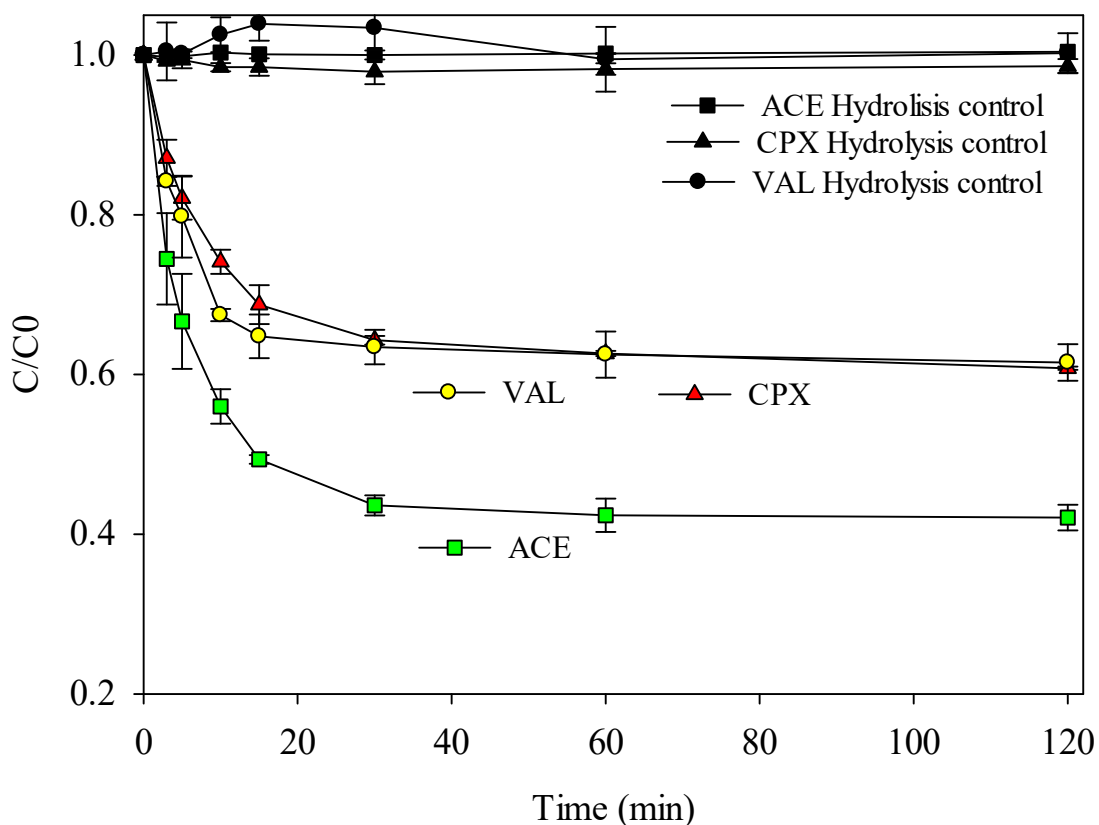


**Figure 3.** Adsorption of acetaminophen (ACE), cephalexin (CPX), and valsartan (VAL) at natural pH (5.5) using the biochar from palm fiber. Experimental conditions: V=100 mL; $C_{CPX}=C_{ACE}=C_{VAL}=16$ μM; $C_{Biochar} = 1 gL^{-1}$; pH =5.5±0.2; temperature=25°C.

The interaction with the functional groups on the pharmaceuticals plays an important role in the adsorption process. Hence, to study the interactions during the adsorption of the considered pharmaceuticals, FT-IR analyses of the BP before and after the adsorption process were performed (Fig. 4). The comparison between the spectra of the adsorbent material before and after the adsorption process indicated that the band at 3000-3300 $cm^{-1}$ modifies its form and intensity, which suggests that -OH groups on the BP (e.g., phenolic or carboxylic moieties) can form hydrogen bonds with the free electronic pairs of N, O or S present in the structure of the pharmaceuticals. Furthermore, after adsorptions, there is a modification of intensity of the band at ~1700 $cm^{-1}$, which could be related to interactions of C=O on carboxylic acids and lactones of BP with the phenolic hydrogen of ACE (Paredes-Laverde et al., 2019), or with the carboxylic/carboxylate groups of CPX and VAL. Also, the shoulder at ~1510 $cm^{-1}$, (which is related to the aromatic C=C portion of BP) is more intense in the presence of the target pollutants, suggesting the possibility of π-π interactions between the biochar and the aromatic rings of the considered pharmaceuticals. Additionally, the increase of band intensities in the 1000-1400 $cm^{-1}$ region suggests the interaction of pollutants with the oxygenated moieties on the BP, through alterations of the C–O stretching of acid, alcohol, phenol, ether, and/or ester groups in the adsorbent (Paredes-Laverde et al., 2019).
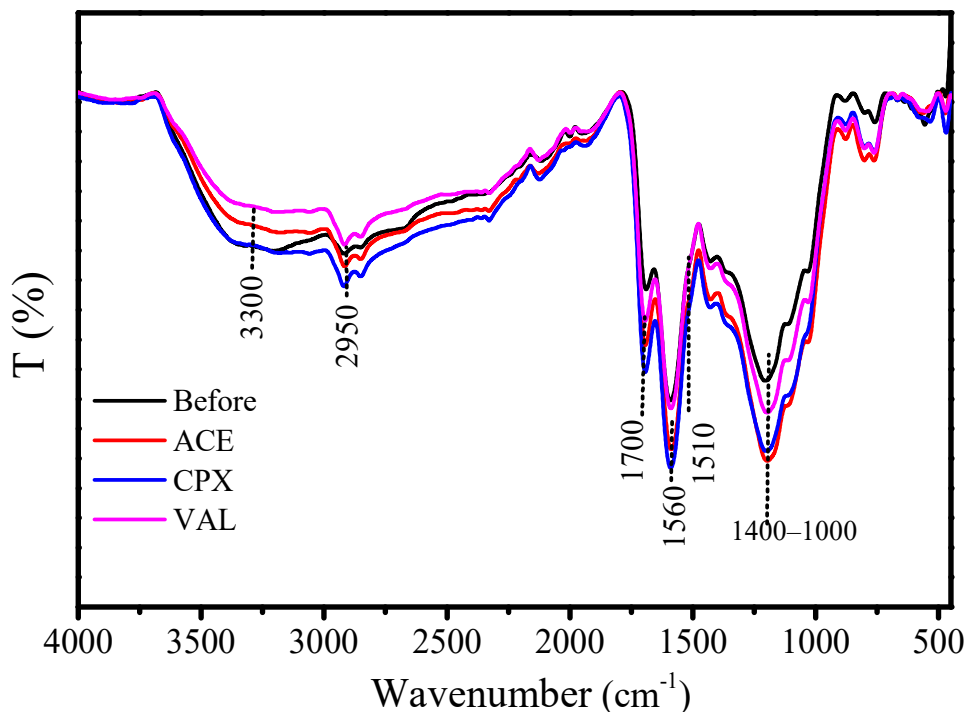
**Figure 4.** FTIR spectra for the BP before (a) and after the adsorption process of (b) VAL (c) CPX (d) ACE. pH= 5.5.

As a strategy to better understand and support the adsorption of each pharmaceutical on the BP, DFT analyses were also carried out. Then, the most favorable interactions between the functional groups on the target pollutants and the BP moieties were determined. Table 8 contains a graphical view of the most favorable interactions. It can be indicated that for ACE, interactions between carboxylate of the BP and phenol and amide on the pharmaceutical are favored. Also, phenolic groups on BP and carbonyl of ACE strongly interact during the adsorption process.

From the computational analysis, it was found that the valsartan molecule has relevant interactions through its carboxylic and carbonyl groups with phenolic parts on the biochar. Furthermore, tetrazole moiety on VAL can also present linkages with carboxylate and ketone groups on the BP (Table 8). In turn, the carboxylic acid, the amine, and the secondary amide of cephalexin exhibit relevant interactions with the ketone groups on the considered biochar. Additionally, the same secondary amide can also interact with the carboxylate on the carbonaceous material strongly.

Most of the above-mentioned interactions are H-bonding-types, which are very common in the adsorption process on carbon-based materials (Paredes-Laverde et al., 2019). Indeed, the computational results are coincident with the FT-IR findings about the interactions of H-bond-type, involving phenol, carbonyl, and carboxyl moieties on the biochar. It must be mentioned that although in our case such interactions predominate, the adsorption of the pharmaceuticals may also involve the simultaneous occurrence of several adsorption mechanisms such as $\pi$-$\pi$ interaction, hydrophobic interaction, electrostatic interaction, and pore-filling, (Peng et al., 2016), which could contribute in a minor degree on the process and then, they cannot be discarded.

It is important to mention that the computational analysis is useful for understanding the individual interactions of the pharmaceuticals with the BP. However, it is necessary to be careful avoiding comparisons among pollutants due to the computational calculations are performed on local effects on the BP-pollutants interactions.

**Table 9**. Graphical views of most favorable interactions between the prepared biochar (BP)
and each pharmaceutical.



| Acetaminophen (ACE) | | |
|---|---|---|
| Carboxylate_OH | Carboxylate_NH | Phenol_CO |

| Valsartan (VAL) | |
|---|---|
| Carboxylate_NH | Phenol_CO |

**Phenol_COO**

**Ketone_NH**

Cephalexin (CPX)

**Carboxylate_HN**

**Ketone_H₂N**

**Ketone_HOOC**

**Ketone_HN**
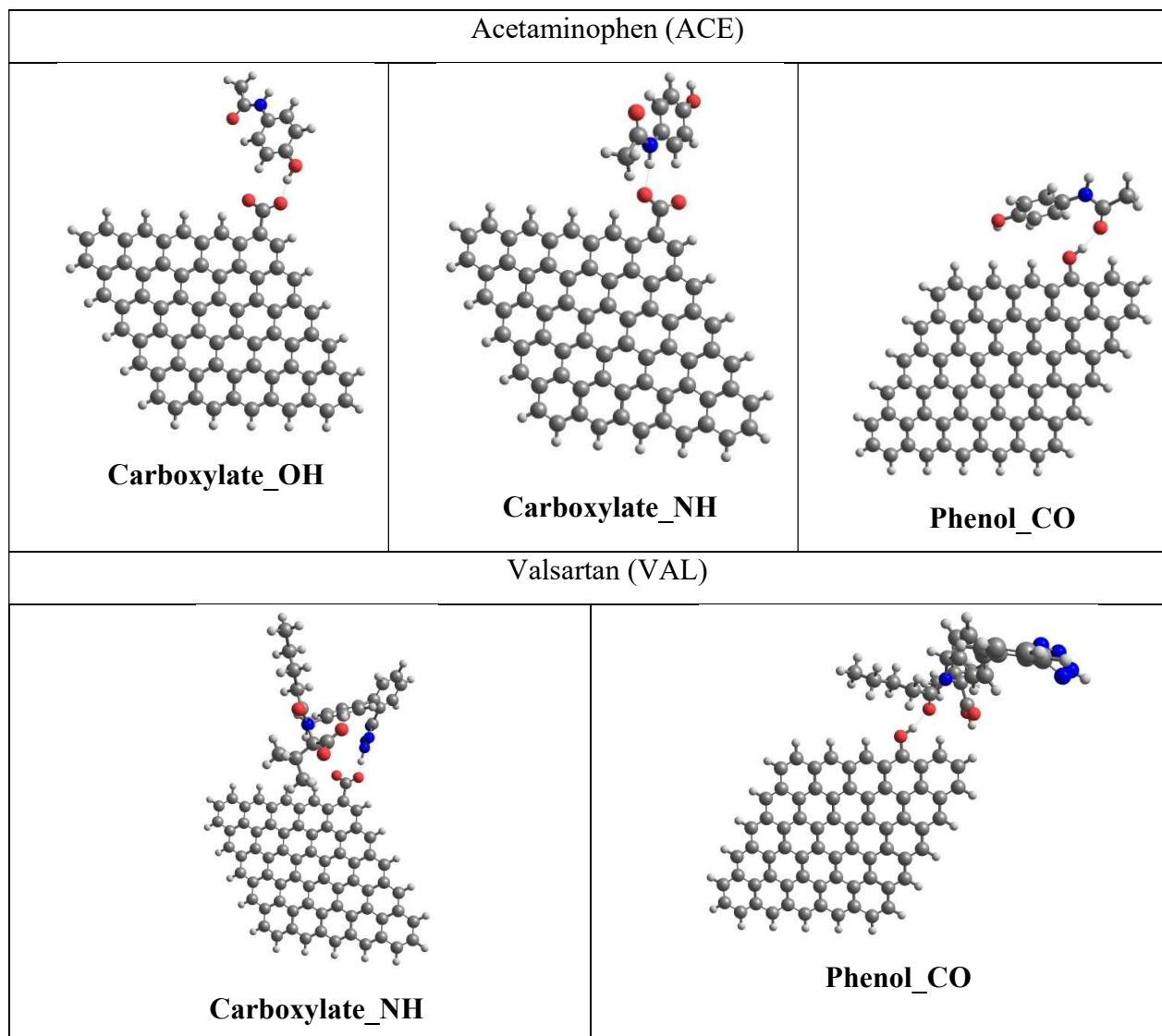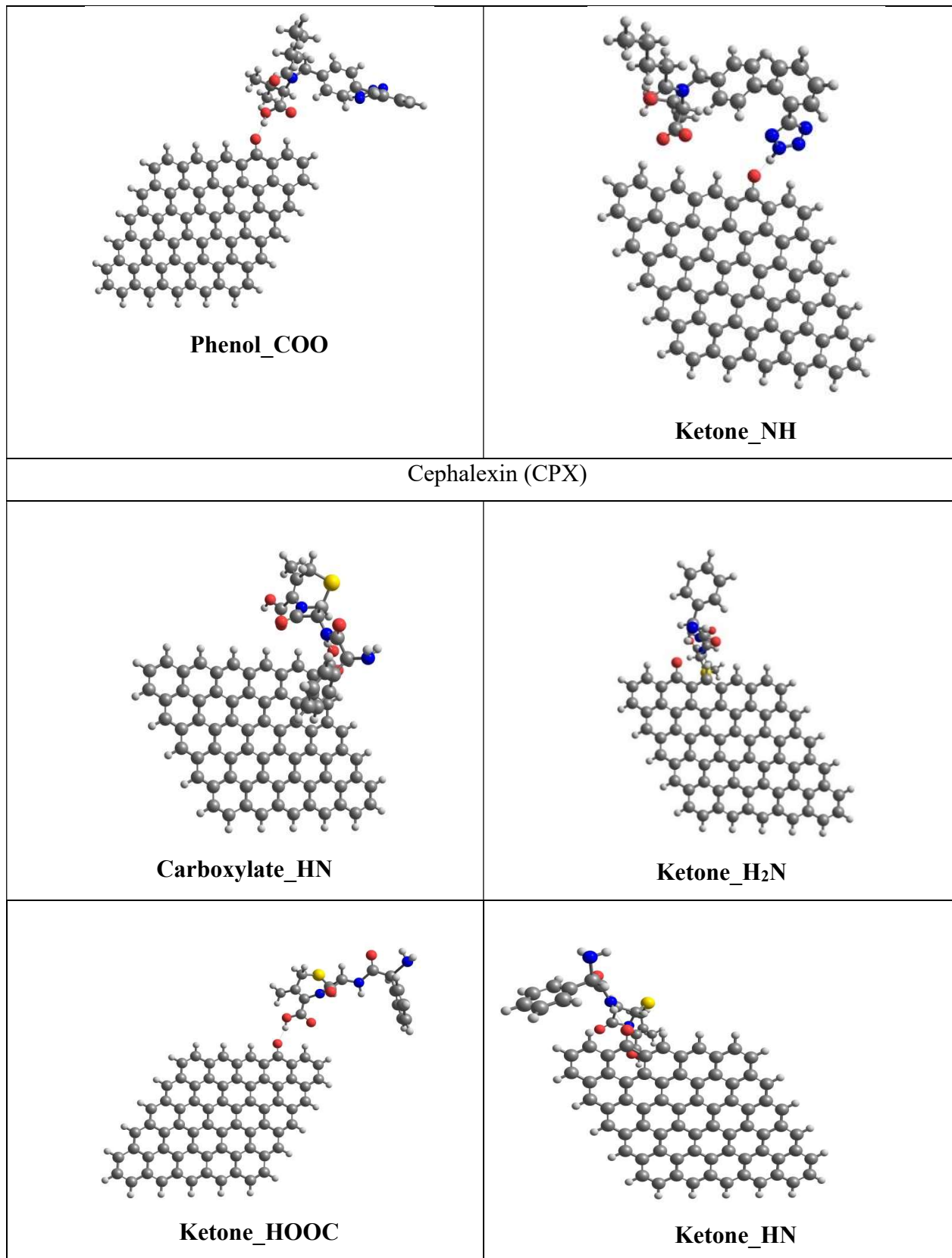
### 3.3.2. Activation properties of the biochar: Effect of the oxidative agent (peroxide, persulfate, and peroxymonosulfate) on the elimination of the pharmaceuticals

After determining the adsorption ability of the BP, the interaction of this carbonaceous material with the three oxidizing agents was studied. Figs. 5-7 show the results for the direct oxidation of $H_2O_2$ (HP), $S_2O_8^{2-}$ (PDS), and $HSO_5^-$ (PMS) and by the combined action of BP and oxidants (carbocatalysis) for CEP, ACE, and VAL removal. It can be noted that after 15 min, the direct action of HP, PDS, and PMS resulted in less than 6% removal for ACE and VAL (Figs. 5 and 7). Only CPX was significantly oxidized by HP, PDS, or PMS (Fig. 6). The highest reactivity of CPX toward the three oxidants can be related to the structural characteristics of this pharmaceutical, which has a reduced form of sulfur (the thioether moiety) in its cephalosporin nucleus, which makes it easier to oxidize by soft oxidizing species such as HP, PDS, or PMS (Bruycker, 2017; Liu et al., 2020a).

For the combination of the BP with the oxidants, the synergy values were calculated (Eq. 5). Fig. 8. Shows the results for each combination, where a positive value of S means a synergistic effect, a negative value of S represents an antagonistic effect, and a zero value stands for an additive effect (Dewil et al., 2017). The results suggested an antagonistic effect by the combination of HP and biochar for the removal of VAL, CPX, and ACE.

In turn, a synergistic effect was obtained by PDS and biochar combination. Also, in the case of PMS synergistic effects were observed. It is important to mention that the biochar can activate PMS or PDS to produce strong degrading agents (e.g., radical species) whose action leads to synergistic effects (Zhao et al., 2021).

The highest synergistic effect was found by combining PMS and BP for the removal of VAL, which, among the studied pharmaceuticals, was the most recalcitrant to the oxidants action and hardly adsorbed on the biochar (see Fig. 7). Therefore, to better understand the catalytic role of the BP, an experimental design was carried out to find the conditions that allow improving the combined system PMS and biochar in the VAL removal, this topic is developed in the next section.
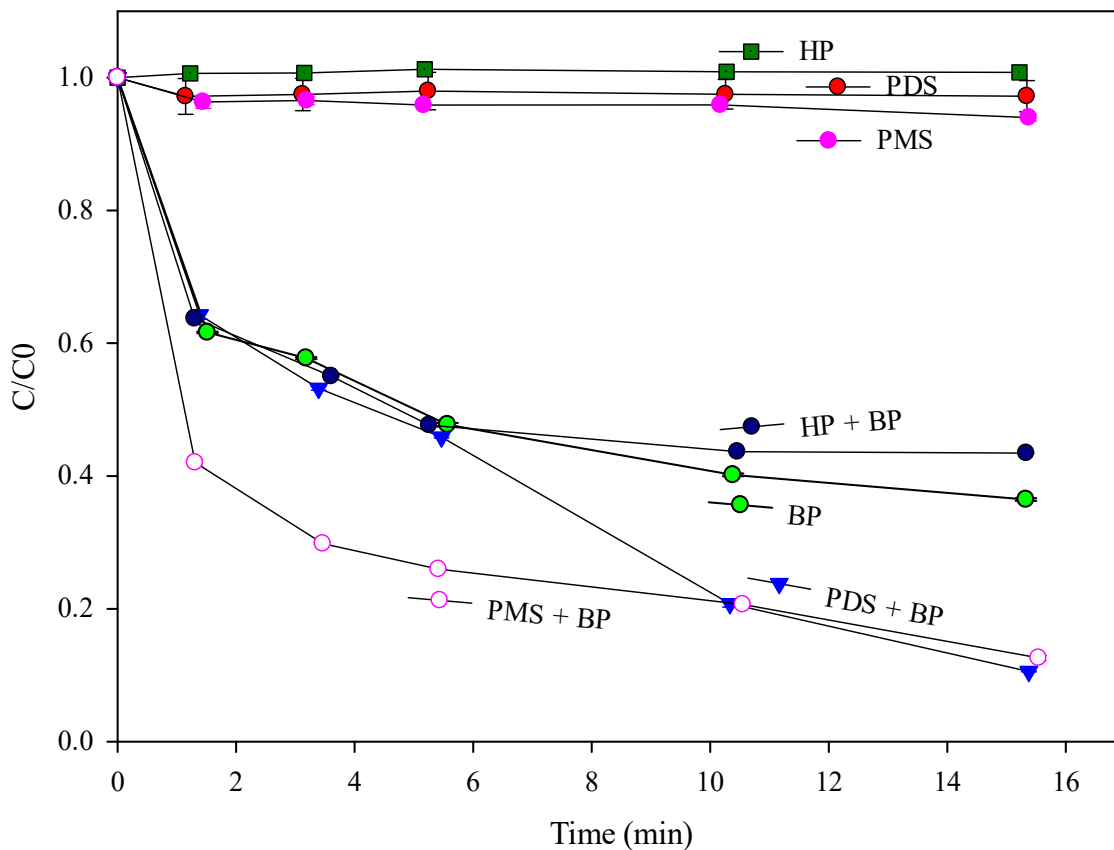
**Figure 5.** Effect of the oxidative agent (HP, PDS, and PMS) on the elimination of the acetaminophen pharmaceutics in water. Experimental conditions: V=100 mL; $C_{ACE}$= 16 μM; $C_{BP}$ = 1g L$^{-1}$; pH =5.5±0.2; temperature=25°C.
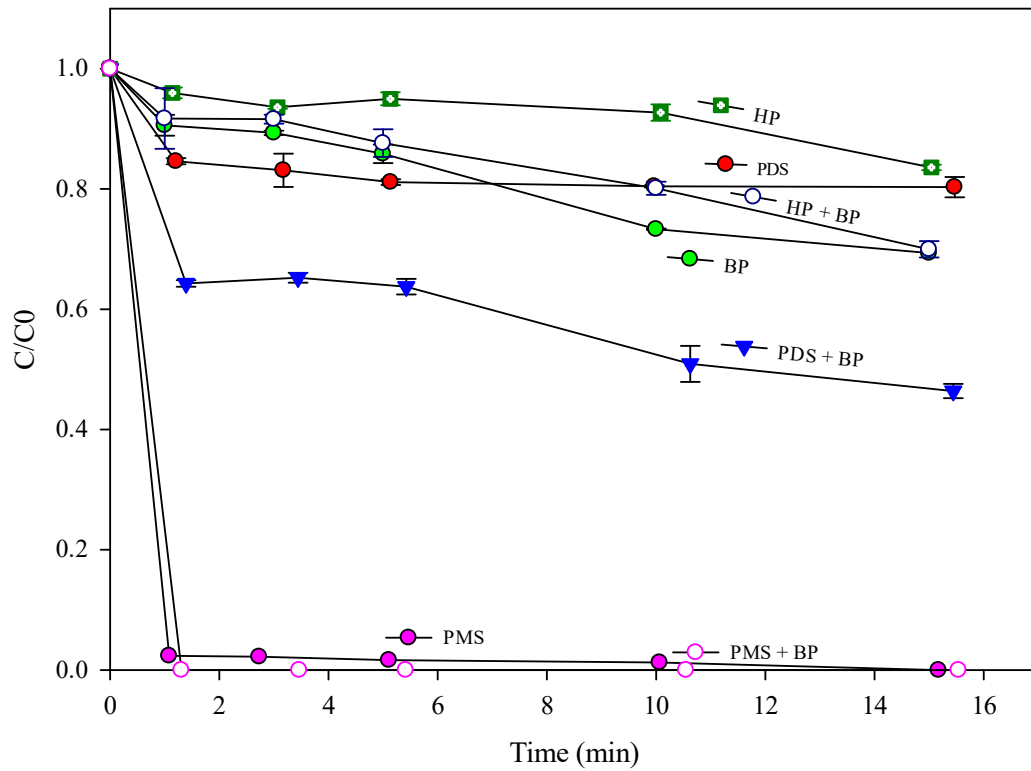
**Figure 6**. Effect of the oxidative agent (HP, PDS, and PMS) on the elimination of the cephalexin
in water. Experimental conditions: V=100 mL; $C_{CPx}$=16 μM; $C_{BP}$ = 1g $L^{-1}$; pH =5.5±0.2;
temperature=25°C.
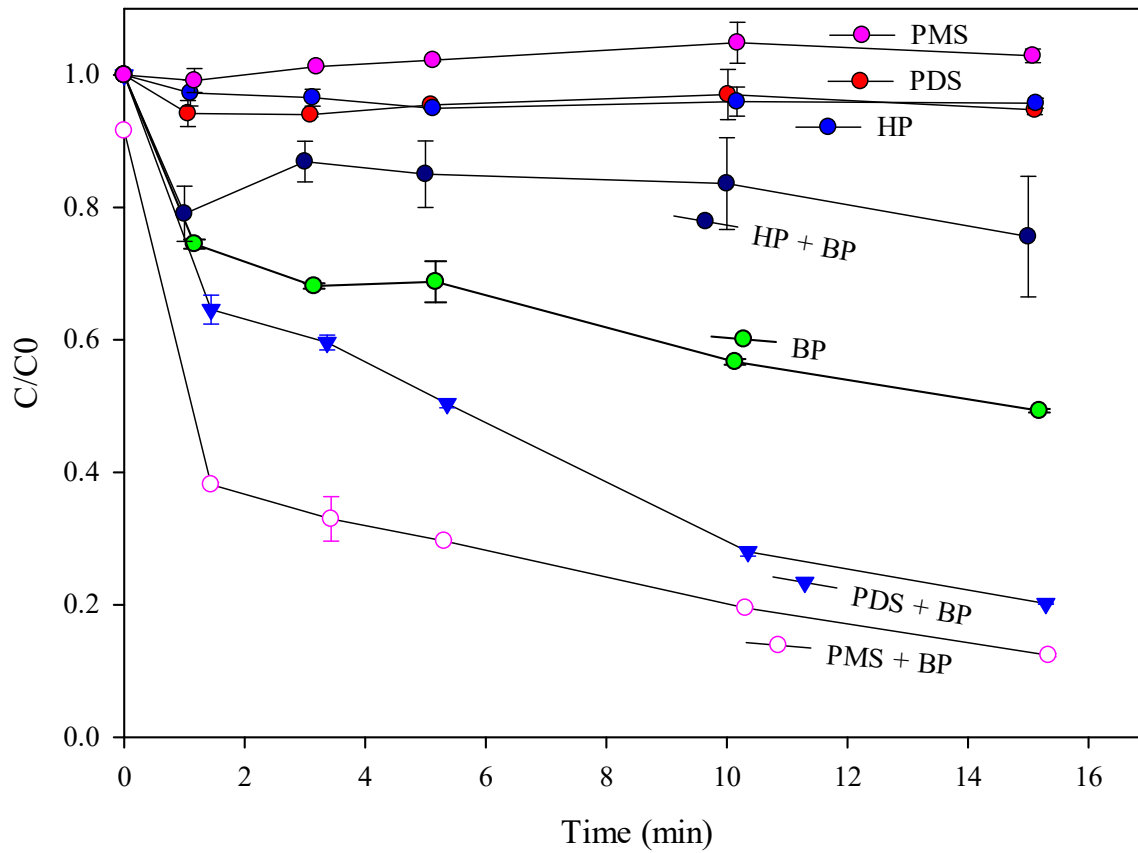
**Figure 7.** Effect of the oxidative agent (HP, PDS, and PMS) on the elimination of the valsartan in water. Experimental conditions: V=100 mL; $C_{VAL}$=16 μM; $C_{BP}$ = 1g $L^{-1}$; pH =5.5±0.2; temperature=25°C.
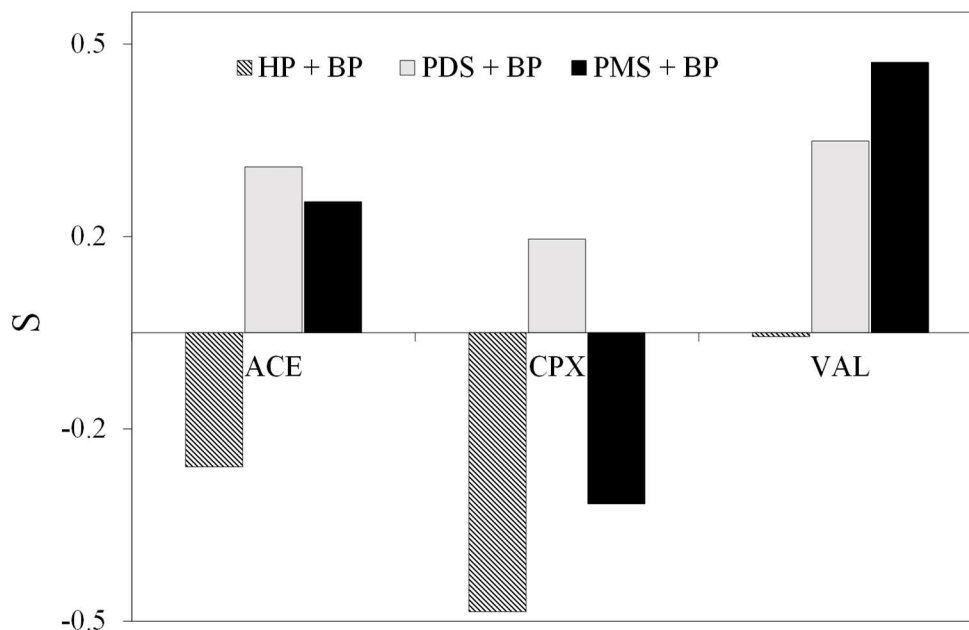
**Figure 8.** Sinergy results of the combination of different oxidizing agents with biochar.

### 3.3.3. Effect of pH, PMS, and biochar concentration on the removal of VAL

An experimental design was performed to examine the effect of three relevant variables, pH, PMS concentration ($C_{PMS}$), and biochar concentration ($C_{BP}$), on the removal of VAL. VAL was selected owing to its highest synergistic elimination (Fig. 8). A Box-Behnken experimental design consisting of 17 experiments (including 5 repetitions of the central point) was carried out. Table 9 depicts the conditions for the set of tests. The range for each variable was as follows: $C_{PMS}$, from 0.02 to 1 mM; $C_{BP}$ from 0.04 to 1.0 g L$^{-1}$; and pH from 3 to 11.

The statistical analysis indicated that a quadratic model (Eq. 7) is adequate to represent the removal of VAL (RP) by means of the BP and PMS combination. F values (F model = 5.29) indicated that the model is significant and that the probability of attributing this value to noise is lower than 0.01%. Values of $r^2$ ($r^2 = 0.87$) and adjusted $r^2$ ($r^2$ adj = 0.72), standard deviation (S.D. = 12.7), and the variation coefficient (V.C. = 20.26%) confirmed that the obtained mathematical model is adequate to represent the removal of VAL Eq. (7).

$$RP\ (\%) =\ 74.4 + 11.16 * PMS + 9.87 * BP - 16.54 * pH + 0.93 * PMS * BP + 5.31 * PMS * pH - 13.94 * BP * pH - 24.74 * PMS^2 - 7.04 * BP^2 + 4.03 * pH^2 \qquad \text{Eq. (7)}$$

**Table 10.** Experimental design set up for the elimination of VAL by the BP and PMS combination.

| Run | PMS (mM) | BP (g L$^{-1}$) | pH |
|-----|----------|-----------------|-----|
| 1 | 0.02 | 0.04 | 7 |
| 2 | 1 | 0.52 | 11 |
| 3 | 0.51 | 0.52 | 7 |
| 4 | 0.51 | 0.52 | 7 |
| 5 | 0.02 | 1 | 7 |
| 6 | 0.51 | 0.04 | 3 |
| 7 | 0.51 | 0.04 | 11 |
| 8 | 0.02 | 0.52 | 11 |
| 9 | 1 | 0.04 | 7 |
| 10 | 0.51 | 0.52 | 7 |
| 11 | 1 | 0.52 | 3 |
| 12 | 0.51 | 1 | 11 |
| 13 | 0.51 | 0.52 | 7 |
| 14 | 0.51 | 0.52 | 7 |
| 15 | 0.51 | 1 | 3 |
| 16 | 0.02 | 0.52 | 3 |
| 17 | 1 | 1 | 7 |

To evaluate the effect of the variables on the process, the response surface analyses from the experimental design were performed (Fig. 9-11). It can be noted that high biochar concentrations

and low pH values have positive effects on the removal of VAL, while PMS dose exerts a positive influence until reaching an optimum concentration; after that, it starts to become negative (Fig. 10 and 11). At pH below PZC, a higher adsorption affinity of VAL (when this pharmaceutical is non-ionized) is expected if compared to pH > PZC (i.e., pH 7.0 and 11). At neutral and basic pH, the electrostatic repulsion between the negative biochar surface and the deprotonated VAL decreases the adsorption process (see Table 10). Indeed, there is a negative influence of increasing pH from 3 to 11, during the process (as observed in Fig. 9 and 10). Also, at the basic pH, the negative charge of biochar surface disfavors the degradation of VAL by the carbocatalytic process because PMS is doubly deprotonated (increasing the repulsion), which limits the interaction between the BP and PMS to generate degrading species. When PMS is in excess, a self-scavenging effect is triggered, in which the target pollutant and PMS compete for the radical species generated (Eq. 8-9) (Solís et al., 2020). Additionally, the sulfur pentoxide radical ($SO_5^{\bullet-}$, $E° = 1.1$ V), species produced from the self-scavenger effect, has an oxidizing power lower than $HO\bullet$ or $SO_4^{\bullet-}$ (Rodríguez-Chueca, Giannakis, et al., 2019). These aspects explain the decrease in the VAL degradation efficiency at high concentrations of PMS.

$$BP + HSO_5^- \rightarrow HO\bullet \text{ or } SO_4^{\bullet-} \hspace{4cm} \text{Eq. (8)}$$

$$HSO_5^- + HO\bullet/SO_4^{\bullet-} \rightarrow SO_5^{\bullet-} + H_2O/HSO_4^- \hspace{3cm} \text{Eq. (9)}$$

**Table 11.** Species at different pH.

| Material | PZC/pKa | Acid (3.0) | Natural (7.0) | Basic (11) |
|----------|---------|------------|---------------|------------|
| **Biochar** | 4.1 (PZC) | **Positive** | **Negative** | **Negative** |
| **Valsartan** | 4.7 (pKa) | **Neutral** | **Negative** | **Negative** |
| **PMS** | 9.4 (pKa) | **Neutral** | **Neutral** | **Negative** |
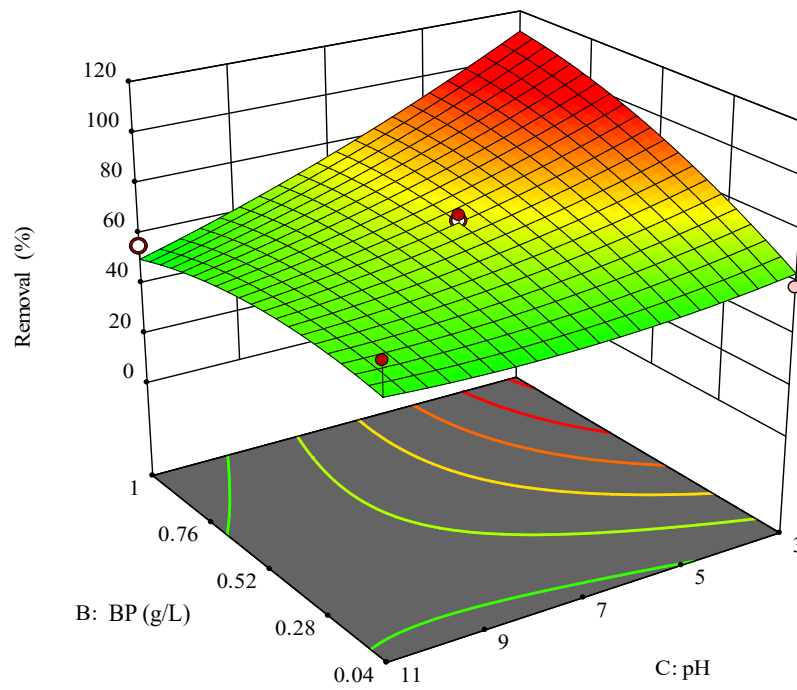
**Figure 9.** Response surface analysis for the degradation of VAL. Variation effect of biochar and pH. Experimental conditions: V=100 mL; $C_{VAL}$=16 μM; $C_{BP}$ values= 0.04- 1gL$^{-1}$;$C_{PMS}$ values= 0.02- 1 mM; pH values=3- 11.
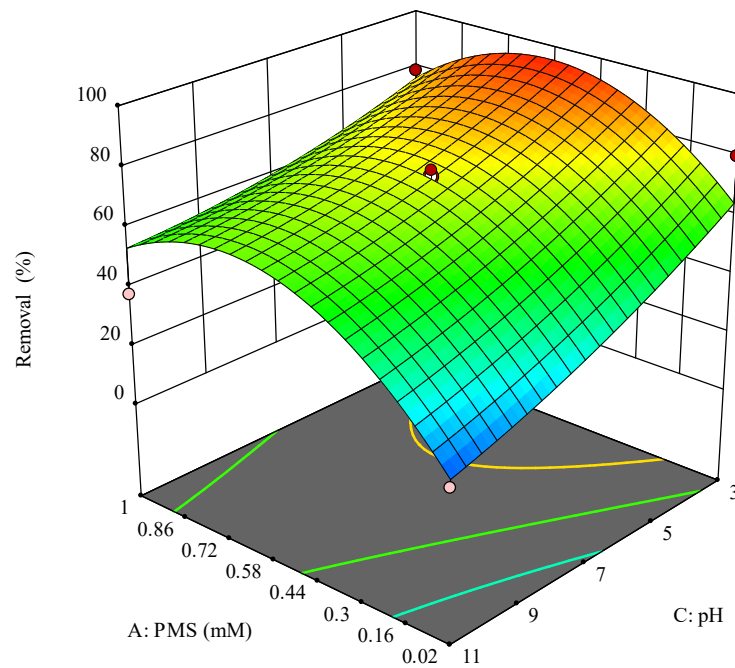
**Figure 10.** Response surface analysis for the degradation of VAL. Variation effect of PMS –

pH. Experimental conditions: V=100 mL; $C_{VAL}$=16μM; $C_{BP}$ values= 0.04- 1gL$^{-1}$;$C_{PMS}$ values=

0.02- 1 mM; pH values=3- 11.
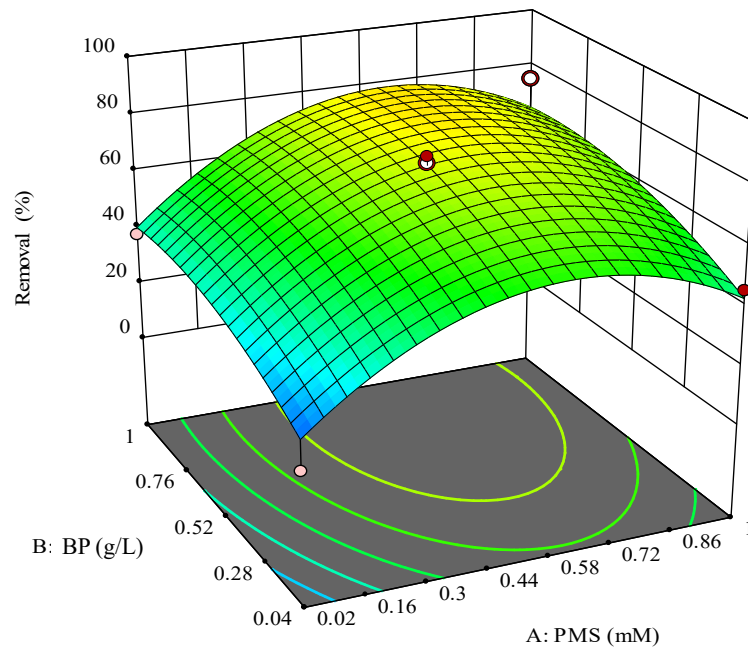
**Figure 11.** Response surface analysis for the degradation of VAL. Variation effect of biochar
– PMS. Experimental conditions: V=100 mL; $C_{VAL}$=16μM; $C_{BP}$ values= 0.04- 1gL$^{-1}$;$C_{PMS}$
values= 0.02- 1 mM; pH values=3- 11.

On the other hand, to achieve an optimal condition based on the experimental design it was
established an objective function while imposing operational restrictions. Thus, it was done an
optimization considering the reduction of the PMS consumption (to reduce both the environmental
impact and cost of treatment, without affecting the removal efficiency of the target pollutant). It
should be mentioned that from an environmental point of view, recent studies have noticed that in
advanced oxidation processes, the consumptions of reagents represent 30 to 90% of the total carbon
footprint of the processes (Belalcázar-Saldarriaga et al., 2018b; Farré et al., 2007; Foteinis,
Monteagudo, et al., 2018; Grisales et al., 2019; Luis Miguel Salazar et al., 2019). It is important to
remember that the used BP was made from palm fiber wastes, which could reduce the inappropriate
management and final disposal of agricultural wastes.

The best operational condition for VAL removal was selected through the Desing-Expert®
software and the concept of global desirability (D) (Myers, RH.; Mongotmery, DC.; Anderson,
1997). Such analyses indicated that 90% of VAL removal can be achieved using the following
experimental conditions: pH = 6.1, PMS= 0.462 mM, and BP = 1 g L$^{-1}$. From these optimal

conditions, two keypoint deserve special attention: the operation at near-neutral pH, and the significant reduction of PMS consumption (~60%) compared with the initial experiments (see Section 3.3.2). Finally, the optimal conditions were validated. As depicted in Figure 12, the combination PMS-BP removed up to 90% in 15 min, effectively.
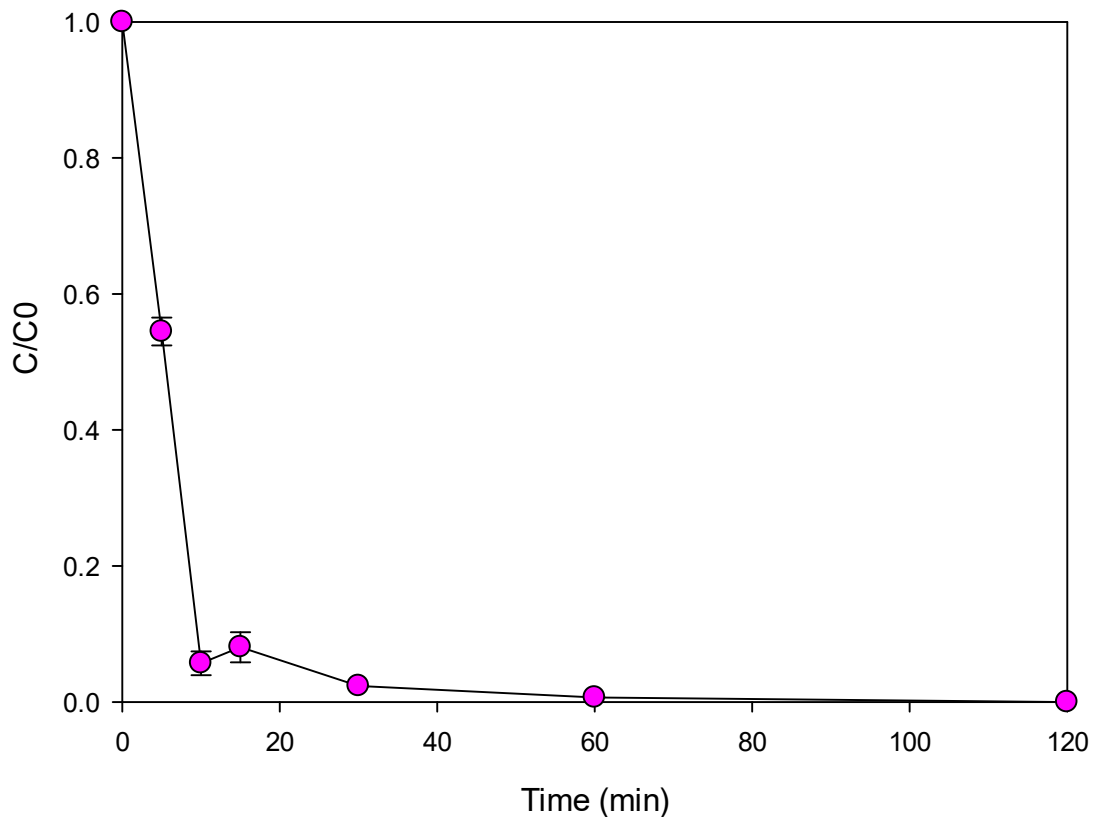


**Figure 12.** Validation of optimal conditions for the removal of VAL using the combination PMS-BP (Carbocatalysis).

### 3.3.4. Study of the oxidative pathways

The mechanism of activation of PMS by carbon-based materials, such as biochars, can involve both radical (e.g. $HO\bullet$, $SO_4\bullet^-$, or $O_2\bullet^-$) and non-radical pathways (e.g. singlet oxygen, $^1O_2$) (Zhao et al., 2021). Then, the participation of both radical and non-radical species in the degradation of VAL by the carbocatalytic process using BP was studied. Quenching tests allowed to identify the activity of reactive oxidative species (ROS) produced during this oxidative process (Mian & Liu, 2020; Jia Wang et al., 2020). In this work, methanol (MeOH), tert-butanol (TBA), furfuryl alcohol (FFA), and benzoquinone (BQ) were used as probe substances for the quenching tests. To better

evidence the phenomenon, the amount of BP was diminished up to 0.2 g L$^{-1}$. MeOH can scavenge SO$_4$•$^-$ ((1.2–2.8) × 10$^9$ M$^{-1}$ s $^{-1}$) and HO• ((1.6–7.7) × 10$^7$ M$^{-1}$ s$^{-1}$) efficiently, and TBA is a powerful scavenger for HO• ((3.8–7.6) × 10$^8$ M$^{-1}$ s$^{-1}$ ) but not that sensitive on SO$_4$•$^-$ ((4.0–9.1) × 10$^5$ M$^{-1}$ s$^{-1}$) (Jia Wang et al., 2020). In turn, FFA is a specific scavenger of $^1$O$_2$ (1.2 × 10$^8$ M$^{-1}$ s$^{-1}$) (Chen et al., 2018), whereas BQ can scavenge O$_2$•$^-$ (9 × 10$^8$ M$^{-1}$ s$^{-1}$) (Bielski et al., 1985).

Fig. 13 depicts the effect of different scavengers on VAL removal during carbocatalysis with PMS and BP. Fig. 13 reveals inhibition of VAL removal in the presence of all the considered scavengers, indicating the participation of both radical and non-radical mechanisms in the process. It can be noted that the presence of MeOH and TBA inhibited the VAL decay during the process in 20.8% and 36%, respectively. These results indicate that HO• has a stronger contribution than SO$_4$•$^-$ on VAL degradation. Furthermore, when FFA was added to the system, the removal of VAL decreased in 31.4%. Meanwhile, BQ addition led to a decay in the VAL removal of 17.8%. The results for the scavengers addition suggest the predominance of HO• and $^1$O$_2$ species in the carbocatalytic process. Our findings are in agreement with previous works, which report that during the activation of PMS (or PDS) with carbon-based materials for pollutants elimination, singlet oxygen $^1$O$_2$ has a relevant role as a degrading species (Sun et al., 2020; Yin et al., 2019; Zhang et al., 2020).
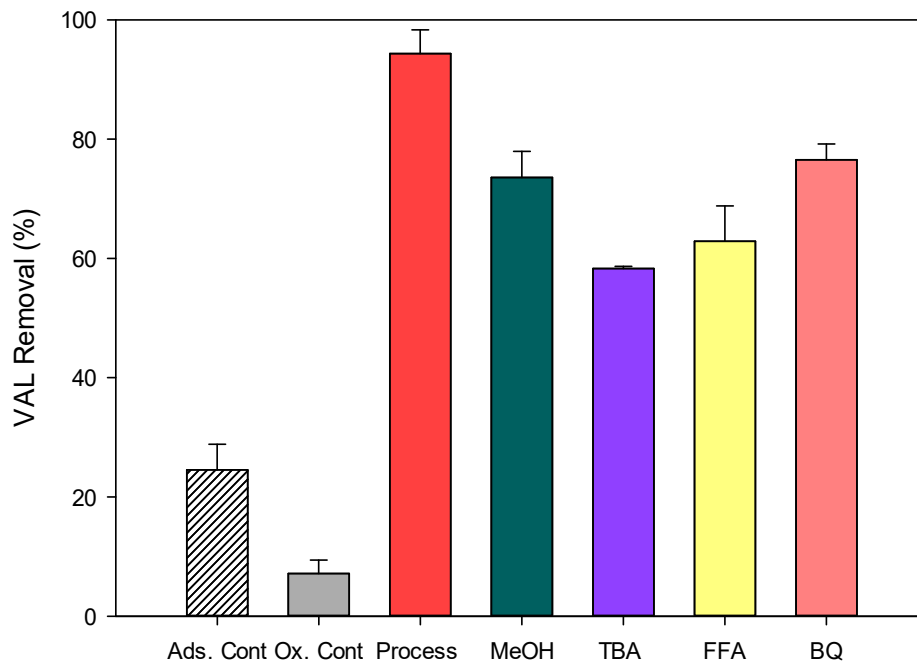
**Figure 13.** Effect of scavengers on VAL removal during the PMS-catalysis with biochar.
Experimental conditions: V=100 mL; $C_{VAL}$=16 μM; $C_{BP}$ = 0.2 g $L^{-1}$; $C_{PMS}$ = 0.462 mM; pH =6.1.

Biochar-based catalysts can be used as both electron acceptors and electron donors, and the
production of ROS is dependent on such behavior. The generation of HO• and $SO_4•^-$ from PMS
involves the action of biochar as electron donor capability related to structural defects and oxygen-
containing functional groups. The defect structures of biochar (edge defects, curvature, vacancies,
etc.) can generate dangling σ bonds, which can keep the π-electrons of biochar from being limited
by the edge carbon atoms, thereby transferring electrons from biochar to PMS to produce the
radicals. Also, the lone pair of electrons in the Lewis basic site in the biochar-based catalysts (such
as the oxygen atom in C = O moieties. Indeed, our BP has these functional groups (Grisales-
Cifuentes et al., 2021), and the free-flowing π-electrons in the sp2 -hybridized carbon are able to
transfer electrons (Eq. 10-11) (Zhao et al., 2021).

$$HSO_5^- + BP \rightarrow OH^- + SO_4^{\cdot-} + BC^+ \qquad \text{Eq. (10)}$$

$$HSO_5^- + BP \rightarrow SO_4^{2-} + HO\cdot + + BC^+ \qquad \text{Eq. (11)}$$
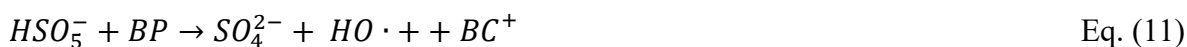
The formation of $^1O_2$ can be explained considering the electron acceptor characteristics of BP. Electron deficient moieties on the biochar can accept an electron from the PMS, producing $SO_5^{\bullet-}$ (Eq. 12), which further produces $^1O_2$ (Eqs. 13)(Zhao et al., 2021). Singlet oxygen can be generated by the self-decomposition of $SO_5^{\bullet-}$ (Eq. 13) or PMS (Eq. 14). Moreover, $O_2^{\bullet-}$ is produced by the interaction of the BP with the oxygen present in the aqueous media as illustrated by Eq. 15 (Ouyang et al., 2019).

$$HSO_5^- + BP \rightarrow H^+ + SO_5^{\bullet-} + BP^- \qquad \text{Eq. (12)}$$

$$2SO_5^{\bullet-} \rightarrow {}^1O_2 + S_2O_8^{2-} \qquad \text{Eq. (13)}$$

$$HSO_5^- + SO_5^{2-} \rightarrow {}^1O_2 + SO_4^{2-} + HSO_4^- \qquad \text{Eq. (14)}$$

$$BP + O_2 \rightarrow O_2^{\cdot-} + BC^+ \qquad \text{Eq. (15)}$$
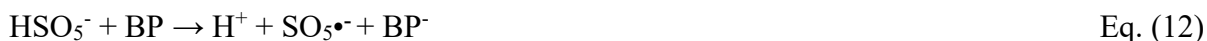
It is important to mention that ROS, such as HO•, attack VAL on its carboxylic, tetrazole, and amide groups (Martínez-Pachón et al., 2021; E.A. Serna-Galvis et al., 2019). In turn, singlet oxygen could transform the functional groups attached to the biphenyl tetrazole nucleus as reported for losartan (another sartan antihypertensive structurally related to valsartan) (Seburg et al., 2006).

### 3.3.5. Reusability of biochar in adsorption vs. reaction with PMS

The reusability of the biochar plays an important role in terms of economic and environmental feasibility (Mian & Liu, 2020). Therefore, the reuse of BP was evaluated four times (Fig. 14). The adsorption and carbocatalysis processes were also compared. The adsorption process became inefficient after the 2$^{nd}$ run as the active centers are occupied by the adsorbed VAL molecules. In fact, some studies have been also reported that the removal efficiency of organic pollutants, gradually declined after the third time of biochar reuse (Li et al., 2020; Mian & Liu, 2020; Jia Wang et al., 2020).

From Fig. 14, it can be noted that the efficiency of VAL removal by the carbocatalytic system achieved high values (~80%) even after the fourth cycle, indicating that this process is less affected than the adsorption system. These results indicate that carbocatalysis with PMS could be an interesting alternative because this system increases the biochar lifetime use. On the other hand, the decrease in the efficiency of the BP/PMS combination during the reuse cycles could be associated with the pollutant absorbed and/or the intermediates products remaining on the BP

surface, which inhibit the interaction between biochar and the oxidant (Li et al., 2020; Mian & Liu, 2020). However, it is important to mention that some studies have shown the catalytic activity of recycled biochars can be recovered by thermal treatment under high temperatures, which allows removing substances remaining on the surface of used biochar (Li et al., 2020). Such regeneration of biochar could be applied in the future to extend the utilization of this carbonaceous material.
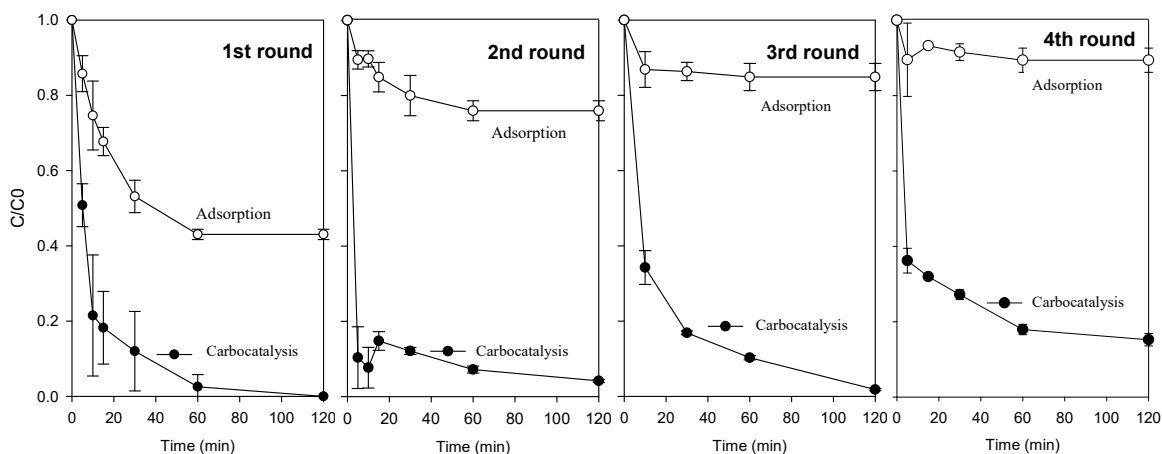


**Figure 14.** Biochar reusability test during adsorption and PMS catalytic tests. V=100 mL; $C_{VAL}$=16μM; $C_{BP}$ = 1gL$^{-1}$; $C_{PMS}$ = 0.462 mM; pH =6.1.

### 3.3.6. Matrix effect

Due to the fact that valsartan can be found in complex hospital wastewaters (Efraím A. Serna-Galvis et al., 2019a), the degradation of this pharmaceutical by carbocatalysis was carried out in SHWW (composition in Table 7) and RHWW (composition Tables 2 and 5). Fig. 15 shows the VAL removal in these matrices. The VAL removal in SHWW (~94% removal at 60 min) is slightly affected when compared with the treatment in distilled water (DW, ~99% at 60 min). In contrast, VAL removal decay in the RHWW matrix is strongly affected (~ 20% removal at 60 min).

The SHWW is composed of organic (e.g., urea and acetate) and inorganic (e.g., chloride, sulfate, or dihydrogen phosphate) substances, which have low reactivity toward singlet oxygen and superoxide anion radical (Díez-Mato et al., 2014; Hayyan et al., 2016; Liu et al., 2020b), whose participation in the VAL elimination was shown previously. Although the inorganic anions such as chloride or bicarbonate, and organic substances like urea and acetate, in SHWW, have relatively high-rate constants with the hydroxyl radicals, they also lead to the formation of other radical

species (Table 11) that may contribute to the VAL degradation; which may explain the low affectation to the VAL degradation by the SHWW components observed in Fig. 15. This contrasts with high competition for matrix components in the RHWW. It must be highlighted that the RHWW is a matrix much more complex than SHWW. The RHWW has a high content of organic matter and solids (non-present in SHWW), which can cover some active sites on the BP, limiting the PMS activation. Furthermore, the organic components and solids in the RHWW matrix also compete with VAL by the ROS, inducing a decrease in the removal efficiency of the process when compared to DW or SHWW.
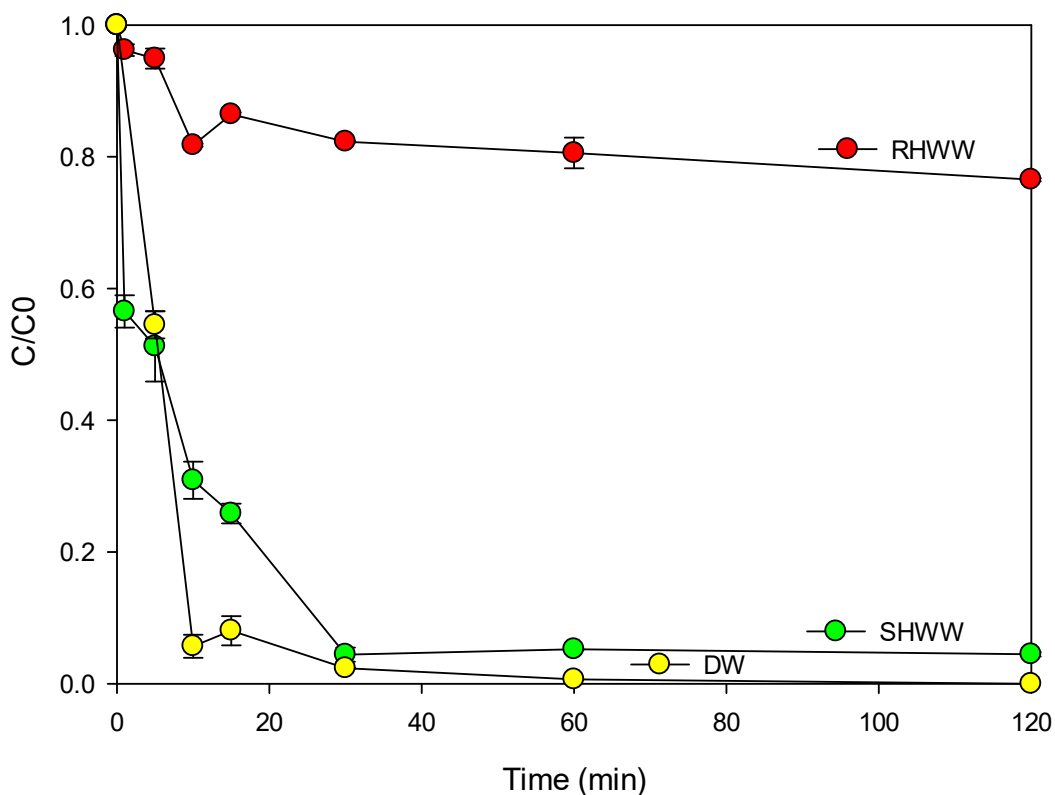


**Figure 15.** Results of the matrix effects on Carbocatalysis process using RHWW (Real Hospital Wastewater), SHWW (Simulated Hospital Wastewater) and DW (Distilled Water) dopped with VAL. V=100 mL; $C_{VAL}$=16μM; $C_{BP}$ = 1g L$^{-1}$; $C_{PMS}$ = 0.462 mM; pH =6.1.

**Table 12.** Rate constants of the reactions between hydroxyl radical and the diverse components of fresh urine.

| Reaction | Second-order rate constant ($k^{2nd}$, $M^{-1}$ $s^{-1}$) | References |
|---|---|---|
| $HO^\bullet + Cl^- \rightarrow ClOH^{\bullet-}$ | $4.3 \times 10^9$ | (Lian et al., 2017) |
| $HO^\bullet + H_2PO_4^- \rightarrow HO^- + H_2PO_4^\bullet$ | $\sim 2 \times 10^4$ | (Buxton et al., 1988) |
| $HO^\bullet + CH_3COO^- \rightarrow H_2O + CH_2COO^{\bullet-}$ | $7.0 \times 10^7$ | (Minakata et al., 2011) |
| $HO^\bullet + H_2NCONH_2 \rightarrow products$ | $7.9 \times 10^5$ | (Buxton et al., 1988) |
| $HO^\bullet + HCO_3^- \rightarrow CO_3^{\bullet-} + H_2O$ | $8.5 \times 10^6$ | (Toth et al., 2012) |

### 3.3.7. Phytotoxicity

High concentrations of recalcitrant compounds present in wastewater systems (e.g, hospital, wastewaters) or even organic by-products during the carbocatalytic process may cause toxic effects to organisms. Thus, it is necessary to assess the toxicity of the treated water, which allows evaluating the effectiveness of the treatment systems (Carvalho Neves et al., 2020; Li et al., 2020; Zhang et al., 2020). The use of toxicity assays reduces the need to identify large numbers of compounds present in effluents. Among the available methods to investigate the toxic effects of compounds released to the environment, phytotoxicity assays are widely used (Belalcázar-Saldarriaga et al., 2018b; Carvalho Neves et al., 2020; Libralato et al., 2016).

To determine the extent of the carbocatalytic process, phytotoxicity tests were performed. Phytotoxicity essays were carried out evaluating the matrices of DW, SHWW, and RHWW before, during, and after the carbocatalytic process (Fig. 16). It can be mentioned that several studies suggest the presence of a nonphytotoxic effluent when the G.I. value is in the range of 60% and 100% (Belalcázar-Saldarriaga et al., 2018b). From Fig. 16, it is observed that the G.I. value for

each water matrix without treatment (0 min) is different. Indeed, the non-treated DW and RHWW are less phytotoxic than the SHWW, this could be related to the high content of salts in the simulated matrix, which may affect the germination of the seeds.

The results in Fig. 16 also revealed that the carbocatalytic process in distilled water matrix led to a significant increase in the G.I. as the treatment time increased from 120 min (G.I.: 68.49%) to 240 min (G.I.: 87.66%), which indicates that the process transformed the initial VAL into less phytotoxic compounds. In turn, the G.I. in SHWW and RHWW was lower than 60% after carbocatalysis application. These results could be related to the matrix effects. In the case of SHWW, the high presence of ions such as chloride may lead to the generation of organochlorinated products that are phytotoxic (Jayaraj et al., 2016). Meanwhile, in the RHWW, where VAL was not completely degraded (see Fig. 15), some of the primary transformation products from the target pharmaceutical or other by-products coming from the action of the process on the intrinsic matrix components may be responsible for the increased toxicity.
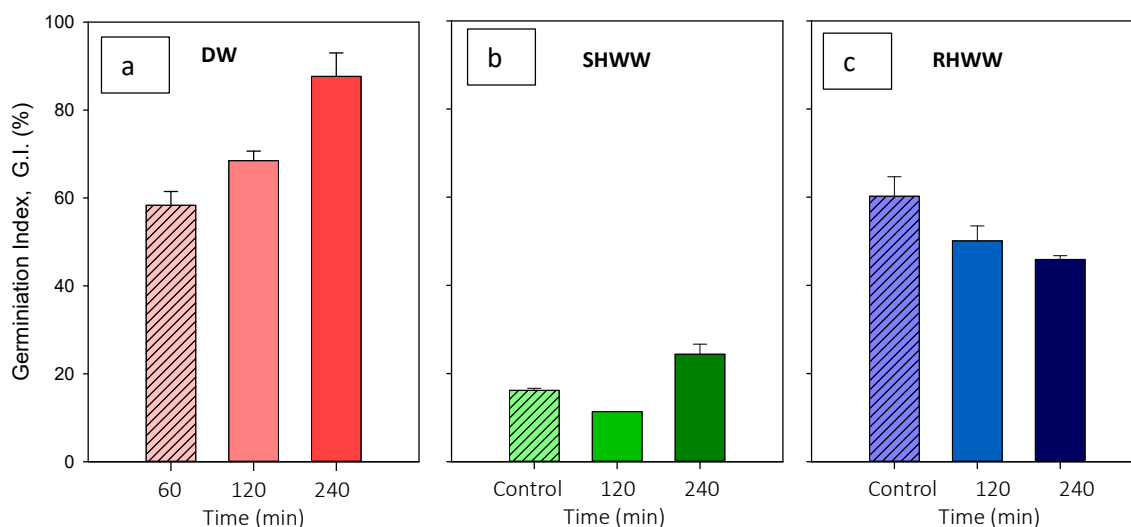


**Figure 16.** Germination index (G.I.) results. a) Distilled water (DW); b) Simulated Hospital wastewater (SHWW); c) Real Hospital wastewater (RHWW). using carbocatalysis. The matrixes were dopped with VAL. V=100 mL; CVAL=16μM; CBP = 1g L$^{-1}$; CPMS = 0.462 mM; pH =6.1.

### 3.4. Conclusions

The used biochar (BP, prepared from agro-industrial wastes of oil fiber palm) had oxygenated functional groups which favored the adsorption of pharmaceuticals. The theoretical calculations indicated that the most favorable interactions between the tested pharmaceuticals and the BP were H-bonding-types due to the presence of oxygenated functional groups (e.g., carbonyl/ketone, carboxyl, and phenol) on the biochar. Such oxygenated moieties also favored the interaction with PMS to generate ROS, which leads to a synergistic degradation of target pharmaceuticals such as VAL.

The tests using scavengers demonstrated that the carbocatalytic process involved the main action of hydroxyl radical and singlet oxygen in the degradation of pollutants. The experimental design allowed us to determine that a near neutral-pH and low amounts of PMS (which may minimize environmental impacts and reagent costs) led to high degradation of the target pharmaceutical. Interestingly, the combination of the BP with PMS (i.e., the carbocatalytic process) extends the biochar lifetime use, showing high efficiencies (~80%) even after the fourth reuse cycle. Finally, the carbocatalytic process in distilled water was able to transform VAL into less phytotoxic compounds; however, the presence of other components in very complex matrices such as hospital wastewater (SHWW or RHWW) induces the formation of phytotoxic products.

**CHAPTER IV**

# ELIMINATION OF VALSARTAN BY THE PHOTO-FENTON PROCESS (Fe (II)+PMS+UVA) AT NATURAL pH USING PMS AS OXIDIZING AGENT

## 4.1 Introduction

This chapter begins by depicting the main effect of power, PMS, and iron concentration on valsartan degradation using an experimental design, followed by the validation of the process optimization. Then, the degradation route, the effect of the HWW, and the enhancement of the process by a complexing agent of iron were studied. Finally, the phytotoxicity of the treated solutions is also discussed.

## 4.2. Materials and methods

### 4.2.1.  Reagents

Valsartan (VAL, $C_{24}H_{29}N_5O_3$, MK®). Oxone® ($2KHSO_5 \cdot KHSO_4 \cdot K_2SO_4$) from Sigma-Aldrich® was used as a source of peroxymonosulfate (PMS).  Iron sulfate heptahydrate ($FeSO_4 \times 7H_2O$, Fisher Scientific, ACS, 99%). Citric Acid ($HOC(COOH)(CH_2COOH)_2$, Sigma Aldrich, ACS reagent, $\geq 99.5\%$). All solutions were prepared with distilled water, except for solutions used for chromatographic analyses, which were made with purified water from a Millipore Milli-Q® system.

### 4.2.2.  Reaction system

All tests were carried out using a homemade aluminum reflective reactor equipped with 5 Philips UVA lamps (BLB, with the main emission at 365 nm, Figure 17). For this process, 15, 45, or 75 W of light power were applied to 100 mL of sample. Assays were performed at near-neutral pH ($5.8 \pm 0.3$).
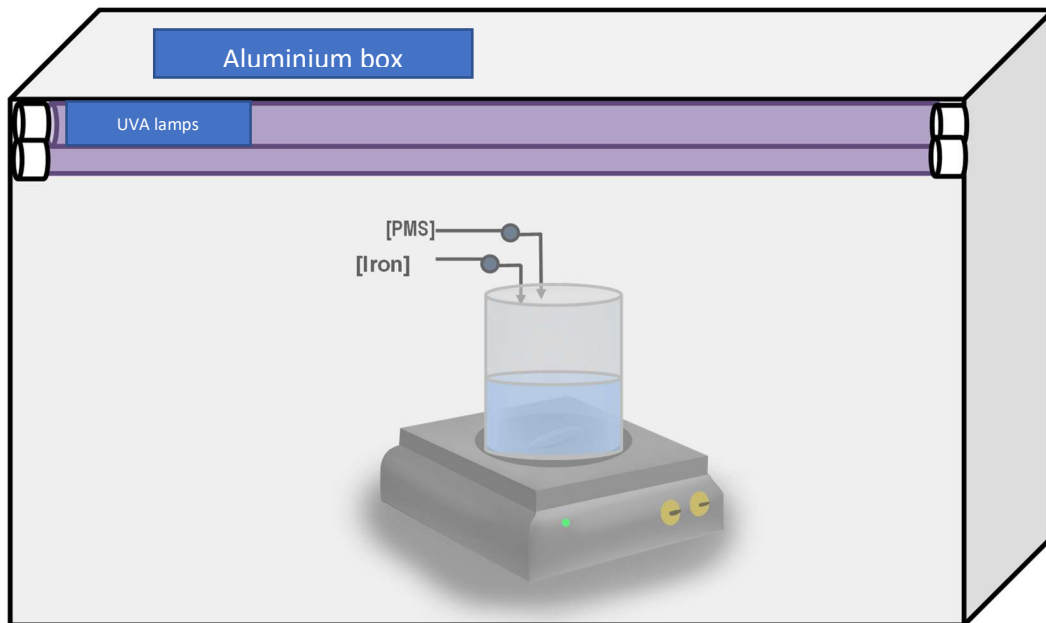
**Figure 17.** Scheme of the reaction system for the photo-Fenton process.

### 4.2.3. Analytical determinations

The concentration of aqueous organic pollutants was determined following the methodology described in Section 3.2.3 (Table 6).

### 4.2.4. Experimental Design

A Box-Behnken experimental design was used to determine the effect of concentration of the oxidizing agent, iron concentration, and power on the removal of VAL. The best operational conditions were found following the methodology described in Section 3.2.5 using the Design Expert® software.

### 4.2.5. Determination of degradation routes

Similar to section 3.2.6 quenching experiments were used to identify the contribution of radical species produced during the oxidative degradation of the pollutants by the Fe (II)+PMS+UVA process.

### 4.2.6. Matrix effect

Similar to section 3.2.7 we evaluated the Fe (II)+PMS+UVA process selected using simulated hospital wastewater (SHWW, see Table 7) and real hospital wastewater (i.e., RHWW, see Tables 2 and 5) to identify the matrix effect on the system.

### 4.2.7. Treatment extent-Phytotoxicity

Similar to the methodology described in Section 3.2.8 phytotoxicity tests were carried out to evaluate the effluent characteristics of the Fe (II)+PMS+UVA process.

## 4.3. Results and discussion

### 4.3.1. Effect of power, PMS, and iron concentrations on the pollutant degradation

To study the effect of power, PMS, and Fe (II) concentration on the removal of VAL by the photo-Fenton process, a design of experiments (DOE) using the response surface methodology (RSM) was carried out. The design consisted of a set of 17 experiments (including 6 repetitions of the central point). Table 12 shows the experimental conditions. The iron concentration range was chosen according to the experience acquired in previous works by the GIRAB research group. Also, it is important to mention that a high concentration of iron may have negative environmental impacts, then, we used low amounts (0.05-0.1 mM).

**Table 13.** Experimental conditions for the DOE.

| Run | Power (Watts) | PMS (mM) | Fe (II) (mM) |
|---|---|---|---|
| 1 | 75 | 0.51 | 0.05 |
| 2 | 45 | 0.51 | 0.075 |
| 3 | 45 | 0.51 | 0.075 |
| 4 | 75 | 0.51 | 0.1 |
| 5 | 15 | 0.51 | 0.05 |
| 6 | 45 | 0.51 | 0.075 |
| 7 | 45 | 1 | 0.1 |
| 8 | 75 | 0.02 | 0.075 |
| 9 | 15 | 1 | 0.075 |
| 10 | 15 | 0.02 | 0.075 |
| 11 | 45 | 0.02 | 0.1 |
| 12 | 15 | 0.51 | 0.1 |
| 13 | 45 | 0.02 | 0.05 |

| 2 | 45 | 1 | 0.05 |
|---|----|---|------|
| 15 | 45 | 0.51 | 0.075 |
| 16 | 45 | 0.51 | 0.075 |
| 17 | 75 | 1 | 0.075 |

The statistical analysis indicated that a quadratic model is adequate to represent the removal of VAL by means of the Fe (II)+PMS+UVA process. F values (p model = < 0.0001) indicated that the model is significant and that the probability of attributing this value to noise is lower than 0.01%. Values of $r^2$ ($r^2 = 0.99$) and adjusted $r^2$ ($r^2$ adj = 0.98), standard deviation (S.D. = 4.05), and the variation coefficient (V.C. = 5.74%) confirmed that the obtained mathematical model (Eq. 16) is adequate to represent the removal of VAL.

$$RP\ (\%) = 92.60 + 36.75 * PMS + 10.13 * power + 2.88 * iron + 5.50 * PMS * power + 3.00 * PMS * iron - 3{,}25 * power * iron - 36{,}92 * PMS^2 - 5{,}68 * power^2 - 4{,}17 * iron^2$$

Eq. (16)

The RSM analyses from the experimental design (Fig. 18 and 20) showed that the increment in the concentrations of the ferrous ions and the ultraviolet light power has positive effects on the removal of VAL. As the iron concentration is increased, its interaction with the oxidant (PMS) is favored (Eq. 3), then higher production of radicals occurs (Giraldo-Aguirre et al., 2018). Also, when the light power is augmented, the photo-regeneration of iron is favored (Eq. 17, (Pignatello et al., 2006)), improving the catalytic cycle of iron, and the production of radicals. Consequently, more molecules of VAL are degraded.

$$Fe^{3+} + H_2O + UVA \rightarrow Fe^{2+} + HO\bullet + H^+ \qquad\qquad Eq.\ (17)$$

Regarding the PMS dose effect, we can mention that the increment in this parameter leads to the formation of more radicals (Eq. 3), improving the pharmaceutical elimination. Nevertheless, when PMS is in excess, self-scavenging becomes important (Eq. 9), and the target pollutant and PMS compete for the radical species generated (Solís et al., 2020). Moreover, undesired reactions with iron (Eq. 18 and 19) can take place. Also, it should be said that $SO_5\bullet^-$ (Eq. 9) is a radical less powerful than hydroxyl radical or sulfate radical (Rodríguez-Chueca, Giannakis, et al., 2019), which limits its ability to degrade VAL. For these reasons, it is very important to control the amount of PMS in the photo-Fenton system.

$$SO_4^{\cdot-} + Fe^{2+} \rightarrow Fe^{3+} + SO_4^{2-} \qquad \text{Eq. (18)}$$

$$Fe^{2+} + HO^{\cdot} \rightarrow Fe^{3+} + HO^{-} \qquad \text{Eq. (19)}$$

The concept of global desirability (D) using the Desing-Expert® software (Myers, RH.; Mongotmery, DC.; Anderson, 1997) was used to select the best operational condition for VAL removal by the photo-Fenton process. The results of such analysis indicate that 90% removal can be achieved using the following conditions: Power = 45 W, PMS= 0.475 mM, and Fe (II)= 0.075 mM. These conditions allow us to reach three aspects that deserve special attention in the photo-Fenton process: operation at near-neutral pH, reduction of PMS consumption, and decrease in electricity consumption. It is important to mention that Fe (II) was not considered in the desirability function since this reagent could be presented in wastewater intrinsically and its price is lower than PMS.
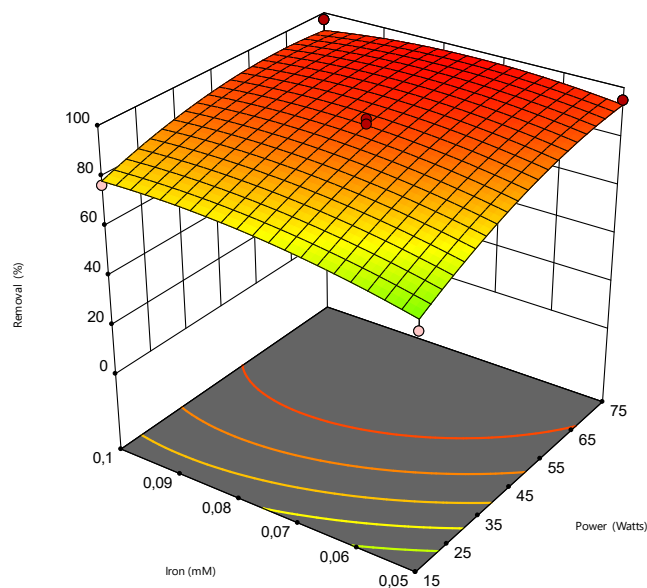


**Figure 18**. Response surface analysis for the degradation of VAL. Variation effect of iron - power. Experimental conditions V=100 mL; $C_{VAL}$=16μM; $C_{Fe(II)}$ = 0.05-0.1 mM; $C_{PMS}$ = 0.02-1 mM; Power= 15 -75 Watts; pH: 7 ± 0.3.
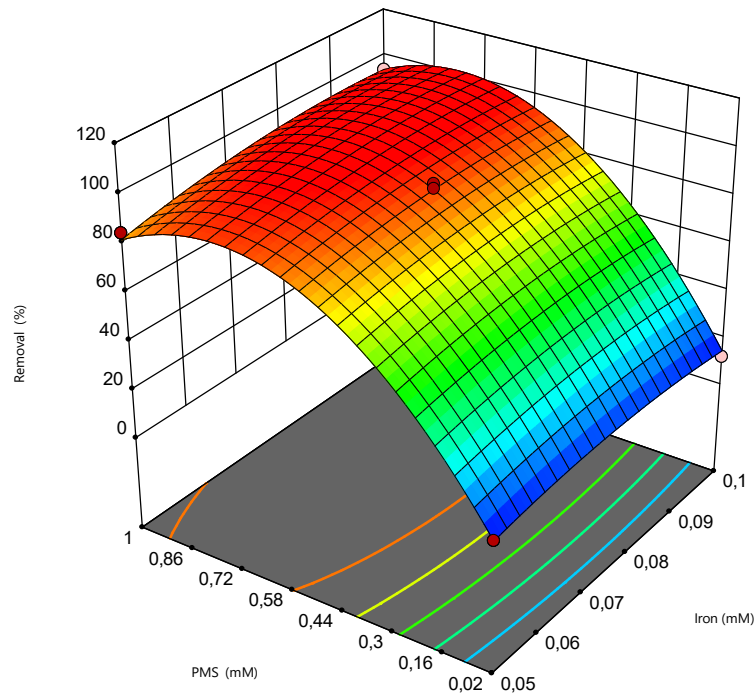
**Figure 19.** Response surface analysis for the degradation of VAL. Variation effect of PMS -
Iron. Experimental conditions: V=100 mL; $C_{VAL}$=16µM; $C_{Fe(II)}$ = 0.05-0.1 mM; $C_{PMS}$ = 0.02-1
mM; Power= 15 -75 Watts; pH: 7 ± 0.3.
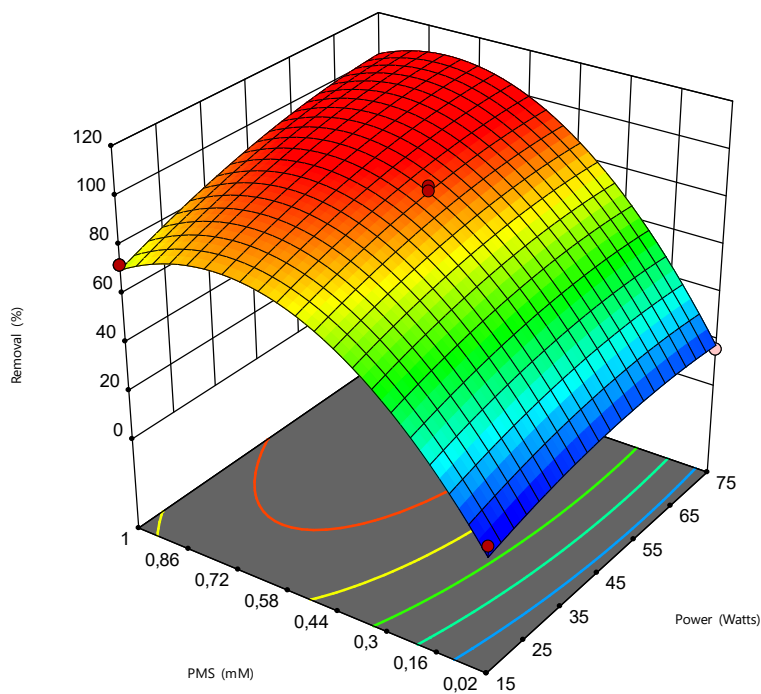
**Figure 20.** Response surface analysis for the degradation of VAL. Variation effect of PMS -
power. Experimental conditions: V=100 mL; $C_{VAL}$=16μM; $C_{Fe(II)}$ = 0.05-0.1 mM; $C_{PMS}$ = 0.02-1
mM; Power= 15 -75 Watts; pH: $7 \pm 0.3$.

### 4.3.2    Validation of the system optimization and routes of the process action

To validate the optimization established in the previous section, VAL was treated using the optimal
operational conditions. Fig. 21 shows the VAL evolution under the photo-Fenton process, and its
control subsystems (i.e., UVA, PMS, Fe (II), and Fe (II)+ PMS. The results confirmed that for the
optimized conditions, the photo-Fenton process achieved 90% of VAL removal in 15 min. From
Fig. 21, it is also observed that the UVA or iron acting individually are not able to degrade VAL.
Furthermore, PMS degraded ~10% of the target pharmaceutical. Meanwhile, the Fe (II)+PMS
achieved up to 48% of VAL removal after 1 min of treatment, but after this time the system
achieved a plateau.

The UVA alone did not degrade VAL because this pollutant had no absorption at 365 nm
(corresponding to the band of emission of the used lamps). The ferrous ion itself has a poor
degrading ability and requires the interaction with an oxidizing agent (such as $H_2O_2$ or PMS) to

produce strong radicals able to attack the target pharmaceutical (Giraldo-Aguirre et al., 2018). PMS itself is an oxidizing agent (E°= 2.01 V, (Rodríguez-Chueca, Giannakis, et al., 2019)) that can induce some degrading effect as observed in Fig. 20. However, this oxidant also requires interaction with Fe (II) to produce stronger degrading agents such as hydroxyl radical and/or sulfate radical (Eq. 3). In turn, the Fe (II)+PMS process produces radical species (Eq. 3). However, the regeneration of ferrous ions from the interaction between the ferric ion and PMS is very slow, producing sulfur pentoxide radical (see Eq. 9) (Rodríguez-Chueca, Giannakis, et al., 2019), which is a soft oxidant with limited degrading ability. This last explains the plateau reached by the Fe (II)+PMS subsystem.
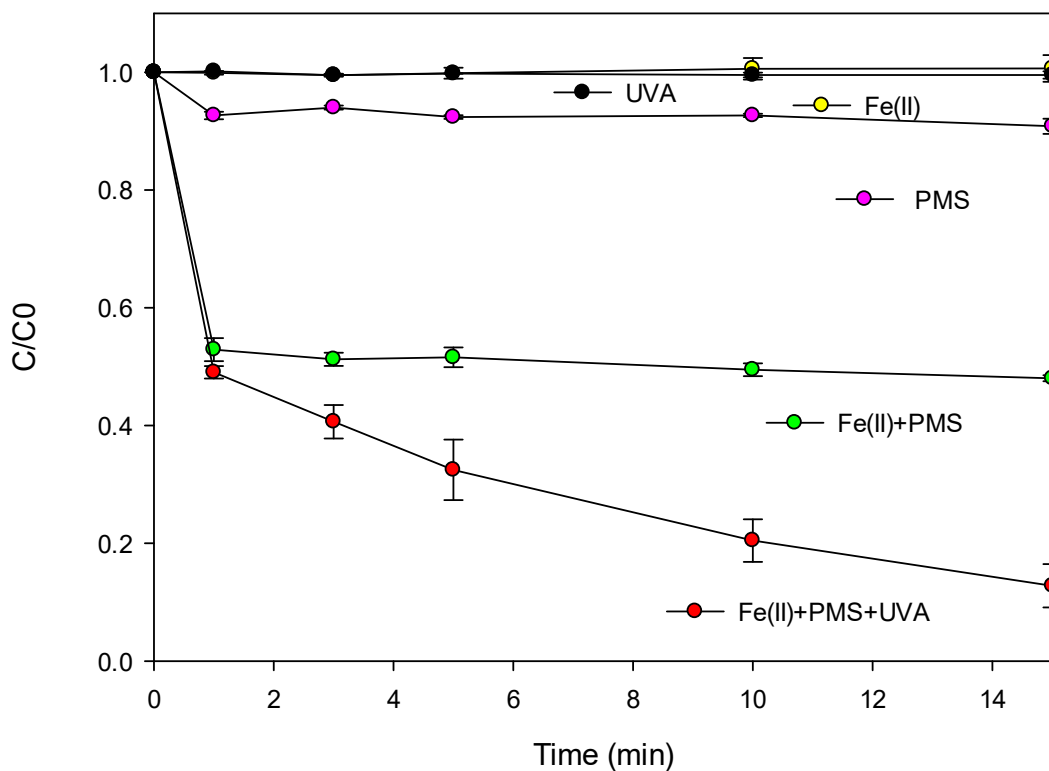


**Figure 21**. Kinetics of VAL elimination by Fe (II) + PMS+UVA process and its components. Experimental conditions: V=100 mL; $C_{VAL}$=16μM; $C_{Fe(II)}$= 0.075 mM; $C_{PMS}$ values= 0.475 mM; Power: 45 Watts.

The comparison between the Fe (II) + PMS and Fe (II)+PMS+UVA processes revealed the relevant role of the UVA light in the whole system. As above mentioned, this light indorses the regeneration of $Fe^{2+}$, and the extra formation of hydroxyl radicals (Eq. 19), contributing to an increase in the

degradation rate for VAL. Moreover, the light avoids the accumulation of $Fe^{3+}$ species, promotes the use of low concentrations of the catalyst, and consequently reduces the sludge disposal problem (Oturan & Aaron, 2014; Pliego et al., 2015). Our results are consistent with those reported by Pereira et al. (Cavalcante et al., 2013), who also compared degradation of the mitoxantrone pharmaceutical by Fenton and photo-Fenton, reporting the superiority of the photo-Fenton process due to the extra action of the light in the process.

### 4.3.3. Verification of participation of radical species in the process
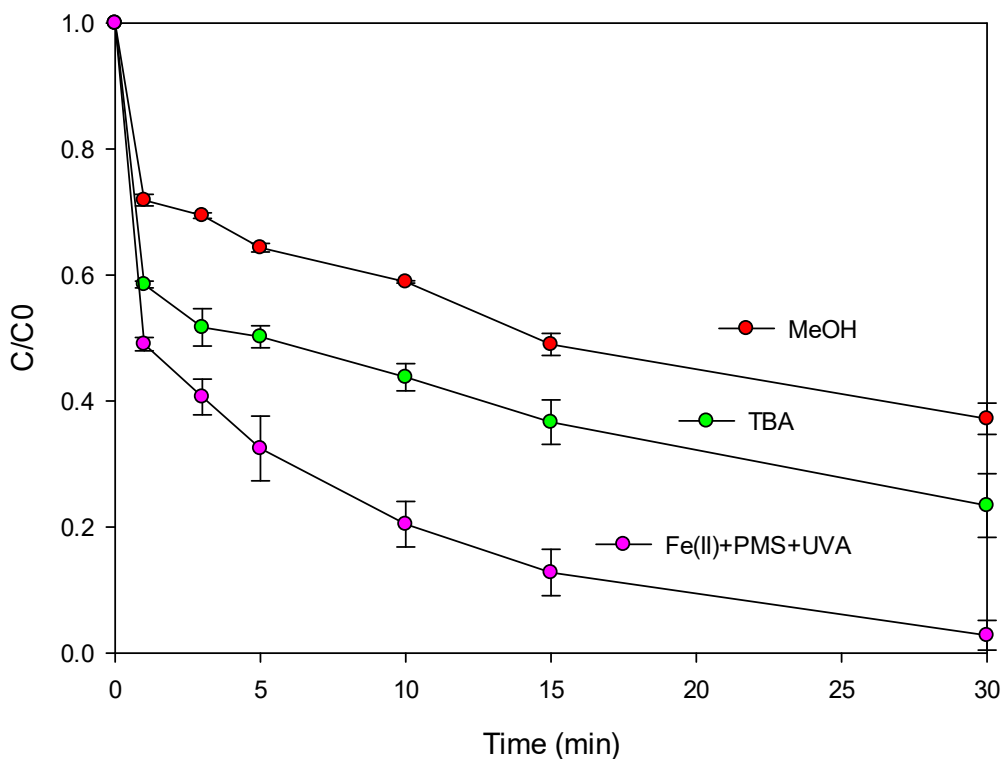


**Figure 22.** Effect of scavengers on VAL removal during the Fe (II)+PMS+UVA. Experimental conditions: V=100 mL; $C_{VAL}$=16μM; $C_{Fe(II)}$= 0.075 mM; $C_{PMS}$ values= 0.475 mM.

According to Solis et al. (Solís et al., 2020) in PMS aqueous chemistry, the main oxidative species are expected to be $HO\bullet$, $SO_4\bullet^-$. Thus, after validation of optimal conditions, experiments in the presence of scavengers were carried out (Fig. 22) to verify the participation of these species during the VAL degradation. It is important to remember that MeOH is able to trap both $HO\bullet$ and $SO_4\bullet^-$, whereas TBA is a powerful scavenger for $HO\bullet$ in presence of $SO_4\bullet^-$ (Jia Wang et al., 2020).

The presence of TBA and MeOH decreased the degradation of the target pharmaceutical. These results indicate that both hydroxyl and sulfate radicals participate in the photo-Fenton process. This is in agreement with those found by (Karimian et al., 2020; Ling et al., 2017; Luo et al., 2019; Ushani et al., 2020). Indeed, our results are also coherent with the proposed activation of PMS by $Fe^{2+}$ as shown in Eq. 3, and activation by UVA light to generate sulfate radical and hydroxyl radical (Eq. 20).

$$HSO_5^- + hv \rightarrow SO_4^{\cdot-} + HO^{\cdot}$$ <div align="right">Eq. (20)</div>

### 4.3.4. Matrix effect

The treatment of VAL by the photo-Fenton process was carried out in SHWW (composition in Table 7) and RHWW (composition Tables 2 and 5). Fig. 23 presents the VAL removal in these matrices and distilled water (DW). The VAL removal in SHWW (~30% removal at 60 min) and RHWW matrices was strongly affected (~ 10% removal at 60 min) when compared with the treatment in distilled water (DW, ~99% at 60 min).

**Figure 23.** Results evaluation matrix effect in Fe (II)+PMS+UVA process using RHWW
(Real Hospital Wastewater), SHWW (Simulated Hospital Wastewater) and DW (Distillated
Water) dopped with VAL. V=100 mL; $C_{VAL}$=16µM; $C_{Fe(II)}$ = 0.075 mM; $C_{PMS}$ = 0.475 mM; pH
=6.1.

The SHWW is composed of organic (e.g., urea and acetate) and inorganic (e.g., chloride, sulfate,
or dihydrogen phosphate) substances, which are very reactive towards the radicals (see Table 11),
affecting the VAL degradation as observed in Fig. 23. Again, it must be considered that the RHWW
is a matrix much more complex than SHWW. The RHWW has a high content of organic matter
and solids (non-present in SHWW), which can diminish the light penetration, limiting the PMS
activation (Eq. 20) and the regeneration of the ferrous ion (Eq. 19). Besides, the organic

components and solids in the RHWW matrix also compete with VAL by the radicals, decreasing the removal efficiency of the Fe (II)+PMS+UVA process compared to DW or SHWW.


### 4.3.5   Improvement of the degradation by addition of a complexing agent of iron

The use of complexing agents has been extensively studied as an alternative to enhance the photo-Fenton process, allowing to reduce reaction time, reagents, and energy consumption, in addition to the possibility of operation at near-neutral pH. These facts may lead to a reduction in operational costs and on the environmental impact of this advanced oxidation process (Pliego et al., 2015; Luis Miguel Salazar et al., 2019; Efraim A. Serna-Galvis et al., 2020). Hence, to improve the performance of the photo-Fenton process, and considering that citric acid (CA) is commonly found in hospital wastewaters that have dialysis units (Efraim A. Serna-Galvis et al., 2020), this organic acid was added to the reaction system.
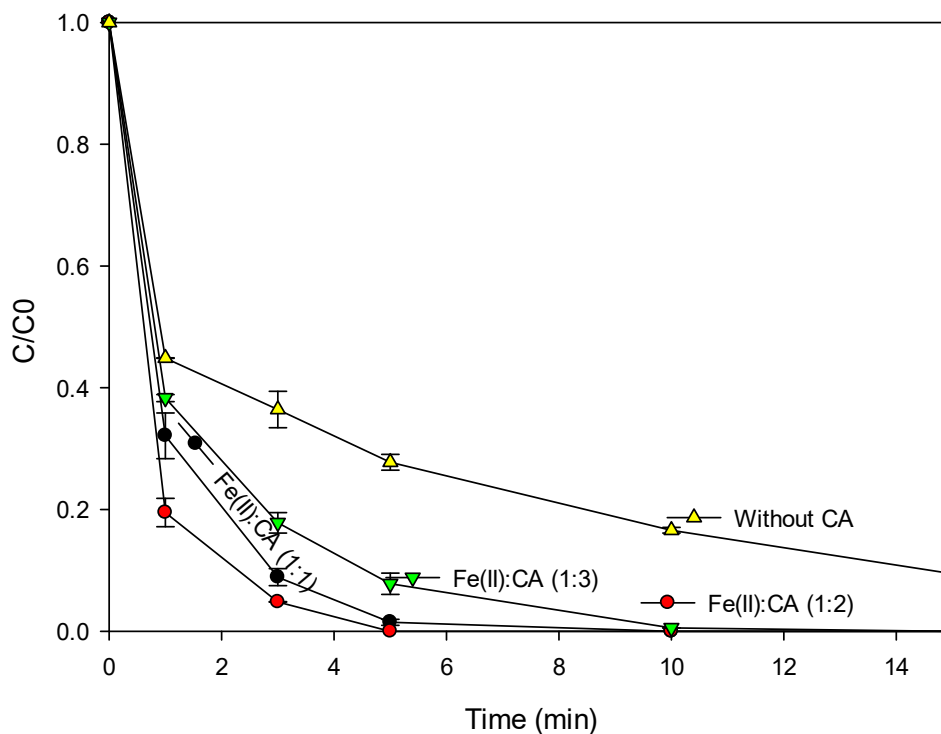
**Figure 24.** Effect of scavengers on VAL removal during the Fe (II)+PMS+UVA process in presence of citric acid (CA). Experimental conditions: V=100 mL; $C_{VAL}$=16 µM; $C_{Fe(II)}$ values= 0.075 mM; $C_{PMS}$ values= 0.475 mM; $C_{citric\ acid}$=0.15 mM.

Initially, it was evaluated three different Fe (II):CA molar ratios (1:1, 1:2, and 1:3) in DW (Fig. 24). As seen, in all cases, the addition of citric acid improves the VAL degradation. As the citric acid concentration is augmented from a 1:1 to 1:2 ratio, the complexation of ferric ions occurs more efficiently (Ahile et al., 2020b, 2020a). However, when the CA concentration is further augmented (1:3 ratio) the excess of the organic acid may induce competition by the radicals thus decreasing the degradation of the target pollutant (Ahile et al., 2020a, 2020b). Then, the results indicate that the 1:2 ratio is the most convenient to enhance the performance of our Fe (II)+PMS+UVA process.

The addition of citric acid at the 1:2 condition in SHWW and RHWW was also evaluated (Fig. 25). It can be noted that the elimination of VAL in both SHWW and RHWW was significantly increased concerning the acid absence (Fig. 25). It is important to mention that the use of complexing agents

of the ferric ion (e.g., citric acid) have benefits such as i) expansion of the useful range of the solar spectrum up to 450-580 nm allowing to increase the oxidation efficiency of the Fe (II)+PMS+UVA process; ii) the photolysis of the ferric complexes provides extra oxidizing species (Eq. 21-24) that may improve the efficiency of the process; iii) these complexes keep ferric ions in soluble forms, allowing to work at neutral pH values, favoring the catalytic cycle of iron in the photo-Fenton process (Monteagudo et al., 2008, 2010; Souza et al., 2014).

$$[Fe(Citrate)\ ]\ + hv \rightarrow Fe^{2+} + Citrate * - \qquad \text{Eq. (21)}$$

$$Citrate * - \ + O_2 \rightarrow Products + O_2^{*-} \qquad \text{Eq. (22)}$$

$$O_2^- + H^+ \rightarrow HO_2^{\cdot} \qquad \text{Eq. (23)}$$

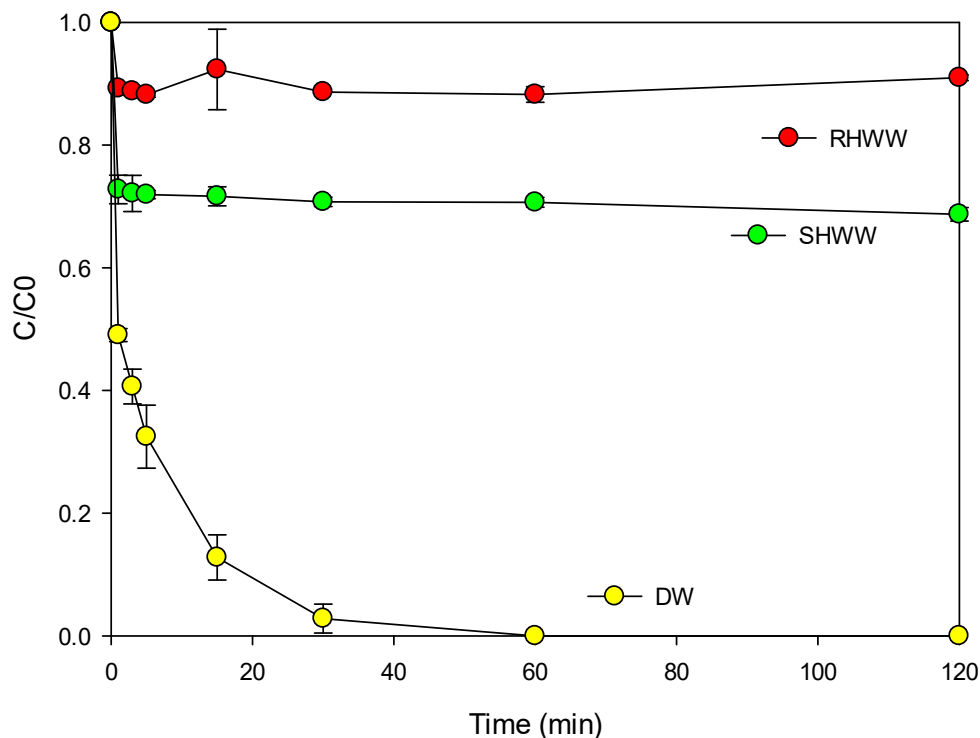$$HO_2^{\cdot} + HO_2^{\cdot} \rightarrow H_2O_2 + O_2 \qquad \text{Eq. (24)}$$
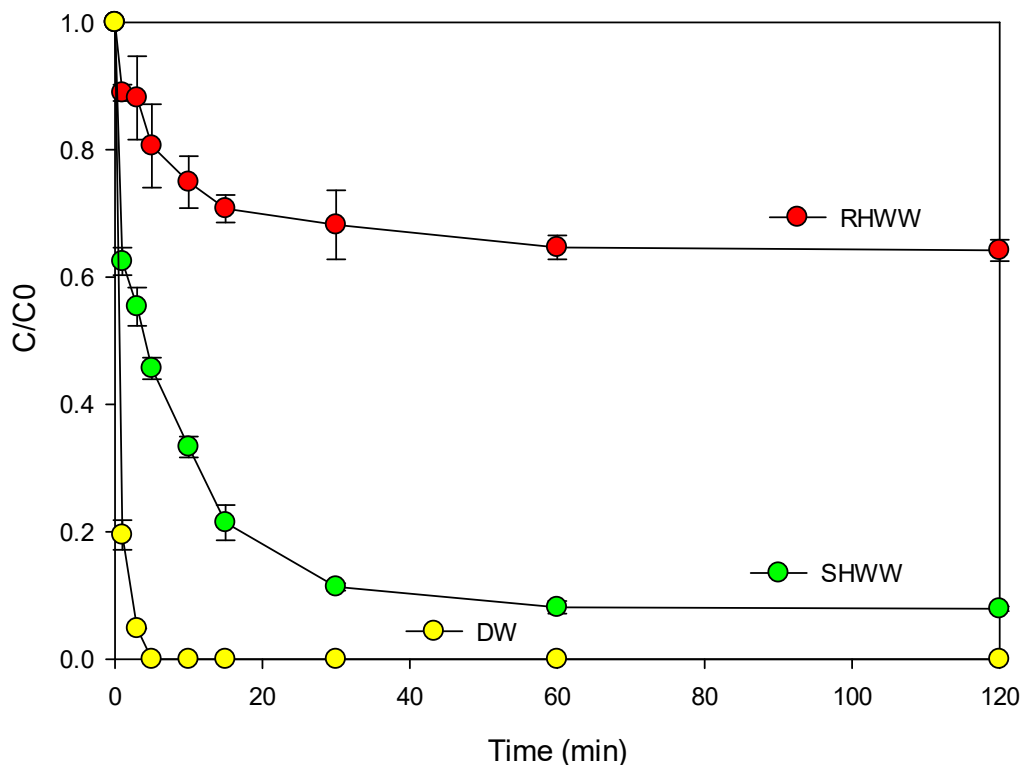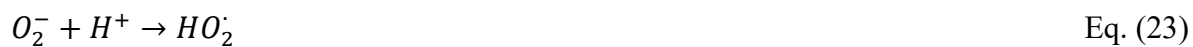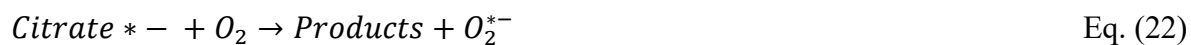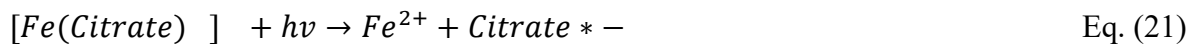


**Figure 25.** Matrix effects on the Fe (II)+PMS+UVA (CA) process using RHWW (Real Hospital Wastewater), SHWW (Simulated Hospital Wastewater) and DW (Distillated Water)

dopped with VAL. V=100 mL; $C_{VAL}$=16μM; $C_{iron}$ = 0.075 mM; $C_{PMS}$ = 0.475 mM; $C_{citric\ acid}$:

0.15 mM; pH =6.1.

### 4.3.6. Extent of the process - phytotoxicity

To determine the extent of the Fe (II)+PMS+UVA process improved with citric acid (CA) at the 1:2 ratio, the phytotoxicity was tested. Phytotoxicity essays were carried out for DW, SHWW, and RHWW (Fig. 26). Different treatment times were considered. It was found that in distilled water, the process increased the G.I. regarding the non-treated sample, when VAL was treated for 60 min (G.I.: ~70%), indicating that at the end of the process are produced compounds less phytotoxic than the parent pharmaceutical (Belalcázar-Saldarriaga et al., 2018b; Elghniji et al., 2012; Hanafi et al., 2011).

The G.I. for the SHWW was below 60% after 60 min of treatment. Again, this behavior could be related to the matrix effects. This water has a high presence of ions such as chloride, which may lead to the generation of organochlorinated products that are phytotoxic (Jayaraj et al., 2016). Interestingly, in the case of RHWW, despite VAL was not completely degraded (Fig. 22), after 60 min of treatment using the Fe (II)+PMS+UVA (CA) process, this led to a G.I. value of ~60%, indicating that the resultant water is a non-phytotoxic effluent (Belalcázar-Saldarriaga et al., 2018b; Elghniji et al., 2012; Hanafi et al., 2011).
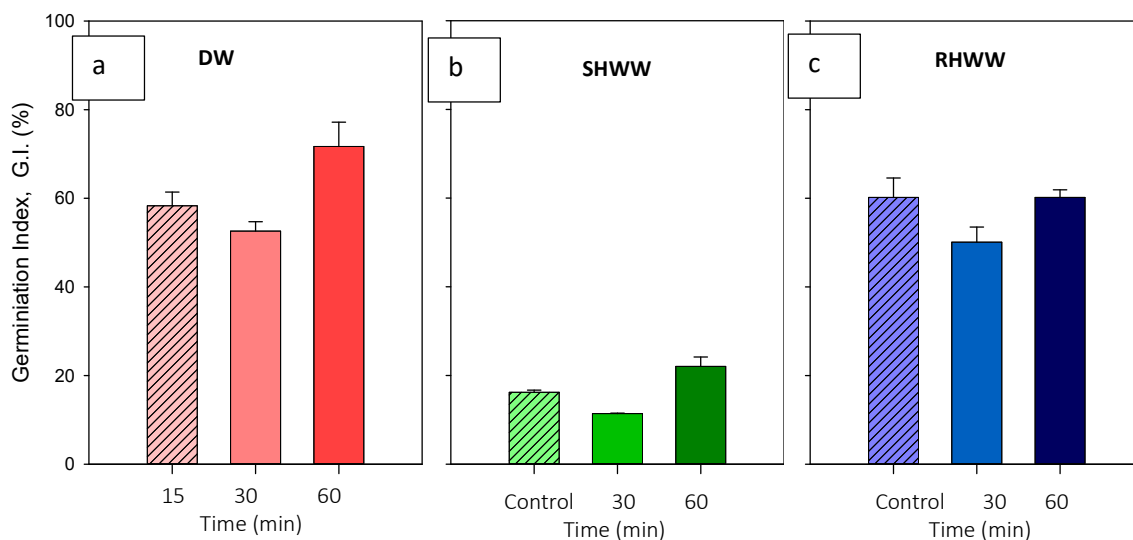
**Figure 26.** Germination index (G.I.) results. a) Distilled water; b) Simulated hospital wastewater (SHWW), and c) Real hospital wastewater (RHWW) using Fe (II)+PMS+UVA (CA). The matrixes were dopped with VAL. V=100 mL; $C_{VAL}$=16μM; $C_{iron}$ = 0.075 mM; $C_{PMS}$ = 0.475 mM; $C_{citric\ acid}$: 0.15 mM; pH =6.1.

## 4.4.  Conclusions

The evaluation of the photo-Fenton process using PMS (Fe (II)+PMS+UVA), as an oxidizing agent at near-neutral pH, to remove valsartan in distilled water showed that the optimal conditions (obtained through the experimental design) required low light power (45 W), and small concentrations of PMS (0.475 mM) and iron (0.075 mM). It was confirmed that in the used photo-Fenton system, hydroxyl and sulfate radicals were the main responsible for the pollutant elimination. Moreover, the addition of citric acid at the 1:2 ratio, significantly improved the degradation of the target pollutant in DW, SHWW, and RHWW. Finally, the treatment of VAL in the RHWW led to a non-phytotoxic effluent, which could be evaluated for crop irrigation potentially.

## CHAPTER V

## ECONOMIC AND ENVIRONMENTAL ASSESSMENT (COMPARISON OF CARBOCATALYSIS AND MODIFIED PHOTO-FENTON PROCESS (Fe (II)+PMS+UVA (CA))

### 5.1. Introduction

In this chapter, the environmental and economic performance of carbocatalysis and photo-Fenton (the main processes under study) were evaluated. In this sense, reagents and energy consumption during the operation were considered. A Life Cycle Assessment (LCA) was carried out to determine the environmental impacts, and then the economic impact associated with the operational costs was calculated.

### 5.2. Methodology

### 5.2.1 Life Cycle Assessment

The environmental assessment was carried out using the Life Cycle Assessment (LCA) methodology. As described in the ISO 14040 technical standard. LCA considers four stages: i) goal and scope (functional unit), ii) inventory analysis, ii) impact evaluation, and iv) interpretation of results (Guinée et al., 2001). For the evaluation of the environmental impact, IPCC-2013 analysis was used (Goedkoop, 2008). This analysis uses the equivalent greenhouse gas emissions ($CO_2$-Eq) as an indicator of the environmental performance of a process the $CO_2$-Eq parameter eases the communication of results to both specialized a non-specialized audiences (Belalcázar-Saldarriaga et al., 2018b; Grisales et al., 2019; Luis Miguel Salazar et al., 2019). In our research, the methodological aspects for the LCA were the following:

### -Goal and scope (functional unit)

The LCA was performed for the treatment of 1 $m^3$ (this considering the projection for the operation at pilot scale) of HWW with a concentration of 16 μM of valsartan as a functional unit (FU). Photo-Fenton intensified with citric acid (Fe (II)+PMS+UVA (CA)) and carbocatalysis were the processes subjected to the LCA (the boundaries for this analysis are depicted in Fig. 27). The

percentage of removal (PR) of the target pollutant established for the processes was 90%. The LCA considered a useful lifetime of 20 years for each treatment system (as typically used, (Belalcázar-Saldarriaga et al., 2018b; Grisales et al., 2019; Luis Miguel Salazar et al., 2019)). Since post-treatment of the generated effluents in each process will take place in a conventional treatment facility, in our study the cradle-to-gate approach was applied.
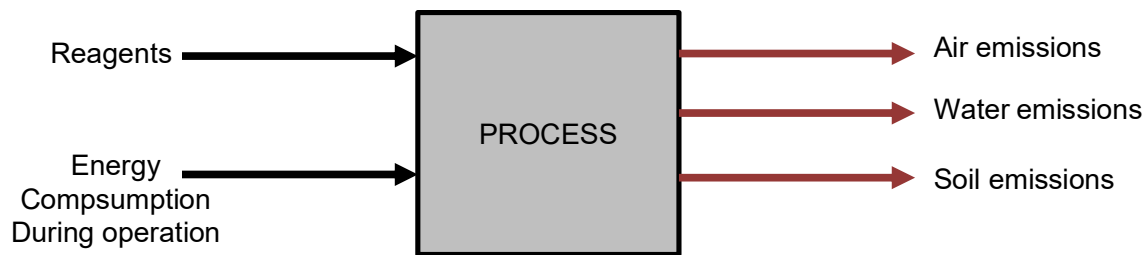


**Figure 27.** System boundaries of system under study.

### -System boundaries and main assumptions

As operative specifications for the LCA, are the following: location (Colombia), operation mode (batch), catalyst (no reuse for iron and biochar was reused during four cycles), and oxidant (fully consumed in the processes).

According to the literature, in advanced oxidation processes, reagents and electricity consumption during the operating stage are the most environmentally aggressive (Belalcázar-Saldarriaga et al., 2018b; Chatzisymeon et al., 2013; Foteinis, Monteagudo, et al., 2018; Giménez et al., 2015; Grisales et al., 2019; Lida Ioannou-Ttofa et al., 2017b; Mufioz et al., 2008; Rodríguez et al., 2016). Thereby, in the evaluated systems, the production of reactants (oxidizing agent and catalyst); and electricity consumption (production and voltage transformation, from high to medium voltage) were considered. It should be highlighted that in Colombia, the energy is mainly generated in hydroelectric power stations (70%). The remaining 30% of energy is generated in thermal power stations that use carbon (15%) and natural gas (15%) as raw materials.

### -Inventory analysis and environmental impact method

Information regarding the unitary processes utilized in this study was obtained from the most recent Ecoinvent v 3.6 database. The OpenLCA version 1.10.3 software was used for the environmental analysis of the treatment systems.

**5.2.2. Economic assessment**

To determine the operational cost of the processes under study, the reagents and electricity consumption for treating one cubic meter ($1 m^3$) of hospital wastewater were considered (Table 13). The energy prices were consulted in the EPM (Empresas Públicas de Medellín) websites, and the reagents prices were established based on the average values for Colombia during 2021.

**Table 14.** Reference values for the economic assessment.

| Reagents | | | |
|---|---|---|---|
| **Reagent** | **Used amount (Kg m$^{-3}$)** | | **Price per Kg (USD)** |
| | **Carbocatalysis** | **Fe (II)+PMS+UVA (CA)** | |
| PMS | 0.052 | 0.054 | 35.78 |
| Iron sulfate | | 0.024 | 36.88 |
| Citric Acid | | 0.029 | 70.19 |
| Zinc Chloride | 0.852 | | 6.01 |
| Hydrochloric acid | 0.152 | | 18.80 |
| **Electric energy consumption per m$^3$** | | | |
| **Activity** | **Carbocatalysis** | **Fe (II)+PMS+UVA (CA)** | **Price of kWh (USD)** |
| Energy Consumption | 6.45 | 0.510 | 0.19 |

**5.3. Results and discussion**

**5.3.1. Environmental impact assessment**

Fig. 28 shows the environmental impact of Fe (II) + PMS + UVA (CA) and carbocatalysis processes in terms of the equivalent greenhouse gas emissions $CO_2$-Eq, also named carbon footprint or global warming potential (GWP). It can be noted that among the two tested systems, Carbocatalysis had a higher carbon footprint (2.87 Kg $CO_2$-Eq) than Fe (II) + PMS + UVA (CA) (0.517 Kg $CO_2$-Eq).
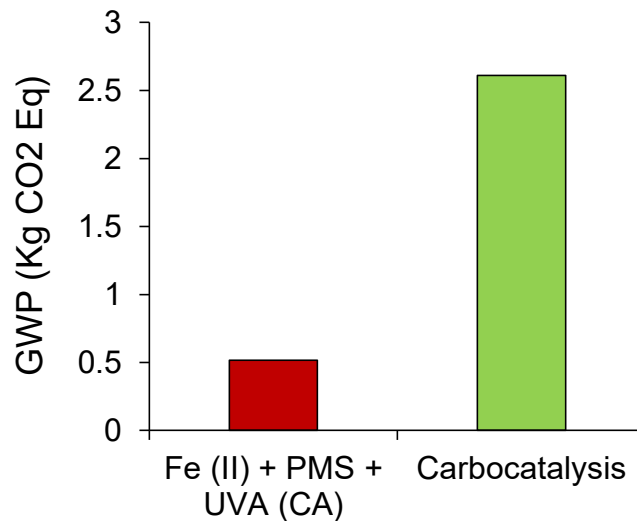
**Figure 28.** LCA results for the systems under study. Photo-Fenton intensified with citric acid
(Fe (II) + PMS + UVA (CA)) and carbocatalysis (the two systems used PMS as the precursor of
ROS).

LCA is a key guide to identify the environmental hotspots of a process (Belalcázar-Saldarriaga et
al., 2018a; Grisales et al., 2019; Luis Miguel Salazar et al., 2019). Thus, from LCA, the contribution
of each process component was analyzed to determine the actual weight of each component on the
environmental impact. Fig. 29 depicts the percentual contribution of the operative components for
the carbocatalytic process. It was evidenced that the biochar preparation represented the most
relevant carbon footprint in carbocatalysis. This behavior was associated with the use of $ZnCl_2$ (the
activating agent) plus the electric energy consumption during the stirring and carbonization steps
to prepare the biochar (BP). Our results were according to different authors, which say that the
preparation of activated carbons or similar CBM is environmentally aggressive due to the very high
energy consumption and the utilization of inorganic acids or salts in the activation step (Magdy et
al., 2021; Muñoz et al., 2007).
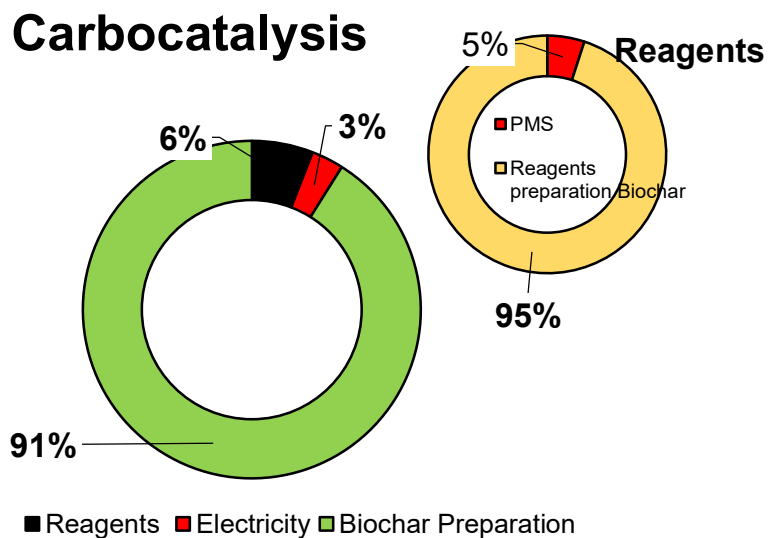
**Figure 29.** Contribution of the Carbocatalysis process components to the Carbon Footprint.

Fig. 30 shows the separated contribution of the operative components for the Fe (II) + PMS + UVA (CA) process. The results indicated that the reagents consumption is more aggressive footprint (~69%) than the electricity consumption. The electrical impact was essentially related to the consumption of energy for pumping and recirculation steps in the process at the pilot scale.

From Fig. 30, the carbon footprint caused by the consumption of the catalyst (iron in this case) is scarcely significant, it represents 2% of the total $CO_2$-Eq emissions. It can also be noted that the PMS had a greater impact, which agrees with other studies, where the use of oxidizing agents is recognized as one of the environmental critical impacts of AOPs (Belalcázar-Saldarriaga et al., 2018b; Grisales et al., 2019; Luis Miguel Salazar et al., 2019). This behavior is associated with the synthesis process of PMS, which involves the intensive use of electricity, petroleum, and other fossil fuels (like coal and natural gas), plus the utilization of reagents for the oxidant preparation (Belalcázar-Saldarriaga et al., 2018b; Foteinis, Monteagudo, et al., 2018; Giménez et al., 2015; Grisales et al., 2019; Lida Ioannou-Ttofa et al., 2017a; Magdy et al., 2021; Luis Miguel Salazar et al., 2019). Furthermore, this catalyst at low concentration (as used in this work) is non-toxic (Belalcázar-Saldarriaga et al., 2018a; Grisales et al., 2019; L. Ioannou-Ttofa et al., 2016; Lida Ioannou-Ttofa et al., 2017a; L.M. Salazar et al., 2019).

Besides, we can mention that the PMS and citric acid induced the most relevant carbon footprint on the reagents item, due to the use of electricity and fossil fuels during their synthesis (Sbardella

et al., 2020). However, it is worth mentioning that the addition of citric acid allowed to achieve the degradation of 80% of VAL of SHWW in 60 minutes, while the FF process removed up to 30% in 120 minutes (see the previous Chapter).
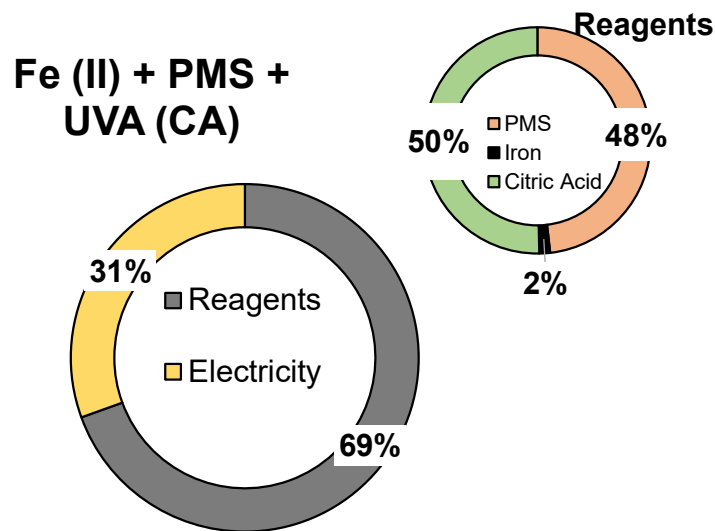


**Figure 30.** Contribution of components of the Fe (II) +PMS +UVA (CA) to the carbon footprint.

### 5.3.2. Economic impact assessment

Once established the environmental impact of the tested processes. The economic assessment was performed. Fig. 31 summarizes the operational cost of processes. The results indicate that from an economic point of view, carbocatalysis presented higher costs (USD 11.05 m$^{-3}$) than Fe (II) +PMS +UVA (CA) (PF (CA), (USD 4.92 m$^{-3}$). The costs associated with the biochar preparation in the carbocatalysis process represented 82% of the value reported for the total operational cost in Fig. 31, this result was essential due to the high cost of the activating agent (i.e., ZnCl$_2$) and energy consumption for BP preparation. These findings are congruent with the results found in the LCA (Section 5.3.1) and allowed us to infer that although the carbon source of the biochar is an agro-industrial waste, the BP preparation is a critical stage, and it is necessary to develop strategies toward reduction of the environmental and economic impacts of this stage in the carbocatalytic system.

Finally, the operational costs associated with PF (CA) process are until 65% lower than carbocatalysis. In this process, the reagents consumption represented ~ 98% of the value reported

for the operational costs. Therefore, the PF (CA) process could be evaluated for applying at the pilot scale for treating HWW.
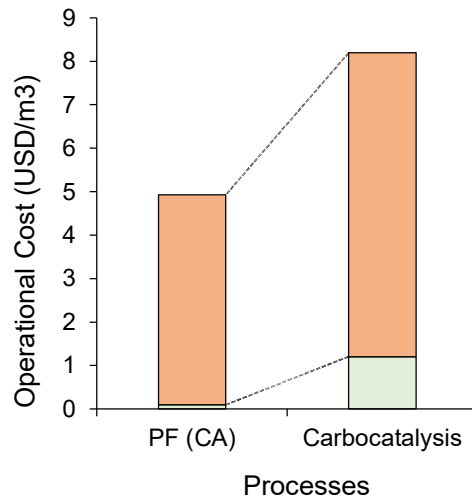


**Figure 31.** Operational costs of the system under study. Fe (II)+PMS+UVA (CA) (PF (CA) process) and carbocatalysis (the two systems using PMS as the precursor of ROS).

### 5.4. Conclusions

After the development of the environmental and economic assessments, it can be concluded that:

- The environmental footprint of the Fe (II)+PMS+UVA(CA) process was up to six times lower than that for carbocatalysis, respectively.

- LCA was key to guide to identify the hotspots of the processes, indicating that for carbocatalysis the preparation of BP was the critical point, whereas in Fe (II)+PMS+UVA (CA) the electric and reagents consumption had a relevant environmental impact.

- The Fe (II)+PMS+UVA (CA) had less economic costs than carbocatalysis. It was noted that the Fenton-based processes (even considering the addition of citric acid) were very competitive alternatives for future pilot-scale applications.

## CONCLUDING REMARKS AND OUTLOOKS

From the development of this research work, it can be highlighted that the considered RHWW is a source of environmental pollution. Interestingly, this pollution was effectively faced by catalytic processes such the carbocatalysis using a biochar from agro-industrial wastes, which presented superficial oxygenated functional groups that favored the interaction with PMS and generate ROS able to degrade the target pharmaceuticals. The interaction of this material with PMS exhibited remarkable characteristics as the extension of lifetime use. The tested carbocatalysis process is a promising alternative from a technical point of view. However, this process had economic and environmental limitations, which could be overcome by testing/using the raw material (oil palm fiber wastes) directly, or a carbonized material prepared at lower temperatures, instead of the preparation of BP.

The photo-Fenton process at near-neutral pH using PMS and citric acid was also useful as an alternative to remove pollution associated with HWW. Simultaneous action of hydroxyl radical and sulfate radical made this process efficient for the degradation of pharmaceuticals. Indeed, from technical, economic, and environmental criteria, this treatment system was more suitable than carbocatalysis. Nevertheless, the use of citric acid, as an intensifying agent, is an important variable to be considered in terms of the environmental impacts and economic costs. Thus, the use of effluents from the renal care units, which are rich in this organic acid could be an alternative to decrease the high economic and environmental weights associated with the addition of citric acid in the photo-Fenton process.

Finally, future research on this topic could be addressed in reactor design to evaluate the photo-Fenton process at the pilot-scale to treat actual HWW *in situ*. Also, it is necessary to test the simultaneous degradation of several pharmaceuticals in the actual HWW, even to assess the elimination of pathogens (such as antibiotic-resistant bacteria) by the photo-Fenton process.

# REFERENCES

Ahile, U. J., Wuana, R. A., Itodo, A. U., Sha'Ato, R., & Dantas, R. F. (2020a). A review on the use of chelating agents as an alternative to promote photo-Fenton at neutral pH: Current trends, knowledge gap and future studies. *Science of the Total Environment*, *710*, 134872. https://doi.org/10.1016/j.scitotenv.2019.134872

Ahile, U. J., Wuana, R. A., Itodo, A. U., Sha'Ato, R., & Dantas, R. F. (2020b). Stability of iron chelates during photo-Fenton process: The role of pH, hydroxyl radical attack and temperature. *Journal of Water Process Engineering*, *36*(October 2019), 101320. https://doi.org/10.1016/j.jwpe.2020.101320

Al-Riyami, I. M., Ahmed, M., Al-Busaidi, A., & Choudri, B. S. (2018). Antibiotics in wastewaters: a review with focus on Oman. *Applied Water Science*, *8*(7), 1–10. https://doi.org/10.1007/s13201-018-0846-z

Álvarez, L., Colmenares, B., Mina, A., Montealegre, L., & Ruiz, F. (2012). *Automedicación con antibióticos en Bogotá, Cali, Zipaquira, Facatativa y Santander de Quilichao "una realidad vigente en nuestro país.* 1–79.

Alvarino, T., García-Sandá, E., Gutiérrez-Prada, I., Lema, J., Omil, F., & Suárez, S. (2020). A new decentralized biological treatment process based on activated carbon targeting organic micropollutant removal from hospital wastewaters. *Environmental Science and Pollution Research*, *27*(2), 1214–1223. https://doi.org/10.1007/s11356-018-2670-2

Anjali, R., & Shanthakumar, S. (2019). Insights on the current status of occurrence and removal of antibiotics in wastewater by advanced oxidation processes. *Journal of Environmental Management*, *246*(January), 51–62. https://doi.org/10.1016/j.jenvman.2019.05.090

Bangari, R. S., & Sinha, N. (2019). Adsorption of tetracycline, ofloxacin and cephalexin antibiotics on boron nitride nanosheets from aqueous solution. *Journal of Molecular Liquids*, *293*, 111376. https://doi.org/10.1016/j.molliq.2019.111376

Belalcázar-Saldarriaga, A., Prato-Garcia, D., & Vasquez-Medrano, R. (2018a). Photo-Fenton processes in raceway reactors: Technical, economic, and environmental implications during

treatment of colored wastewaters. *Journal of Cleaner Production*, *182*, 818–829.
https://doi.org/10.1016/j.jclepro.2018.02.058

Belalcázar-Saldarriaga, A., Prato-Garcia, D., & Vasquez-Medrano, R. (2018b). Photo-Fenton
processes in raceway reactors: Technical, economic, and environmental implications during
treatment of colored wastewaters. *Journal of Cleaner Production*, *182*, 818–829.
https://doi.org/10.1016/j.jclepro.2018.02.058

Berkner, S., & Thierbach, C. (2014). Biodegradability and transformation of human
pharmaceutical active ingredients in environmentally relevant test systems. *Environmental
Science and Pollution Research*, *21*(16), 9461–9467. https://doi.org/10.1007/s11356-013-
1868-6

Bielski, B. H. J., Cabelli, D. E., Arudi, R. L., & Ross, A. B. (1985). Reactivity of HO2/O−2
Radicals in Aqueous Solution. *Journal of Physical and Chemical Reference Data*, *14*(4),
1041–1100. https://doi.org/10.1063/1.555739

Boillot, C., Bazin, C., Tissot-Guerraz, F., Droguet, J., Perraud, M., Cetre, J. C., Trepo, D., &
Perrodin, Y. (2008). Daily physicochemical, microbiological and ecotoxicological
fluctuations of a hospital effluent according to technical and care activities. *Science of the
Total Environment*, *403*(1–3), 113–129. https://doi.org/10.1016/j.scitotenv.2008.04.037

Botero-Coy, A. M., Martínez-Pachón, D., Boix, C., Rincón, J. R., Castillo, N., Arias-Marín, L.
P., Manrique-Losada, L., Torres-Palma, R. A., Moncayo-Lasso, A., & Hernández, F. (2018).
An investigation into the occurrence and removal of pharmaceuticals in colombian
wastewater. *Science of The Total Environment*, *62*, 842–853.

Botero-Coy, A. M., Martínez-Pachón, D., Boix, C., Rincón, R. J., Castillo, N., Arias-Marín, L.
P., Manrique-Losada, L., Torres-Palma, R., Moncayo-Lasso, A., & Hernandez, F. (2018).
'An investigation into the occurrence and removal of pharmaceuticals in Colombian
wastewater.' *Science of The Total Environment*, *642*, 842–853.
https://doi.org/10.1016/j.scitotenv.2018.06.088

Bruycker, K. De. (2017). RSC Advances Recyclable cross-linked hydroxythioether particles with
tunable structures via robust and e ffi cient thiol-epoxy dispersion polymerizations †. *RSC*

*Advances*, *7*, 51763–51772. https://doi.org/10.1039/C7RA10481B

Buxton, G. V, Greenstock, C. L., Helman, W. P., & Ross, A. B. (1988). Critical Review of rate
constants for reactions of hydrated electron, hydrogen atoms and hydroxyl radicals (·OH/·O
in Aqueous Solution). *Journal of Physical and Chemical Reference Data*, *513*.
https://doi.org/10.1063/1.555805

Carraro, E., Bonetta, S., Bertino, C., Lorenzi, E., Bonetta, S., & Gilli, G. (2016). Hospital
effluents management: Chemical, physical, microbiological risks and legislation in different
countries. *Journal of Environmental Management*, *168*, 185–199.
https://doi.org/10.1016/j.jenvman.2015.11.021

Carvalho Neves, L., Beber de Souza, J., de Souza Vidal, C. M., Herbert, L. T., de Souza, K. V.,
Geronazzo Martins, K., & Young, B. J. (2020). Phytotoxicity indexes and removal of color,
COD, phenols and ISA from pulp and paper mill wastewater post-treated by UV/H2O2 and
photo-Fenton. *Ecotoxicology and Environmental Safety*, *202*, 110939.
https://doi.org/10.1016/j.ecoenv.2020.110939

Castillo Meza, L., Piotrowski, P., Farnan, J., Tasker, T. L., Xiong, B., Weggler, B., Murrell, K.,
Dorman, F. L., Vanden Heuvel, J. P., & Burgos, W. D. (2020). Detection and removal of
biologically active organic micropollutants from hospital wastewater. *Science of the Total
Environment*, *700*, 134469. https://doi.org/10.1016/j.scitotenv.2019.134469

Cavalcante, R. P., da Rocha Sandim, L., Bogo, D., Barbosa, A. M. J., Osugi, M. E., Blanco, M.,
de Oliveira, S. C., de Fatima Cepa Matos, M., Machulek, A., & Ferreira, V. S. (2013).
Application of Fenton, photo-Fenton, solar photo-Fenton, and UV/H2O2 to degradation of
the antineoplastic agent mitoxantrone and toxicological evaluation. *Environmental Science
and Pollution Research*, *20*(4), 2352–2361. https://doi.org/10.1007/s11356-012-1110-y

Chatzisymeon, E., Foteinis, S., Mantzavinos, D., & Tsoutsos, T. (2013). Life cycle assessment of
advanced oxidation processes for olive mill wastewater treatment. *Journal of Cleaner
Production*. https://doi.org/10.1016/j.jclepro.2013.05.013

Chen, X., Oh, W. Da, & Lim, T. T. (2018). Graphene- and CNTs-based carbocatalysts in
persulfates activation: Material design and catalytic mechanisms. *Chemical Engineering*

*Journal*, *354*, 941–976. https://doi.org/10.1016/j.cej.2018.08.049

Chiarello, M., Minetto, L., Giustina, S. V. D., Beal, L. L., & Moura, S. (2016). Popular
pharmaceutical residues in hospital wastewater: quantification and qualification of
degradation products by mass spectroscopy after treatment with membrane bioreactor.
*Environmental Science and Pollution Research*, *23*(16), 16079–16089.
https://doi.org/10.1007/s11356-016-6766-2

Chonova, T., Labanowski, J., & Bouchez, A. (2018). Contribution of hospital effluents to the
load of micropollutants in WWTP influents. *Handbook of Environmental Chemistry*,
*60*(April 2017), 135–152. https://doi.org/10.1007/698_2017_21

ClinClac. (2018). *Valsartan-number of prescriptions over time (2007-2017)*. Clincalc.Com.

Devi, P., Das, U., & Dalai, A. K. (2016). In-situ chemical oxidation: Principle and applications of
peroxide and persulfate treatments in wastewater systems. In *Science of the Total
Environment* (Vol. 571). https://doi.org/10.1016/j.scitotenv.2016.07.032

Dewil, R., Mantzavinos, D., Poulios, I., & Rodrigo, M. A. (2017). New perspectives for
Advanced Oxidation Processes. *Journal of Environmental Management*, *195*, 93–99.
https://doi.org/10.1016/j.jenvman.2017.04.010

Díez-Mato, E., Cortezón-Tamarit, F. C., Bogialli, S., García-Fresnadillo, D., & Marazuela, M. D.
(2014). Phototransformation of model micropollutants in water samples by photocatalytic
singlet oxygen production in heterogeneous medium. *Applied Catalysis B: Environmental*,
*160–161*(1), 445–455. https://doi.org/10.1016/j.apcatb.2014.05.050

Dong, H., Qiang, Z., Hu, J., & Sans, C. (2017). Accelerated degradation of iopamidol in iron
activated persulfate systems: Roles of complexing agents. *Chemical Engineering Journal*,
*316*, 288–295. https://doi.org/10.1016/j.cej.2017.01.099

Du, L., Xu, W., Liu, S., Li, X., Huang, D., Tan, X., & Liu, Y. (2020). Activation of persulfate by
graphitized biochar for sulfamethoxazole removal: The roles of graphitic carbon structure
and carbonyl group. *Journal of Colloid and Interface Science*, *577*, 419–430.
https://doi.org/10.1016/j.jcis.2020.05.096

Elghniji, K., Hentati, O., Mlaik, N., Mahfoudh, A., & Ksibi, M. (2012). Photocatalytic
    degradation of 4-chlorophenol under P-modified TiO 2/UV system: Kinetics, intermediates,
    phytotoxicity and acute toxicity. *Journal of Environmental Sciences*, *24*(3), 479–487.
    https://doi.org/10.1016/S1001-0742(10)60659-6

Emmanuel, E., Perrodin, Y., Keck, G., Blanchard, J., & Vermande, P. (2005). Ecotoxicological
    risk assessment of hospital wastewater : a proposed framework for raw effluents discharging
    into urban sewer network. *Journa of Hazardous Materials*, *117*, 1–11.
    https://doi.org/10.1016/j.jhazmat.2004.08.032

Farré, M. J., García-Montaño, J., Ruiz, N., Muñoz, I., Domènech, X., & Peral, J. (2007). Life
    cycle assessment of the removal of Diuron and Linuron herbicides from water using three
    environmentally friendly technologies. *Environmental Technology*, *28*(7), 819–830.
    https://doi.org/10.1080/09593332808618830

Foteinis, S., Maria, J., Durán, A., & Chatzisymeon, E. (2018). Science of the Total Environment
    Environmental sustainability of the solar photo-Fenton process for wastewater treatment and
    pharmaceuticals mineralization at semi-industrial scale. *Science of the Total Environment*,
    *612*, 605–612. https://doi.org/10.1016/j.scitotenv.2017.08.277

Foteinis, S., Monteagudo, J. M., Durán, A., & Chatzisymeon, E. (2018). Environmental
    sustainability of the solar photo-Fenton process for wastewater treatment and
    pharmaceuticals mineralization at semi-industrial scale. *Science of the Total Environment*,
    *612*, 605–612. https://doi.org/10.1016/j.scitotenv.2017.08.277

García, P. A. C. (2010). *Utilización de antibióticos de uso humano en caninos y felinos atendidos
    en la clínica de pequeños animales de la Universidad Nacional de Colombia*. *9*(1), 76–99.

Giménez, J., Bayarri, B., González, Ó., Malato, S., Peral, J., & Esplugas, S. (2015). Advanced
    Oxidation Processes at Laboratory Scale: Environmental and Economic Impacts. *ACS
    Sustainable Chemistry and Engineering*. https://doi.org/10.1021/acssuschemeng.5b00778

Giraldo-Aguirre, A. L., Serna-Galvis, E. A., Erazo-Erazo, E. D., Silva-Agredo, J., Giraldo-
    Ospina, H., Flórez-Acosta, O. A., & Torres-Palma, R. A. (2018). Removal of β-lactam
    antibiotics from pharmaceutical wastewaters using photo-Fenton process at near-neutral pH.

*Environmental Science and Pollution Research*, *25*(21), 20293–20303.
https://doi.org/10.1007/s11356-017-8420-z

Goedkoop, M. J. (2008). *ReCiPE 2008 : A life cycle impact assessment method which comprises
harmonised category indicators at the ... ReCiPe 2008*. *June 2016*.

Grisales-Cifuentes, C. M., Serna Galvis, E. A., Porras, J., Flórez, E., Torres-Palma, R. A., &
Acelas, N. (2021). Kinetics, isotherms, effect of structure, and computational analysis
during the removal of three representative pharmaceuticals from water by adsorption using a
biochar obtained from oil palm fiber. *Bioresource Technology*, *326*.
https://doi.org/10.1016/j.biortech.2021.124753

Grisales, C. M., Salazar, L. M., & Garcia, D. P. (2019). Treatment of synthetic dye baths by
Fenton processes: evaluation of their environmental footprint through life cycle assessment.
*Environmental Science and Pollution Research*, *26*(5), 4300–4311.
https://doi.org/10.1007/s11356-018-2757-9

Guinée, J., Gorree, M., Heijungs, R., Huppes, G., Kleijn, R., Haes, H., & Voet, E. (2001). *Life
cycle assessment An operational guide to the ISO standards* (Issue May).

Hamjinda, N. S., Chiemchaisri, W., Watanabe, T., Honda, R., & Chiemchaisri, C. (2018).
Toxicological assessment of hospital wastewater in different treatment processes.
*Environmental Science and Pollution Research*, *25*(8), 7271–7279.
https://doi.org/10.1007/s11356-015-4812-0

Hanafi, F., Belaoufi, A., Mountadar, M., & Assobhei, O. (2011). Augmentation of
biodegradability of olive mill wastewater by electrochemical pre-treatment: Effect on
phytotoxicity and operating cost. *Journal of Hazardous Materials*, *190*(1–3), 94–99.
https://doi.org/10.1016/j.jhazmat.2011.02.087

Hayyan, M., Hashim, M. A., & Alnashef, I. M. (2016). Superoxide Ion: Generation and Chemical
Implications. *Chemical Reviews*, *116*(5), 3029–3085.
https://doi.org/10.1021/acs.chemrev.5b00407

Huong, P. T., Jitae, K., Al Tahtamouni, T. M., Le Minh Tri, N., Kim, H. H., Cho, K. H., & Lee,
C. (2020). Novel activation of peroxymonosulfate by biochar derived from rice husk toward

oxidation of organic contaminants in wastewater. *Journal of Water Process Engineering*, *33*(October 2019), 101037. https://doi.org/10.1016/j.jwpe.2019.101037

Ioannou-Ttofa, L., Foteinis, S., Chatzisymeon, E., & Fatta-Kassinos, D. (2016). The environmental footprint of a membrane bioreactor treatment process through Life Cycle Analysis. *Science of the Total Environment*. https://doi.org/10.1016/j.scitotenv.2016.06.032

Ioannou-Ttofa, Lida, Foteinis, S., Chatzisymeon, E., Michael-Kordatou, I., & Fatta-Kassinos, D. (2017a). Life cycle assessment of solar-driven oxidation as a polishing step of secondary-treated urban effluents. *Journal of Chemical Technology and Biotechnology*, *92*(6), 1315–1327. https://doi.org/10.1002/jctb.5126

Ioannou-Ttofa, Lida, Foteinis, S., Chatzisymeon, E., Michael-Kordatou, I., & Fatta-Kassinos, D. (2017b). Life cycle assessment of solar-driven oxidation as a polishing step of secondary-treated urban effluents. *Journal of Chemical Technology and Biotechnology*, *92*(6), 1315–1327. https://doi.org/10.1002/jctb.5126

Jayaraj, R., Megha, P., & Sreedev, P. (2016). Review Article. Organochlorine pesticides, their toxic effects on living organisms and their fate in the environment. *Interdisciplinary Toxicology*, *9*(3–4), 90–100. https://doi.org/10.1515/intox-2016-0012

Karimian, S., Moussavi, G., Fanaei, F., Mohammadi, S., Shekoohiyan, S., & Giannakis, S. (2020). Shedding light on the catalytic synergies between Fe(II) and PMS in vacuum UV (VUV/Fe/PMS) photoreactors for accelerated elimination of pharmaceuticals: The case of metformin. *Chemical Engineering Journal*, *400*(June), 125896. https://doi.org/10.1016/j.cej.2020.125896

Keith, T. A., & Frisch, M. J. (1994). Inclusion of Explicit Solvent Molecules in a Self-Consistent-Reaction Field Model of Solvation. In *Modeling the Hydrogen Bond* (Vol. 569, pp. 3–22). American Chemical Society. https://doi.org/doi:10.1021/bk-1994-0569.ch003

Khan, A. H., Khan, N. A., Ahmed, S., Dhingra, A., Singh, C. P., Khan, S. U., Mohammadi, A. A., Changani, F., Yousefi, M., Alam, S., Vambol, S., Vambol, V., Khursheed, A., & Ali, I. (2020). Application of advanced oxidation processes followed by different treatment technologies for hospital wastewater treatment. *Journal of Cleaner Production*, *269*.

https://doi.org/10.1016/j.jclepro.2020.122411

Khan, N. A., Khan, S. U., Ahmed, S., Farooqi, I. H., Yousefi, M., Mohammadi, A. A., &
    Changani, F. (2020). Recent trends in disposal and treatment technologies of emerging-
    pollutants- A critical review. *TrAC - Trends in Analytical Chemistry*, *122*.
    https://doi.org/10.1016/j.trac.2019.115744

Kim, J., Coulibaly, G. N., Yoon, S., Assadi, A. A., Hanna, K., & Bae, S. (2020). Red mud-
    activated peroxymonosulfate process for the removal of fluoroquinolones in hospital
    wastewater. *Water Research*, *184*, 116171. https://doi.org/10.1016/j.watres.2020.116171

Kumari, A., Maurya, N. S., & Tiwari, B. (2020). Hospital wastewater treatment scenario around
    the globe. In *Current Developments in Biotechnology and Bioengineering*. BV.
    https://doi.org/10.1016/b978-0-12-819722-6.00015-8

Li, F., Duan, F., Ji, W., & Gui, X. (2020). Biochar-activated persulfate for organic contaminants
    removal: Efficiency, mechanisms and influencing factors. *Ecotoxicology and Environmental
    Safety*, *198*. https://doi.org/10.1016/j.ecoenv.2020.110653

Lian, L., Yao, B., Hou, S., Fang, J., Yan, S., & Song, W. (2017). Kinetic Study of Hydroxyl and
    Sulfate Radical-Mediated Oxidation of Pharmaceuticals in Wastewater Effluents. *Environ.
    Sci. Technol.*, *51*(5), 2954–2962. https://doi.org/10.1021/acs.est.6b05536

Liang, J., Xu, X., Qamar Zaman, W., Hu, X., Zhao, L., Qiu, H., & Cao, X. (2019). Different
    mechanisms between biochar and activated carbon for the persulfate catalytic degradation of
    sulfamethoxazole: Roles of radicals in solution or solid phase. *Chemical Engineering
    Journal*, *375*(June), 121908. https://doi.org/10.1016/j.cej.2019.121908

Libralato, G., Costa Devoti, A., Zanella, M., Sabbioni, E., Mičetić, I., Manodori, L., Pigozzo, A.,
    Manenti, S., Groppi, F., & Volpi Ghirardini, A. (2016). Phytotoxicity of ionic, micro- and
    nano-sized iron in three plant species. *Ecotoxicology and Environmental Safety*, *123*.
    https://doi.org/10.1016/j.ecoenv.2015.07.024

Lima, D. R., Lima, E. C., Umpierres, C. S., Thue, P. S., El-Chaghaby, G. A., da Silva, R. S.,
    Pavan, F. A., Dias, S. L. P., & Biron, C. (2019). Removal of amoxicillin from simulated
    hospital effluents by adsorption using activated carbons prepared from capsules of cashew

of Para. *Environmental Science and Pollution Research*, *26*(16), 16396–16408.
https://doi.org/10.1007/s11356-019-04994-6

Ling, L., Zhang, D., Fan, C., & Shang, C. (2017). A Fe(II)/citrate/UV/PMS process for
carbamazepine degradation at a very low Fe(II)/PMS ratio and neutral pH: The mechanisms.
*Water Research*, *124*, 446–453. https://doi.org/10.1016/j.watres.2017.07.066

Liu, T., Zhang, D., Yin, K., Yang, C., Luo, S., & Crittenden, J. C. (2020a). Degradation of
thiacloprid via unactivated peroxymonosulfate: The overlooked singlet oxygen oxidation.
*Chemical Engineering Journal*, *388*, 124264.
https://doi.org/https://doi.org/10.1016/j.cej.2020.124264

Liu, T., Zhang, D., Yin, K., Yang, C., Luo, S., & Crittenden, J. C. (2020b). Degradation of
thiacloprid via unactivated peroxymonosulfate: The overlooked singlet oxygen oxidation.
*Chemical Engineering Journal*, *388*(November 2019), 124264.
https://doi.org/10.1016/j.cej.2020.124264

López, J. J., & Garay, A. M. (2016). Study of the use of antibiotics in the outpatient service of a
public hospital in Bogotá, D. C. *Revista Colombiana de Ciencias Químico-Farmacéuticas*,
*45*(1), 456.

Luo, K., Yang, Q., Pang, Y., Wang, D., Li, X., Lei, M., & Huang, Q. (2019). Unveiling the
mechanism of biochar-activated hydrogen peroxide on the degradation of ciprofloxacin.
*Chemical Engineering Journal*, *374*. https://doi.org/10.1016/j.cej.2019.05.204

Lykoudi, A., Frontistis, Z., Vakros, J., Manariotis, I. D., & Mantzavinos, D. (2020). Degradation
of sulfamethoxazole with persulfate using spent coffee grounds biochar as activator. *Journal
of Environmental Management*, *271*. https://doi.org/10.1016/j.jenvman.2020.111022

Machado-Alba, J. E., & González-Santos, D. M. (2009). Dispensación de antibióticos de uso
ambulatorio en una población colombiana. *Revista de Salud Pública*, *11*(5), 734–744.
https://doi.org/10.1590/S0124-00642009000500006

Mackuľak, T., Grabic, R., Špalková, V., Belišová, N., Škulcová, A., Slavík, O., Horký, P., Gál,
M., Filip, J., Híveš, J., Vojs, M., Staňová, A. V., Medveďová, A., Marton, M., & Birošová,
L. (2019). Hospital wastewaters treatment: Fenton reaction vs. BDDE vs. ferrate(VI).

*Environmental Science and Pollution Research*, *26*(31), 31812–31821.
https://doi.org/10.1007/s11356-019-06290-9

Magdy, M., Gar, M., & El-etriby, H. K. (2021). Comparative life cycle assessment of fi ve
chemical methods for removal of phenol and its transformation products. *Journal of Cleaner
Production*, *291*, 125923. https://doi.org/10.1016/j.jclepro.2021.125923

Martínez-Pachón, D., Serna-Galvis, E. A., Ibañez, M., Hernández, F., Ávila-Torres, Y., Torres-
Palma, R. A., & Moncayo-Lasso, A. (2021). Treatment of two sartan antihypertensives in
water by photo-electro-Fenton using BDD anodes: Degradation kinetics, theoretical
analyses, primary transformations and matrix effects. *Chemosphere*, *270*.
https://doi.org/10.1016/j.chemosphere.2020.129491

Mian, M. M., & Liu, G. (2020). Activation of peroxymonosulfate by chemically modified sludge
biochar for the removal of organic pollutants: Understanding the role of active sites and
mechanism. *Chemical Engineering Journal*, *392*. https://doi.org/10.1016/j.cej.2019.123681

Minakata, D., Song, W., & Crittenden, J. (2011). Reactivity of Aqueous Phase Hydroxyl Radical
with Halogenated Carboxylate Anions: Experimental and Theoretical Studies. *Environ. Sci.
Technol.*, *45*(14), 6057–6065.

Mir-Tutusaus, J. A., Parladé, E., Llorca, M., Villagrasa, M., Barceló, D., Rodriguez-Mozaz, S.,
Martinez-Alonso, M., Gaju, N., Caminal, G., & Sarrà, M. (2017). Pharmaceuticals removal
and microbial community assessment in a continuous fungal treatment of non-sterile real
hospital wastewater after a coagulation-flocculation pretreatment. *Water Research*, *116*, 65–
75. https://doi.org/https://doi.org/10.1016/j.watres.2017.03.005

Monteagudo, J. M., Durán, A., & López-Almodóvar, C. (2008). Homogeneus ferrioxalate-
assisted solar photo-Fenton degradation of Orange II aqueous solutions. *Applied Catalysis
B: Environmental*, *83*(1–2), 46–55. https://doi.org/10.1016/j.apcatb.2008.02.002

Monteagudo, J. M., Durán, A., Martín, I. S., & Aguirre, M. (2010). Catalytic degradation of
Orange II in a ferrioxalate-assisted photo-Fenton process using a combined UV-A/C-solar
pilot-plant system. *Applied Catalysis B: Environmental*, *95*(1–2), 120–129.
https://doi.org/10.1016/j.apcatb.2009.12.018

Mufioz, I., Malato, S., Rodriguez, A., & Domenech, X. (2008). Integration of environmental and economic performance of processes. Case study on advanced oxidation processes for wastewater treatment. *Journal of Advanced Oxidation Technologies*, *11*(2), 270–275.

Municipio de Tumaco. (2018). *Hospital San Andres de Tumaco E.S.E. Web site*.

Muñoz, I., Feral, J., Ayllón, J. A., Malato, S., Martin, M. J., Perrot, J. Y., Vincent, M., & Domènech, X. (2007). Life-cycle assessment of a coupled advanced oxidation-biological process for wastewater treatment: Comparison with granular activated carbon adsorption. *Environmental Engineering Science*, *24*(5), 638–651. https://doi.org/10.1089/ees.2006.0134

Myers, RH.; Mongotmery, DC.; Anderson, C. . (1997). Response surface methodology: Process and product optimization using designed experiments. *Journal of Statistical Planning and Inference*, *59*(1), 185–186. https://doi.org/10.1016/s0378-3758(97)81631-x

Nguyen, T. T., Bui, X. T., Luu, V. P., Nguyen, P. D., Guo, W., & Ngo, H. H. (2017). Removal of antibiotics in sponge membrane bioreactors treating hospital wastewater: Comparison between hollow fiber and flat sheet membrane systems. *Bioresource Technology*, *240*, 42–49. https://doi.org/10.1016/j.biortech.2017.02.118

Nidheesh, P. V., Gopinath, A., Ranjith, N., Praveen Akre, A., Sreedharan, V., & Suresh Kumar, M. (2021). Potential role of biochar in advanced oxidation processes: A sustainable approach. In *Chemical Engineering Journal* (Vol. 405). Elsevier B.V. https://doi.org/10.1016/j.cej.2020.126582

Nödler, K., Hillebrand, O., Idzik, K., Strathmann, M., Schiperski, F., Zirlewagen, J., & Licha, T. (2013). Occurrence and fate of the angiotensin II receptor antagonist transformation product valsartan acid in the water cycle - A comparative study with selected β-blockers and the persistent anthropogenic wastewater indicators carbamazepine and acesulfame. *Water Research*, *47*(17), 6650–6659. https://doi.org/10.1016/j.watres.2013.08.034

Oh, W. Da, Dong, Z., & Lim, T. T. (2016). Generation of sulfate radical through heterogeneous catalysis for organic contaminants removal: Current development, challenges and prospects. *Applied Catalysis B: Environmental*, *194*, 169–201. https://doi.org/10.1016/j.apcatb.2016.04.003

Oturan, M. A., & Aaron, J. J. (2014). Advanced oxidation processes in water/wastewater
treatment: Principles and applications. A review. *Critical Reviews in Environmental Science
and Technology*, *44*(23), 2577–2641. https://doi.org/10.1080/10643389.2013.829765

Ouarda, Y., Bouchard, F., Azaïs, A., Vaudreuil, M. A., Drogui, P., Dayal Tyagi, R., Sauvé, S.,
Buelna, G., & Dubé, R. (2019). Electrochemical treatment of real hospital wastewaters and
monitoring of pharmaceutical residues by using surrogate models. *Journal of Environmental
Chemical Engineering*, *7*(5), 103332. https://doi.org/10.1016/j.jece.2019.103332

Ouyang, D., Chen, Y., Yan, J., Qian, L., Han, L., & Chen, M. (2019). Activation mechanism of
peroxymonosulfate by biochar for catalytic degradation of 1,4-dioxane: Important role of
biochar defect structures. *Chemical Engineering Journal*, *370*, 614–624.
https://doi.org/10.1016/j.cej.2019.03.235

Paredes-Laverde, M., Salamanca, M., Silva-Agredo, J., Manrique-Losada, L., & Torres-Palma,
R. A. (2019). Selective removal of acetaminophen in urine with activated carbons from rice
(Oryza sativa) and coffee (Coffea arabica) husk: Effect of activating agent, activation
temperature and analysis of physical-chemical interactions. *Journal of Environmental
Chemical Engineering*, *7*(5). https://doi.org/10.1016/j.jece.2019.103318

Paredes-Laverde, M., Silva-Agredo, J., & Torres-Palma, R. A. (2018). Removal of norfloxacin in
deionized, municipal water and urine using rice (Oryza sativa) and coffee (Coffea arabica)
husk wastes as natural adsorbents. *Journal of Environmental Management*, *213*, 98–108.
https://doi.org/10.1016/j.jenvman.2018.02.047

Peña, V. (2015). *Evaluación del uso de antibióticos en el municio de Cajicá, Cundinamarca,
Colombia.* 1–78.

Peng, B., Chen, L., Que, C., Yang, K., Deng, F., Deng, X., Shi, G., Xu, G., & Wu, M. (2016).
Adsorption of Antibiotics on Graphene and Biochar in Aqueous Solutions Induced by π-π
Interactions. *Scientific Reports*, *6*(August), 1–10. https://doi.org/10.1038/srep31920

Perrodin, Y., & Orias, F. (2018). Ecotoxicity of hospital wastewater. *Handbook of Environmental
Chemistry*, *60*, 33–47. https://doi.org/10.1007/698_2017_8

Pham, V. L., Kim, D. G., & Ko, S. O. (2020). Advanced oxidative degradation of acetaminophen

by carbon catalysts: Radical vs non-radical pathways. *Environmental Research*, *188*(June), 109767. https://doi.org/10.1016/j.envres.2020.109767

Pignatello, J. J., Oliveros, E., & MacKay, A. (2006). Advanced oxidation processes for organic contaminant destruction based on the fenton reaction and related chemistry. In *Critical Reviews in Environmental Science and Technology* (Vol. 36, Issue 1, pp. 1–84). https://doi.org/10.1080/10643380500326564

Pirsaheb, M., Hossaini, H., & Janjani, H. (2020). Reclamation of hospital secondary treatment effluent by sulfate radicals based–advanced oxidation processes (SR-AOPs) for removal of antibiotics. *Microchemical Journal*, *153*(July 2019), 104430. https://doi.org/10.1016/j.microc.2019.104430

Pliego, G., Zazo, J. A., Garcia-Muñoz, P., Munoz, M., Casas, J. A., & Rodriguez, J. J. (2015). Trends in the Intensification of the Fenton Process for Wastewater Treatment: An Overview. *Critical Reviews in Environmental Science and Technology*, *45*(24), 2611–2692. https://doi.org/10.1080/10643389.2015.1025646

Rodríguez-Chueca, J., Garcia-Cañibano, C., Sarro, M., Encinas, Á., Medana, C., Fabbri, D., Calza, P., & Marugán, J. (2019). Evaluation of transformation products from chemical oxidation of micropollutants in wastewater by photoassisted generation of sulfate radicals. *Chemosphere*, *226*, 509–519. https://doi.org/10.1016/j.chemosphere.2019.03.152

Rodríguez-Chueca, J., Giannakis, S., Marjanovic, M., Kohantorabi, M., Gholami, M. R., Grandjean, D., de Alencastro, L. F., & Pulgarín, C. (2019). Solar-assisted bacterial disinfection and removal of contaminants of emerging concern by Fe2+-activated HSO5- vs. S2O82- in drinking water. *Applied Catalysis B: Environmental*, *248*(November 2018), 62–72. https://doi.org/10.1016/j.apcatb.2019.02.018

Rodriguez-Mozaz, S., Lucas, D., & Barceló, D. (2018). Full-scale plants for dedicated treatment of hospital effluents. *Handbook of Environmental Chemistry*, *60*, 189–208. https://doi.org/10.1007/698_2017_13

Rodríguez, R., Espada, J. J., Pariente, M. I., Melero, J. A., Martínez, F., & Molina, R. (2016). Comparative life cycle assessment (LCA) study of heterogeneous and homogenous Fenton

processes for the treatment of pharmaceutical wastewater. *Journal of Cleaner Production*, *124*, 21–29. https://doi.org/10.1016/j.jclepro.2016.02.064

Saitoh, T., Shibata, K., Fujimori, K., & Ohtani, Y. (2017). Rapid removal of tetracycline antibiotics from water by coagulation-flotation of sodium dodecyl sulfate and poly(allylamine hydrochloride) in the presence of Al(III) ions. *Separation and Purification Technology*, *187*, 76–83. https://doi.org/10.1016/j.seppur.2017.06.036

Salazar, L.M., Grisales, C. M., & Garcia, D. P. (2019). How does intensification influence the operational and environmental performance of photo-Fenton processes at acidic and circumneutral pH. *Environmental Science and Pollution Research*, *26*(5). https://doi.org/10.1007/s11356-018-2388-1

Salazar, Luis Miguel, Grisales, C. M., & Garcia, D. P. (2019). How does intensification influence the operational and environmental performance of photo-Fenton processes at acidic and circumneutral pH. *Environmental Science and Pollution Research*, *26*(5), 4367–4380. https://doi.org/10.1007/s11356-018-2388-1

Sbardella, L., Gala, I. V., Comas, J., Carbonell, S. M., Rodríguez-Roda, I., & Gernjak, W. (2020). Integrated assessment of sulfate-based AOPs for pharmaceutical active compound removal from wastewater. *Journal of Cleaner Production*, *260*, 121014. https://doi.org/10.1016/j.jclepro.2020.121014

Seburg, R. A., Ballard, J. M., Hwang, T., & Sullivan, C. M. (2006). *Photosensitized degradation of losartan potassium in an extemporaneous suspension formulation*. *42*, 411–422. https://doi.org/10.1016/j.jpba.2006.04.030

Serna-Galvis, E.A., Isaza-Pineda, L., Moncayo-Lasso, A., Hernández, F., Ibáñez, M., & Torres-Palma, R. A. (2019). Comparative degradation of two highly consumed antihypertensives in water by sonochemical process. Determination of the reaction zone, primary degradation products and theoretical calculations on the oxidative process. *Ultrasonics Sonochemistry*, *58*. https://doi.org/10.1016/j.ultsonch.2019.104635

Serna-Galvis, Efraim A., Botero-Coy, A. M., Martínez-Pachón, D., Moncayo-Lasso, A., Ibáñez, M., Hernández, F., & Torres-Palma, R. A. (2019). Degradation of seventeen contaminants

of emerging concern in municipal wastewater effluents by sonochemical advanced oxidation processes. *Water Research*, *154*, 349–360. https://doi.org/10.1016/j.watres.2019.01.045

Serna-Galvis, Efraim A., Cáceres-Peña, A. C., & Torres-Palma, R. A. (2020). Elimination of representative fluoroquinolones, penicillins, and cephalosporins by solar photo-Fenton: degradation routes, primary transformations, degradation improvement by citric acid addition, and antimicrobial activity evolution. *Environmental Science and Pollution Research*, *27*(33), 41381–41393. https://doi.org/10.1007/s11356-020-10069-8

Serna-Galvis, Efraím A., Ferraro, F., Silva-Agredo, J., & Torres-Palma, R. A. (2017). Degradation of highly consumed fluoroquinolones, penicillins and cephalosporins in distilled water and simulated hospital wastewater by UV 254 and UV 254 /persulfate processes. *Water Research*, *122*, 128–138. https://doi.org/10.1016/j.watres.2017.05.065

Serna-Galvis, Efraím A., Silva-Agredo, J., Botero-Coy, A. M., Moncayo-Lasso, A., Hernández, F., & Torres-Palma, R. A. (2019a). Effective elimination of fifteen relevant pharmaceuticals in hospital wastewater from Colombia by combination of a biological system with a sonochemical process. *Science of the Total Environment*, *670*, 623–632. https://doi.org/10.1016/j.scitotenv.2019.03.153

Serna-Galvis, Efraím A., Silva-Agredo, J., Botero-Coy, A. M., Moncayo-Lasso, A., Hernández, F., & Torres-Palma, R. A. (2019b). Effective elimination of fifteen relevant pharmaceuticals in hospital wastewater from Colombia by combination of a biological system with a sonochemical process. *Science of the Total Environment*, *670*, 623–632. https://doi.org/10.1016/j.scitotenv.2019.03.153

Serna-Galvis, Efraim A., Silva-Agredo, J., Giraldo-Aguirre, A. L., & Torres-Palma, R. A. (2015). Sonochemical degradation of the pharmaceutical fluoxetine: Effect of parameters, organic and inorganic additives and combination with a biological system. *Science of the Total Environment*, *524–525*, 354–360. https://doi.org/10.1016/j.scitotenv.2015.04.053

Shan, R., Han, J., Gu, J., Yuan, H., Luo, B., & Chen, Y. (2020). A review of recent developments in catalytic applications of biochar-based materials. In *Resources, Conservation and Recycling* (Vol. 162). Elsevier B.V. https://doi.org/10.1016/j.resconrec.2020.105036

Shi, X., Li, Y., Zhang, Z., Sun, L., & Peng, Y. (2019). Enhancement of ciprofloxacin degradation
in the Fe(II)/peroxymonosulfate system by protocatechuic acid over a wide initial pH range.
*Chemical Engineering Journal*, *372*(January), 1113–1121.
https://doi.org/10.1016/j.cej.2019.04.195

Solís, R. R., Mena, I. F., Nadagouda, M. N., & Dionysiou, D. D. (2020). Adsorptive interaction
of peroxymonosulfate with graphene and catalytic assessment via non-radical pathway for
the removal of aqueous pharmaceuticals. *Journal of Hazardous Materials*, *384*, 121340.
https://doi.org/10.1016/j.jhazmat.2019.121340

Souza, B. M., Dezotti, M. W. C., Boaventura, R. A. R., & Vilar, V. J. P. (2014). Intensification of
a solar photo-Fenton reaction at near neutral pH with ferrioxalate complexes: A case study
on diclofenac removal from aqueous solutions. *Chemical Engineering Journal*, *256*, 448–
457. https://doi.org/10.1016/j.cej.2014.06.111

Suarez, S., Lema, J. M., & Omil, F. (2009). Pre-treatment of hospital wastewater by coagulation-
flocculation and flotation. *Bioresource Technology*, *100*(7), 2138–2146.
https://doi.org/10.1016/j.biortech.2008.11.015

Sun, C., Chen, T., Huang, Q., Zhan, M., Li, X., & Yan, J. (2020). Activation of persulfate by
CO2-activated biochar for improved phenolic pollutant degradation: Performance and
mechanism. *Chemical Engineering Journal*, *380*. https://doi.org/10.1016/j.cej.2019.122519

Toth, J. E., Rickman, K. A., Venter, A. R., Kiddle, J. J., & Mezyk, S. P. (2012). Reaction kinetics
and efficiencies for the hydroxyl and sulfate radical based oxidation of artificial sweeteners
in water. *J Phys Chem A.*, *116*(40), 9819–9824. https://doi.org/10.1021/jp3047246

Ushani, U., Lu, X., Wang, J., Zhang, Z., Dai, J., Tan, Y., Wang, S., Li, W., Niu, C., Cai, T.,
Wang, N., & Zhen, G. (2020). Sulfate radicals-based advanced oxidation technology in
various environmental remediation: A state-of-the–art review. *Chemical Engineering
Journal*, *402*(June), 126232. https://doi.org/10.1016/j.cej.2020.126232

Verlicchi, P., Galletti, A., Petrovic, M., & Barceló, D. (2010). Hospital effluents as a source of
emerging pollutants: An overview of micropollutants and sustainable treatment options.
*Journal of Hydrology*, *389*(3–4), 416–428. https://doi.org/10.1016/j.jhydrol.2010.06.005

Verlicchi, Paola, Galletti, A., & Masotti, L. (2010). Management of hospital wastewaters : the case of the effluent of a large hospital situated in a small town. *Water Science & Technology*, *61*(10), 2507–2519. https://doi.org/10.2166/wst.2010.138

Verlicchi, Paola, Galletti, A., Petrovic, M., & Barceló, D. (2012). Micro-pollutants in Hospital Effluent: Their Fate, Risk and Treatment Options. *Handbook of Environmental Chemistry*, *20*(January), 139–171. https://doi.org/10.1007/698_2011_134

Vo, T. K. Q., Bui, X. T., Chen, S. S., Nguyen, P. D., Cao, N. D. T., Vo, T. D. H., Nguyen, T. T., & Nguyen, T. B. (2019). Hospital wastewater treatment by sponge membrane bioreactor coupled with ozonation process. *Chemosphere*, *230*, 377–383. https://doi.org/10.1016/j.chemosphere.2019.05.009

Wang, H., Guo, W., Liu, B., Wu, Q., Luo, H., Zhao, Q., Si, Q., Sseguya, F., & Ren, N. (2019). Edge-nitrogenated biochar for efficient peroxydisulfate activation: An electron transfer mechanism. *Water Research*, *160*, 405–414. https://doi.org/https://doi.org/10.1016/j.watres.2019.05.059

Wang, Jia, Shen, M., Wang, H., Du, Y., Zhou, X., Liao, Z., Wang, H., & Chen, Z. (2020). Red mud modified sludge biochar for the activation of peroxymonosulfate: Singlet oxygen dominated mechanism and toxicity prediction. *Science of the Total Environment*, *740*. https://doi.org/10.1016/j.scitotenv.2020.140388

Wang, Jianlong, & Wang, S. (2018). Activation of persulfate (PS) and peroxymonosulfate (PMS) and application for the degradation of emerging contaminants. In *Chemical Engineering Journal* (Vol. 334). https://doi.org/10.1016/j.cej.2017.11.059

Wei, J., Liu, Y., Zhu, Y., & Li, J. (2020). Enhanced catalytic degradation of tetracycline antibiotic by persulfate activated with modified sludge bio-hydrochar. *Chemosphere*, *247*. https://doi.org/10.1016/j.chemosphere.2020.125854

Wirtz, V. J., Herrera-Patino, J. J., Santa-Ana-Tellez, Y., Dreser, A., Elseviers, M., & Vander Stichele, R. H. (2013). Analysing policy interventions to prohibit over-the-counter antibiotic sales in four Latin American countries. *Tropical Medicine and International Health*, *18*(6), 665–673. https://doi.org/10.1111/tmi.12096

Xiang, W., Zhang, X., Chen, J., Zou, W., He, F., Hu, X., Tsang, D. C. W., Ok, Y. S., & Gao, B. (2020). Biochar technology in wastewater treatment: A critical review. *Chemosphere*, *252*, 126539. https://doi.org/10.1016/j.chemosphere.2020.126539

Yao, N., Li, C., Yu, J., Xu, Q., Wei, S., Tian, Z., Yang, Z., Yang, W., & Shen, J. (2020). Insight into adsorption of combined antibiotic-heavy metal contaminants on graphene oxide in water. *Separation and Purification Technology*, *236*, 116278. https://doi.org/https://doi.org/10.1016/j.seppur.2019.116278

Yin, R., Guo, W., Wang, H., Du, J., Wu, Q., Chang, J. S., & Ren, N. (2019). Singlet oxygen-dominated peroxydisulfate activation by sludge-derived biochar for sulfamethoxazole degradation through a nonradical oxidation pathway: Performance and mechanism. *Chemical Engineering Journal*, *357*, 589–599. https://doi.org/10.1016/j.cej.2018.09.184

Zhang, R., Li, Y., Wang, Z., Tong, Y., & Sun, P. (2020). Biochar-activated peroxydisulfate as an effective process to eliminate pharmaceutical and metabolite in hydrolyzed urine. *Water Research*, *177*. https://doi.org/10.1016/j.watres.2020.115809

Zhao, C., Shao, B., Yan, M., Liu, Z., Liang, Q., He, Q., Wu, T., Liu, Y., Pan, Y., Huang, J., Wang, J., Liang, J., & Tang, L. (2021). Activation of peroxymonosulfate by biochar-based catalysts and applications in the degradation of organic contaminants : A review. *Chemical Engineering Journal*, *416*(January), 128829. https://doi.org/10.1016/j.cej.2021.128829

Zhou, X., Zeng, Z., Zeng, G., Lai, C., Xiao, R., Liu, S., Huang, D., Qin, L., Liu, X., Li, B., Yi, H., Fu, Y., Li, L., Zhang, M., & Wang, Z. (2020). Insight into the mechanism of persulfate activated by bone char: Unraveling the role of functional structure of biochar. *Chemical Engineering Journal*, *401*(June), 126127. https://doi.org/10.1016/j.cej.2020.126127